Application of Electromagnetic and Electrical Resistivity Methods in Investigating Groundwater Resources of The Sunyani Municipality in The Brong-Ahafo Region of Ghana

by

SOMIAH JOHN, BSc Materials Eng.(Hons)

A Thesis Submitted to the Department of Physics,
Kwame Nkrumah University of Science and Technology
in partial fulfillment of the requirements for the degree

of

MASTER OF SCIENCE (GEOPHYSICS)

College of Science

Department of Physics
Supervisor: Prof. Aboagye Menyeh

Declaration

I hereby declare that this submission is my own work towards the MSc and that, to the best of my knowledge, it contains no material previously published by another person nor material which has been accepted for the award of any other degree of the University, except where due acknowledgement has been made in the text.

.....	.....	.....
Student Name & ID	Signature	Date

Certified by:

.....	.....	.....
Supervisor Name	Signature	Date

Certified by:

.....	.....	.....
Head of Dept. Name	Signature	Date

ABSTRACT

Two geophysical techniques, the Electromagnetic (EM) and Vertical Electrical Soundings (VES) were employed to explore for groundwater in thirteen communities in the Sunyani Municipality. The Geonics EM 34-3 was used for the electromagnetic profiling which employed both the horizontal and vertical dipole modes of recording conductivity values. Vertical Electrical Soundings were also conducted with the ABEM Terrameter SAS 1000C using the Schlumberger protocol. The collected data was analyzed using the Grapher 8 and RES1D softwares. A total of 18 EM profiles of length 2.8 km were traversed and 40 vertical electrical soundings established. The interpretation of the 40 VES points suggested that 13 points were suitable for borehole drilling. From the VES curve analyses, it was also revealed that the subsurface structure of 27 out of the 40 VES points were underlain by three lithological layers while the remaining 13 are of four layer types of varying resistivities. The results are indicated slight to moderate fracture development in the bedrock. Results from the interpretation of the data collected led to the inference of low groundwater potential at Antwikrom, low to moderate groundwater potential at Domsesre and relatively moderate to high groundwater potential in the rest of the eleven (11) communities. The use of the integrated geophysical technique employed for this study shows how the two methods can be applied complimentarily to groundwater exploration. Whereas the Electromagnetic (EM) was used as a reconnaissance tool in determining areas of increasing conductivity with depth, the Vertical Electrical Sounding (VES) technique was used in delineating the sequence of subsurface lithologies in order to identify potential aquifers.

Table of Contents

List of Tables

List of Figures

List of Symbols and Acronyms

E	electric intensity
H	magnetizing force
e	electric field intensity
b	magnetic induction
d	dielectric displacement
h	magnetic field intensity
j	electric current density
ρ	electric charge density
ρ_e	free charge
ε	dielectric permittivity
μ	magnetic permeability
σ	electric conductivity
ω	angular frequency
B	magnetic induction
t	time
T	temperature
P	pressure
z	depth of penetration
A	amplitude
δ	skin depth
f	frequency
FEM	Frequency-domain electromagnetics
σ_a	apparent conductivity
H_s	secondary magnetic field
H_p	primary magnetic field
μ_o	permeability of free space
s, r	distance
EM	electromagnetic
VES	vertical electrical sounding
$\emptyset$	the porosity
S	fraction of pores containing water
ρ_w	resistivity of water
a, m, n	empirically constants
A, B	current electrodes
M, N	potential electrodes
K	geometric factor
V	potential difference
I	current
R	resistance

Acknowledgements

All the glory and honour goes to the Almighty God, without whose faithfulness the beginning and completion of this project work wouldn't have been possible.

My profound appreciations go to my main supervisor, Prof. Aboagye Menyeh who took the trouble and the pain of reading through my work, correcting me and supporting me in the course of writing this thesis. I owe this thesis also to my second supervisor, Mr. R. M. Noye who worked tirelessly in helping me secure this research topic to work on.

To the Head of Department, Prof. S. K. Danuor, I will like to say a big thank you for his assistance in acquisition of the data. Am also grateful for the lives of all the other lecturers of the Physics Department, Mr. D.D Wemegah, Dr. Kwasi Preko, Mr. A. AAnning, Dr. Amekudzi, Mr. M. K. E. Donkor and Mr. Vandycke Asare for the knowledge they imparted into me during my first year of study and even at the time when this project work was ongoing.

I am also grateful to the management and staff of Water Research Institute (WRI) of the Council for Scientific and Industrial Research (C.S.I.R) especially, Dr. Agyekum, Mr. Evans Manu and Mr. Collins Okrah for granting me permission to use their EM and VES data to prepare the thesis. I want to express my gratitude to them for bringing my interest and attention to this research.

I am indebted to my parents, Mr. and Mrs. Somiah and my siblings for their unflinching support both physically and spiritually. My gratitude goes to my pastor and the entire members of the Spoken Word Church for their prayers and words of encouragement.

I would like to finally appreciate my postgraduate colleagues and all my friends who helped in diverse ways to make this research a success.

God richly bless you all.

CHAPTER 1

INTRODUCTION

1.0 Background of the Study

Groundwater has undoubtedly gained increased recognition in many parts of the world today. Water is said to be a requisite resource for livelihood and therefore, its importance cannot be overemphasized. It is however disturbing if this all-important resource is becoming more and more scarce. Worldwide, 1.1 billion people do not have access to safe water (WHO/UNICEF, 2000). The scarcity of water is more intense in the developing countries where statistics show that 67% of the rural population have no access to safe water supply (Rosen and Vincent, 1999). This is so because people in the rural areas tend to depend mostly on surface water (from lakes, streams, ponds and rivers) for sustenance. Surface water bodies however, are not reliable in that they are associated with high evaporation rates usually in high temperate environments and often susceptible to pollution and waterborne diseases. In order to supply water from these sources particularly for domestic purposes, one requires treatment especially in small settlement communities. In deprived communities where people cannot afford such treatment, they use these waters as they exist resulting in outbreaks of water borne diseases, such as guinea worm infection, bilharzia, etc.

Groundwater which is found to exist below the surface in the soil pores, fractures within rocks, fissures and other weak geological features or zones is comparatively protected from pollution and evaporation and can be useful for both domestic and industrial purposes. It comes along with another added advantage over surface waters regarding the

ease with which the resource can be tapped from close point of need. These benefits have made groundwater more reliable for domestic, agricultural and industrial purposes.

Since groundwater cannot be easily located, a variety of scientific techniques are needed to provide information concerning its occurrence and location. The use of geophysics for example provides the tool for both groundwater resource mapping and for water quality evaluations. Many of these geophysical techniques have been applied to groundwater with some showing more success than others. The methods include gravity, magnetics, seismics, electrical and electromagnetic methods (Reynolds, 1997). Potential field methods like gravity and magnetics have been successfully used to map regional aquifers and large scale basin features. Seismic methods on the other hand have been used to delineate bedrock aquifers and fractured rock systems. The methods that have proved particularly effective to groundwater studies are the electrical and electromagnetic. This is because many of the geological formation properties that are critical to hydrogeology such as porosity and permeability of rocks can be correlated with electrical conductivity signatures. Many of these geophysical techniques have subsequently been used for groundwater characterization but once again, the greatest success has been shown with the electrical and electromagnetic methods (Eke and Igboekwe, 2011). This is why this project seeks to use these two methods in the search for groundwater potential zones. It should be noted however, that in this kind of study (groundwater resource mapping), the groundwater itself is not the target of the geophysics but instead the subsurface geological structure in which the water exists, such as fractures, joints, etc (Araffa, 2012).

A lot of geophysical work has been done across the length and breadth of the world in the field of groundwater exploration. These methods are regularly used to solve a wide variety of groundwater problems.

In one such work, Odoh et al. (2012) carried out groundwater prospecting in fractured shale aquifer using an integrated suite of geophysical methods at Kpiri Kpiri in the Ebonyi State of the South Eastern part of Nigeria. The integrated methods included electromagnetic profiling, vertical electrical soundings and azimuthal resistivity surveys. The results of the integrated interpretation of the electromagnetic and resistivity correlated with the geology of the study area. The deeply weathered/fractured zone which ranged from 6 – 23 mmhos/m between 180 and 300 m provided a good correlation for siting boreholes.

Also, Nejad et al. (2011) carried out a geoelectrical survey using the electrical resistivity method in the Curin basin, Iran to investigate the sub-surface layering and to evaluate the aquifer characteristics. The vertical electrical soundings conducted applying the Schlumberger array revealed four geoelectric layers; a superficial layer, dry alluvium layer, third layer corresponding to the aquifer and the bedrock layer. From the quantitative interpretation of the VES curves, the boundary aquifer was determined. The best parts chosen for drilling were the southeastern and northwestern parts of the aquifer.

Gilson et al. (2000) completed a number of projects in which electrical resistivity tomography (ERT) was used to locate potential groundwater bearing zones by identifying buried valleys, and coarser grained deposits within these valleys. This is because, a significant electrical contrast existed between the marine bedrock sediments and

Quaternary derived siliclastic fluvial deposits. Subsequent drilling and testing was done to prove the ERT method.

In many parts of Ghana, groundwater exploration is ongoing. Several geophysical investigations are being done in the quest of locating this all important resource.

Bayor (2004) applied the electromagnetic and electrical resistivity methods in groundwater exploration at the Tolon-Kumbugu district of the Northern Region of Ghana. The study aimed at locating good yielding wells to be fitted with hand pumps to supply the communities with potable water. Results showed that, major aquifers were confined to hard, fractured sandstone formation and no water was found in the weathered zone or fresh rock aquifers.

Bosu (2004) performed groundwater exploration in the granitic basement in the Assin district of the Central Region using the electrical resistivity method. He used this method to delineate regions of fractured zones, faults, and thickness of the top layer, conductivity and impermeable strata which gave clues to the presence of groundwater. Profiling and sounding were both done using the electrical resistivity technique based on the Schlumberger array. Drilling was done to confirm deductions from the interpretation of the geophysical data sets.

This project therefore seeks to contribute to the efforts made by the department of Physics, KNUST and the Ghana government and other non-governmental organisations (NGO's) in the pursuit of helping reduce water crisis in the country. Similarly, the electromagnetic method as well as the vertical electrical soundings will be used in profiling and studying the variations of resistivity with depth respectively in order to locate groundwater bearing zones.

The thesis work comprises five chapters, each of which addresses a principal heading. The first chapter gives an introduction to the subject matter, outlining the background of the research, the problem statement, objectives of the research, scope of the study and the significance of the research.

Chapter two presents a review of literature outlining the main fundamental theory behind the electromagnetic and electrical resistivity methods. Included in this is the general overview of the geological settings of the area, reviewing both the regional and local geology as well as the hydrogeology of the area.

Chapter three discusses the methodology used in conducting the thesis work. The chapter also addresses processing steps employed in the processing of the datasets. The softwares available to enhance the datasets will be also introduced in this chapter.

Chapter four analyses the various graphs obtained from the electromagnetic and electrical resistivity datasets. The chapter will also give interpretations to the deduced graphs providing rankings of sites that are most suitable for the location of boreholes.

The thesis ends with conclusions and recommendations for future works in Chapter five.

1.1 Problem Statement

According to Ghana Statistical Service Computation in 2010, the population of the Sunyani municipality had increased from a previous 101,145 in 2000 to an estimated 147,301 people. The growth rate of 3.8 percent over the period compared to the national growth rate of 2.7 percent indicates a high growth rate. With this increasing population growth it is an undeniable fact that there will be a corresponding pressure on the water resources in the district. The over-reliance of the indigenes on the little water resource

results in acute water shortages. Earlier this year (2013), there were reports on one such shortage in the area where people had to walk several kilometres to fetch water from the Tano River and other nearby streams. However, this river is polluted by activities of the local farmers especially during the dry season for fermentation of cassava, washing of watermelon, clothes, passing of feaces resulting in unhygienic nature making it unsafe for drinking and domestic use. The consequence is that people relying on such water bodies for their livelihood are exposed to water-related diseases thereby contributing negatively to economic activities as well as reducing their life expectancy.

Another important development in the sphere of water resources in the study area is that there is low yield of some of the boreholes that the District has provided. This occurs because little or no geophysical work was done prior to the drilling of these boreholes. This has led to wastage of financial resources. There is therefore the need to carry out geophysical investigations in order to identify suitable sites for the drilling of boreholes to provide potable water for the community.

1.2 Objectives of the study

This project aims at carrying out geophysical investigations in the area of study using electromagnetic methods. These methods are based on the use of Geonics EM 34-3 equipment and the electrical resistivity methods using ABEM SAS 3000 terrameter equipment to determine groundwater potential zones in the Sunyani Municipal District of the Brong Ahafo Region of Ghana. The purpose is to provide boreholes to supply potable water to these deprived communities.

1.3 Scope of the Study

This thesis focuses on locating groundwater potential zones in the Sunyani Municipality which is one of the twenty-two districts of the Brong Ahafo Region of Ghana. Groundwater exploration will be carried out in selected communities in the district. A total of thirteen communities will be considered in this study. Integrated geophysical tools, specifically the electromagnetic and electrical resistivity methods will be used for the survey. The electromagnetic method will be used as a reconnaissance survey tool. Profiling will be done with the Geonics EM 34-3 equipment. On the other hand, the resistivity method will be used to measure variations in the electrical resistivity of the ground with depth. Vertical electrical soundings (VES) based on the Schlumberger array system will be conducted at points indicated from the results of the electromagnetic profiling.

1.4 Significance of the Study

Due to the pressing need for potable water for agricultural, domestic and industrial purposes in the rural communities, any research aimed at the provision of this resource is worth undertaking. The use of geophysical methods in the groundwater investigations will help reduce if not alleviate completely, the problem of borehole failures in the area. Hence boreholes drilled based on these geophysical investigations will yield utmost results for water yield thereby inhibiting the spread of water related diseases, promoting socio-economic activities thereby contributing to poverty alleviation and further increasing the life expectancy of the natives.

CHAPTER 2

LITERATURE REVIEW

2.1 Groundwater

Groundwater is defined as a resource that occurs in the subsurface within sediments, rocks, desertic sand, ice and snow. Kresic (2007) defined groundwater to be water found below the water table and usually fills all void spaces in the saturated zone of rocks. It is the most widely distributed resource of the Earth and forms an invisible component of the natural water resources. Groundwater occurrence within the Earth is influenced by the lithology of geological materials, structure of the regional geology, recharge sources availability and geomorphology of landforms (Hiscock, 2005). Groundwater plays a major role in the global system and water movement known as the hydrologic cycle as shown in Figure 2.1. The cycle begins with precipitation from the atmosphere down to the ground surface as runoff to water bodies, where some penetrate the groundwater. Next, the infiltrated water recovers to the atmosphere again through evaporation and transpiration from water bodies and plants (Hiscock, 2005).

Subsurface water can be grouped into two different zones namely; the saturated and unsaturated zones. In the saturated zones, water is found to fill entirely all the voids in the soil. Groundwater movement through this zone takes place in response to the force of gravity and pressure. The gravitational force acts to pull water downwards and pressure causes water to move upwards. Contrary to the saturated zone, voids are filled with a mixture of air, moisture and water in the unsaturated zones. As a result, the unsaturated zone is divided into three different classes which are; the soil moisture, intermediate and capillary layers. The top-most layer is the soil moisture layer which varies in thickness

and is necessary for plant growth. Movement of water in this layer is either upwards or downwards depending on gravity. The intermediate layer lies below the top-most layer (soil moisture layer). This is where water is held by intermolecular forces against gravitational pull. The capillary layer, as the name suggests is where water is held by capillary forces against gravitational pull. This is the bottommost layer found above the water table in the unsaturated zone (Sen, 1995).

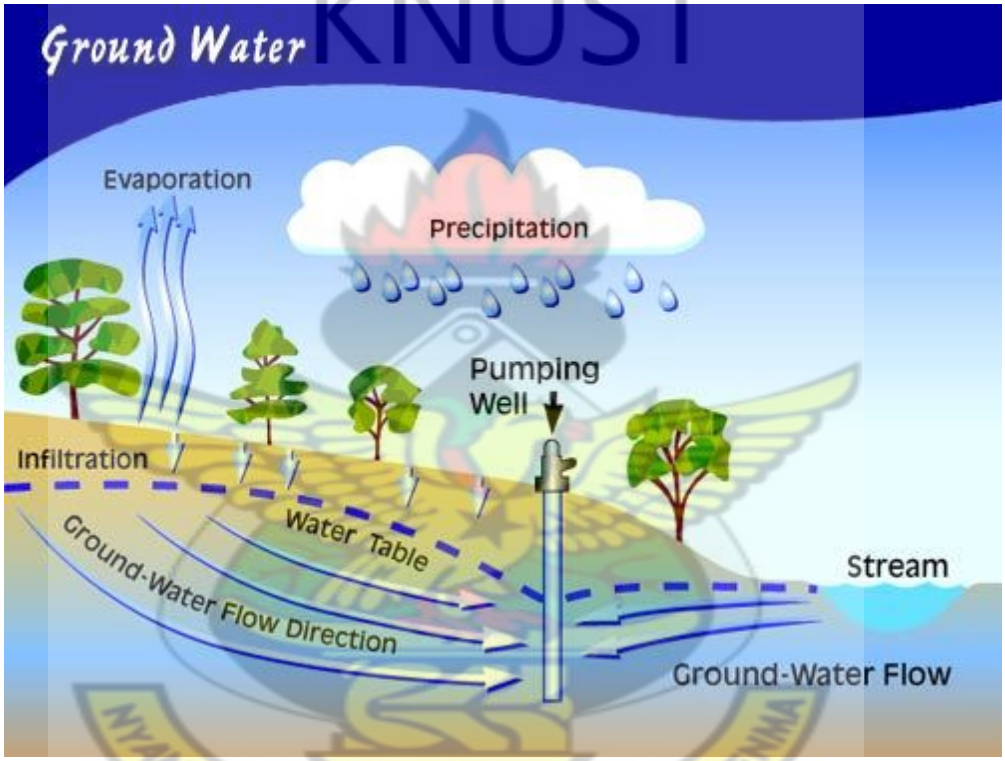

Fig. 2.1 The Hydrologic Cycle Source: (Badrinarayanan, 2002)

2.1.1 Water Table

Water table can be simply defined as the saturated level of groundwater. It is said to be the surface below which all openings in the rock are filled with water. Groundwater usually occurs below the water table. Water table is found everywhere below the Earth's surface. It is always present in desert regions but seldomly intersects the surface but in

humid regions, the water table is able to reach the surface at streams and lakes as shown in Figure 2.1 above. Water table either rises or falls and normally follows the topography of the surface. As a result, the water table is not flat but has peaks and valleys. The depth to the water table varies depending on the season, location and the long-term climatic variations (Freeze and Cherry, 1979). For example, the depth to the water table usually increases during the dry season and decreases in the wet seasons.

.

2.1.2 Aquifer

In simple terms, an aquifer is a rock formation which stores groundwater. It could also be defined as a geological formation which has the capacity to store and provide significant amounts of water. The water yielding capacity of an aquifer to a large extent depends on its constituent materials. Two properties should characterize an aquifer namely; permeability and porosity since the water is held in spaces between the rock formation (Driscoll, 1986). For example, bedrock aquifers mostly yield significant amounts of water if there are cracks in the rock. Rock types that make up good aquifers include; unconsolidated sands, sandstones, gravels, fractured limestones, columnar basalts and conglomerates since they are both permeable and porous. Poor aquifers on the other hand constitute rock types such as mudstone and granites due to their low porosity. Low permeable beds along aquifers are aquitards and solid, impermeable areas underlying or overlying aquifers are aquicludes. Even though aquifers are usually underground layers, there are areas where they are exposed on the surface of the earth. These are areas where aquifers are normally recharged. In the search for groundwater, it is necessary that wells drilled into the ground penetrate the aquifer. If this condition is met, the well becomes

unproductive. One should also be careful in drilling so that the rate at which water is pumped does not exceed the rate at which it is replenished else the water table will be lowered and the well may go dry. There are three types of aquifers which are confined, unconfined and perched aquifers (Freeze and Cherry, 1979).

2.1.2.1 Confined Aquifer

This is an aquifer overlain by low permeability, confining layers mostly made of clay which restrict the movement of groundwater. The confining layers mostly provide protection from surface pollution since they remain deeper down the ground than the unconfined aquifers. Groundwater beneath these confining layers has higher pressures than that of the atmosphere and whenever perforated with a well, the level of water rises over the top of the aquifer (Freeze and Cherry, 1979).

2.1.2.2 Unconfined Aquifer

Unlike the confined aquifer, this has no confining layers between the water level and the ground level. Therefore, groundwater is often in direct contact with the atmosphere through the voids of the overlying rock or soil. Groundwater refill in this aquifer is by direct infiltration by rain or stream water through the overlying rock or soil (Freeze and Cherry, 1979).

2.1.2.3 Perched Aquifer

This is similar to the confined aquifer in that, it has confining layers but these layers lie underneath the groundwater but above the main water table. This type of aquifer occurs where groundwater lies above unsaturated rock formations as a result of a discontinuous impermeable layer (Freeze and Cherry, 1979).

.

2.2 Concepts of Geophysical Techniques Used

Geophysics is basically the application of the principles of Physics to the study of the Earth (Reynolds, 1997). There are two main aspects of geophysics namely; pure and applied geophysics. Pure geophysics deals with the study of the substantial parts of the planet whilst applied geophysics involves investigating the Earth's interior by taking measurements either at or near the surface of the Earth. The latter is of economic benefit since it aims at exploiting resources for economic use. Many geophysical techniques are employed in geophysical exploration ranging from active to passive methods. This classification depends on their source of energy. Active methods are artificial methods whereas passive methods are natural field methods (Reynolds, 1997).

In active methods, artificially generated signals (electrical or electromagnetic fields) are transmitted into the Earth and the response of the Earth to these signals is measured. Examples of active methods include: electrical resistivity, electromagnetic, seismic, induced polarization and ground-probing radar methods (Reynolds, 1997).

Passive methods on the contrary rely on naturally occurring fields and hence, measure the response of the Earth to these signals. Passive methods can normally give information on the properties of the Earth to greater depths and are comparatively easier to carry out than

active methods. Examples of these methods include; magnetic, gravity, telluric, self-potential and radiometric decay methods (Reynolds, 1997).

There are so many geophysical techniques and a wide range of equipment used in geophysical prospecting. Each of these respond to a particular physical property and the kind of property that a method responds to evidently determines its range of applications. For example, the magnetic method is more appropriate for locating buried magnetic ore bodies due to their high magnetic susceptibility. Similarly, the seismic and electrical methods are preferred for the location of buried water table since they are able to differentiate saturated rock from dry rock by virtue of its higher seismic velocity or higher electrical conductivity (Kearey and Brooks, 2002).

Even though geophysical methods have potential ambiguities of interpretation, they offer a comparatively rapid and cost effective measure of inferring really distributed information on subsurface geology. During subsurface resource exploration, these methods are able to detect and delineate local features of potential interest which otherwise couldn't have been detected by any realistic drilling operation (Kearey and Brooks, 2002). Some of the geophysical techniques require sophisticated equipment or complex analysis and consequently are inappropriate for use in rural water supply programmes. The two most appropriate methods as far as rural water supply is concerned are the electrical resistivity and electromagnetic (MacDonald et al., 2005). The concepts and operation of these methods are described below.

2.2.1 The Electromagnetic Method

The electromagnetic method otherwise referred to as the EM method measures the response of induced electromagnetic fields into the ground. The electromagnetic fields comprise alternating electric intensity and magnetic force. Contrary to other conventional resistivity methods, this method does not need ground contact and hence problems related to direct electrical coupling are removed. Therefore, this method provides faster and easier data acquisition and is mostly used as reconnaissance tools. It is often employed in detecting anomalies for further investigation. When a conductive body buried in the subsurface responds to incoming primary electromagnetic field from a transmitter, it produces eddy currents on the conductor which in turn produces a secondary electromagnetic field. The resultant of the primary and secondary fields is detected by the receiver (Oghenekohwo, 2008). All anomalous bodies which have high electrical conductivity produce strong secondary electromagnetic fields. Some ore bodies which contain minerals that are themselves insulators are likely to produce secondary fields if considerable quantities of an accessory mineral with a high conductivity are present (Kearey and Brooks, 2002). In practice, current is induced into the subsurface by a transmitting coil and a receiving coil is positioned a short distance away to measure the induced earth current. The magnitude of the current induced is dependent on the type of geologic material underneath the transmitter and the receiver. The measured quantity is the apparent conductivity with units millimhos/meter (m mhos/m). There are several divisions of the electromagnetic method namely; frequency domain electromagnetic method (FDEM), time-domain electromagnetic method (TDEM), airborne electromagnetic survey, very low frequency (VLF), telluric and magneto-telluric

methods. Among these methods, the frequency domain electromagnetic method (FDEM) and the time-domain electromagnetic method (TDEM) remain the popularly used methods (Oghenekohwo, 2008). Frequency-domain instruments rely on either one or more frequencies for measurements whilst the time-domain electromagnetic equipment are time-dependent; thus they take measurements as a function of time. Also, electromagnetic methods could either be active; which makes use of artificial transmitters either in near-field (as in ground conductivity meters) or in the far-field (as in VLF mapping where remote high-powered military transmitters are used) or passive, which makes use of natural ground signals (for example in magnetotellurics) (Reynolds, 1997).

A few advantages of this method relative to other electrical methods include:

- Since electromagnetic methods are based on induction, they do not require direct contact with the ground hence, electrodes are not required.
- It is faster to carry out surveys over larger areas.
- The method can be used in the air, sea and on land.

In spite of the versatility and efficiency of this survey technique, it suffers a few limitations which include:

- More sophisticated quantitative interpretation of electromagnetic anomalies.
- The depth of investigation is fixed depending on the frequency used and the transmitter to receiver separation.

2.2.1.1 Principles of the Electromagnetic (EM) Method

Electromagnetic methods generally use the response of the ground to the propagation of incident alternating electromagnetic waves which are made up of two orthogonal vector

components, an electric intensity (E) and a magnetizing force (H), in a plane perpendicular to the direction of travel as shown in Figure 2.2. Electromagnetic fields are usually generated by passing electric current through either a small coil (which consists of many turns of wire) or a large loop of wire. Frequencies of electromagnetic radiation range from atmospheric micropulsations which have frequencies less than 10 Hz, through to the radar bands of frequencies between 10^8 and 10^{11} Hz up to X-rays and gamma-rays of frequencies far beyond 10^{16} Hz. Of all these frequency ranges, the visible band of frequency $\approx 10^{15}$ Hz is of vital importance (Reynolds, 1997). For most geophysical applications, the propagation of the primary wave and its associated wave attenuation could be ignored. This is because frequencies of the primary alternating field are normally below a few thousand hertz and the wavelengths usually of the order of 10 – 100 km while typically, source – receiver separation is much less than ≈ 4 – 100 m. On the whole, these primary electromagnetic fields which are transmitted above and below the ground are generated by the transmitter coil (Reynolds, 1997).

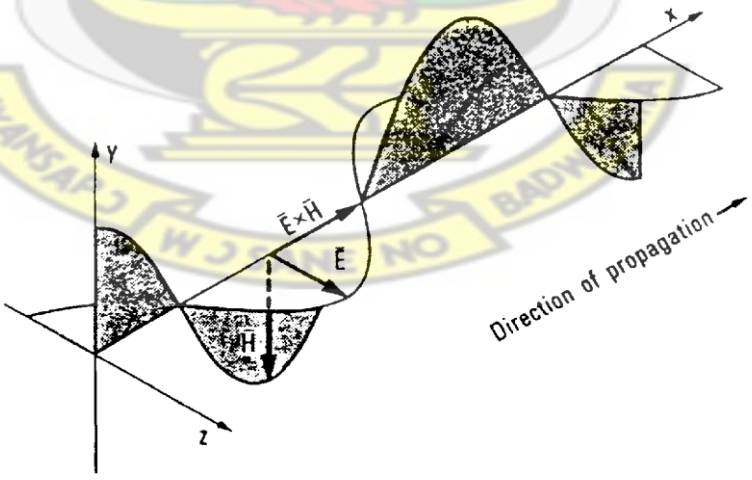

Fig. 2.2 Basic elements of an electromagnetic wave, showing the two principal electric (E) and magnetic (H) components which are orthogonal Source: (Beck, 1981)

Whenever EM radiations are transmitted through the sub-surface, they are modified slightly as compared to that which travels through air. When it meets a conductive medium, the magnetic component of the incident EM wave induces eddy currents within the conductor. The eddy currents in turn generate secondary EM field which is detected by a receiver as shown in Figure 2.3. Since the receiver is also able to detect the primary field which is transmitted through the air, the total response of the receiver is the resultant effect of both the primary and the secondary fields. As a result, the measured response differs from the unmodulated primary field in both phase and amplitude. The extent to which these components vary brings to bear important information about the size, geometry and electrical properties of any buried conductor (Reynolds, 1997).

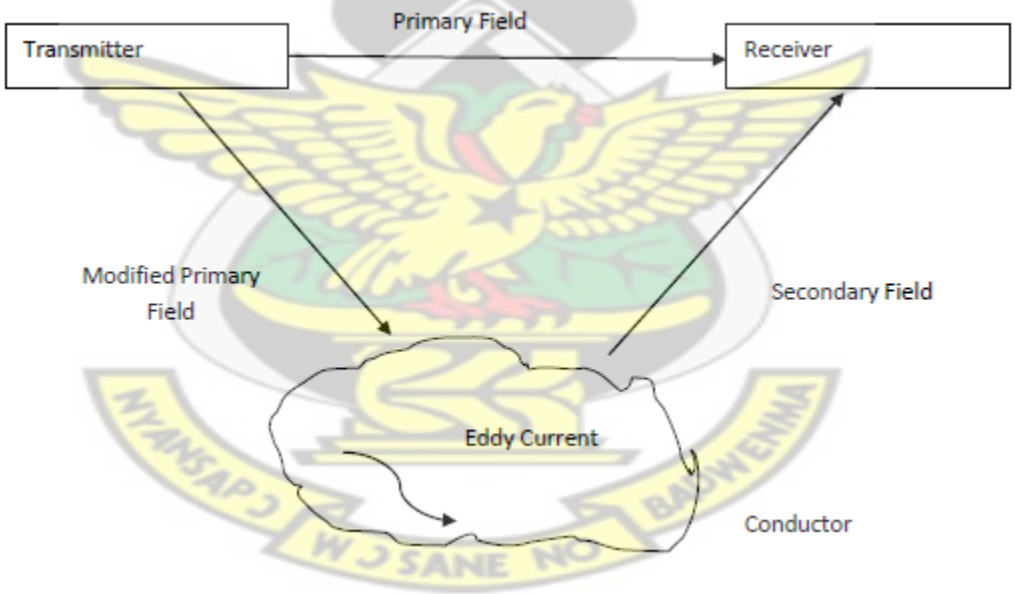

Fig. 2.3 Generalized schematic of the EM surveying method. Source: (Kearey and Brooks, 2002)

2.2.1.2 Fundamental Field Equations

In order to fully understand the interpretational techniques of electrical exploration methods, one has to first know the tools of electromagnetic theory. All electromagnetic phenomena are governed by the empirical Maxwell's equations (Ward and Hohmann, 1987). The wave equation is derived directly from Maxwell's equation. Maxwell's equation is expressed both in the time and frequency domain.

Maxwell's equation in the time domain

According to Ward and Hohmann (1987), an electromagnetic field may be defined as the domain of the four vector functions; E, B, D, H where:

E is the electric field intensity in (V/m)

B is the magnetic induction in (Wb/m^2)

D is the dielectric displacement in C/m^2 and

H is the magnetic field intensity in A/m

Experimental evidence reveals that all electromagnetic phenomena obey Maxwell's equations described in the time domain as

$$\nabla \times E + \frac{\partial B}{\partial t} = 0, \quad \ldots\ldots 2.1$$

$$\nabla \times H - \frac{\partial D}{\partial t} = J, \quad \ldots\ldots 2.2$$

$$\nabla . B = 0, \quad \ldots\ldots 2.3$$

$$\nabla . D = \rho, \quad \ldots\ldots 2.4$$

in which J is the electric current density in A/m^2 and ρ is electric charge density in C/m^2.

For homogenous earth materials of conductivity 10^{-4} S/m or greater, free charge ρ_e, dissipates in less than 10^{-6} s (Straton, 1941). Hence, in geophysical exploration which

involves frequencies less than 10^5 Hz, $\partial\rho_e/\partial t \sim 0$, and by taking the divergence of equation 2.2 we get

$$\nabla . J = 0, \ldots\ldots\ldots\ldots\ldots\ldots\ldots\ldots\ldots\ldots\ldots\ldots\ldots\ldots\ldots\ldots\ldots\ldots\ldots\ldots\ldots\ldots 2.5$$

Equation 2.5 does not apply to inhomogeneous regions; at the interface between two different media, a surface charge accumulates as described subsequently. From equations (2.1) through to (2.4), which are the conventional forms of Maxwell's equations are based on the experiments of Faraday and Ampere. Therefore, they are empirical yet describe most macroscopic electromagnetic phenomena. They could be made symmetric as subsequently shown, by adding a magnetic current source term on the right hand-side of equation (2.1) and the time derivative of a magnetic charge source on the right-hand side of equation (2.4). Significant facility is afforded the solution of certain boundary-value problems by such a generalization.

The constitutive relations

Equations (2.1) through to (2.4) are uncoupled differential equations of the five vector equations E, B, H, D and J. These equations are however coupled through the frequency-domain constitutive relations

$$D = \varepsilon\,(\omega, E, r, t, T, P, \ldots).E, \ldots\ldots\ldots\ldots\ldots\ldots\ldots\ldots\ldots\ldots (2.6)$$

$$B = \mu\,(\omega, H, r, t, T, P, \ldots).H, \ldots\ldots\ldots\ldots\ldots\ldots\ldots\ldots\ldots\ldots (2.7)$$

$$J = \sigma\,(\omega, E, r, t, T, P, \ldots).E, \ldots\ldots\ldots\ldots\ldots\ldots\ldots\ldots\ldots\ldots (2.8)$$

Where the tensors, ε, μ, σ describe the dielectric permittivity, the magnetic permeability and the electric conductivity respectively as functions of angular frequency ω, electric field strength E or magnetic induction B, position r, time t, temperature T, and pressure P. Each one of these three tensors is complex in the general case, allowing the phases of D

and E, of H and B, and of J and E to differ. Certain assumptions are made in most elementary electromagnetic earth problems in order to simplify analysis. These include;

1. all media are linear, isotropic, homogenous and have electrical properties which are not dependent on time, temperature or pressure and
2. the magnetic permeability μ is taken to be that of free space, i.e $\mu = \mu_o$.

However, a few exceptions are made to these assumptions in some applications.

Maxwell's equation in the frequency domain

After utilizing a one-dimensional Fourier transformation and the constitutive relations in equations (2.6), (2.7) and (2.8) above, we get Maxwell's equation in the frequency domain as:

$$\nabla \times E + i\mu\omega H = 0, \ldots\ldots\ldots\ldots\ldots\ldots\ldots\ldots\ldots\ldots\ldots\ldots (2.9)$$

$$\nabla \times H - (\sigma + i\varepsilon\omega)E = 0, \ldots\ldots\ldots\ldots\ldots\ldots\ldots\ldots\ldots\ldots\ldots\ldots (2.10)$$

When the impedivity $\acute{z} = i\mu\omega$ and the admittivity $\hat{y} = \sigma + i\varepsilon\omega$ (Harrington, 1961), equations (2.9) and (2.10) become:

$$\nabla \times E + \acute{z}H = 0, \ldots\ldots\ldots\ldots\ldots\ldots\ldots\ldots\ldots\ldots\ldots\ldots (2.11)$$

and

$$\nabla \times H - \hat{y}E = 0, \ldots\ldots\ldots\ldots\ldots\ldots\ldots\ldots\ldots\ldots\ldots\ldots (2.12)$$

The wave equations

The wave equations for the electric and magnetic fields in the time domain are:

$$\nabla^2 E - \mu\varepsilon\frac{\partial^2 E}{\partial t^2} - \mu\sigma\frac{\partial E}{\partial t} = 0, \ldots\ldots\ldots\ldots\ldots\ldots\ldots\ldots (2.13)$$

and

$$\nabla^2 H - \mu\varepsilon\frac{\partial^2 H}{\partial t^2} - \mu\sigma\frac{\partial H}{\partial t} = 0, \ldots\ldots\ldots\ldots\ldots\ldots\ldots\ldots (2.14)$$

Similarly, in the frequency domain, the wave equations are:

$$\nabla^2 E + (\mu\varepsilon\omega^2 - i\mu\sigma\omega)E = 0, \dots \dots \dots \dots \dots \dots \dots \dots \dots \dots \dots \dots (2.15)$$

and

$$\nabla^2 H + (\mu\varepsilon\omega^2 - i\mu\sigma\omega)H = 0, \dots \dots \dots \dots \dots \dots \dots \dots \dots \dots \dots \dots (2.16)$$

2.2.1.3 Depth of Penetration of Electromagnetic Radiation

In any electromagnetic survey, a consideration of the depth of penetration of the electromagnetic radiation and the resolution as a function of depth is very paramount (Reynolds, 1997). Electromagnetic waves travel almost indefinitely in isotropic resistive medium but have limited penetration depth in the real world where surface conductivities are substantial. The depth of penetration is mostly a function of the conductivity and frequency of the media through which electromagnetic radiation is transmitted. In electromagnetic exploration, effects of attenuation are infinitesimal since frequencies used are usually less than 5 kHz but signal losses take place by diffusion. Depth of penetration, otherwise known as skin depth is defined as the depth at which the amplitude of a plane wave has decreased to 1/e or 37% relative to its initial amplitude A_o (Sheriff, 1991).

Mathematically, the amplitude of electromagnetic radiation as a function of depth (z) relative to its original amplitude A_o is:

$$A_z = A_o e^{-1} \dots\dots\dots\dots\dots\dots \quad 2.17$$

The mathematical expression of skin depth is given by:

$$\delta = \sqrt{\frac{2}{\omega\sigma\mu}} = 503\sqrt{(f\sigma)} \dots\dots\dots\dots\dots\dots \quad 2.18$$

where $\omega = 2\pi f$, f = frequency in Hz, σ = conductivity in S/m and μ = magnetic permeability (usually ≈ 1)

A realistic estimate of the depth to which a conductor would give rise to a detectable EM anomaly is $\approx \delta/5$ (Reynolds, 1997).

For an equipment of known frequency, the unknown is the vertical variation of conductivity with depth. Manufacturers of different equipment systems usually quote effective skin depths for their equipment. An example is the Geonics Ltd who cite the skin depths of their FEM systems as a function of the inter-coil separation.

2.2.1.4 Electrical Conduction in Geological Materials

Electrical conductivity of earth materials is influenced by the metal content (sulfides) in the rock, porosity, clay content, permeability, and degree of pore saturation (Wightman et. al, 2003). The physical quantity measured in electromagnetic surveys is conductivity, which is the inverse of resistivity. Synonymous to electrical resistivity surveys where apparent resistivity is measured, apparent conductivity is also measured in electromagnetic surveys. Mathematically, this apparent conductivity in geological materials (soil and rock types) is given by:

$$\sigma_a = \frac{4}{\omega s^2 \mu_o}\left(\frac{H_s}{H_p}\right) \quad \text{..... 2.19}$$

σ_a = apparent conductivity (mhos/m)

H_s = secondary magnetic field at the receiver coil

H_p = primary magnetic field at the receiver coil

$\omega = 2\pi f$ where f is the frequency of the electromagnetic wave (in Hz)

μ_o = permeability of free space

s = distance between the transmitter and receiver coils (m)

2.2.1.5 Applications of Electromagnetic Method

The electromagnetic method, among other geophysical methods is considered to have the widest range of applications. The range of applications is independent of the instrument type being used. The main use of EM surveys is in the exploration of metalliferous mineral deposits, which differ significantly in their electrical properties from their host rocks. Regardless of the limited depth of penetration, airborne methods are often used in reconnaissance surveys, with aeromagnetic surveys frequently run in conjunction. Also, EM methods are used in follow-up ground surveys which give more accurate information on the target area. On a small scale, EM methods could be used in geotechnical and archaeological surveys to locate buried objects such as pipes, barrels, tanks and walls (Kearey and Brooks, 2002). Other common applications include: groundwater surveys, landfill surveys, geothermal resource investigation, contaminated land mapping, geological mapping, contaminant plumes mapping, natural and artificial cavities detection and location of geological faults.

2.2.2 Electrical Resistivity Method

The electrical resistivity method is by far the longest established geophysical tool for siting boreholes and wells in Africa. This technique involves two main survey methods which include: profiling and depth sounding. Unlike the depth sounding method, the resistivity profiling method is a comparatively slow process for detecting lateral

variations and has been overtaken by electromagnetic conductivity traversing. Even though there are methods available which combine both profiling and depth sounding, such surveys are complex and demand specialists equipment and interpretation. Hence, such methods are rendered inappropriate for small rural water supply projects (MacDonald et. al., 2002).

However, in most parts of Africa, the vertical electrical depth sounding (VES) remains the most popularly used method. This produces a one-dimensional profile of the resistivity beneath the midpoint of the survey. This technique is used to examine the vertical change in resistivity. This method involves progressively increasing the electrode spacings between measurements while the centre of the whole array is kept constant. As the electrode spacing is increased, the current permeates to greater depths (McDowell et. al., 2002). Therefore, a plot of apparent resistivity against electrode spacing produces an image of the variation of resistivity with depth. The data from such surveys could also be interpreted qualitatively to give resistivity and thickness values of subsurface layers.

Electrical resistivity methods measure the bulk resistivity of the subsurface as in electromagnetic methods. The only difference is in the way electric currents are transmitted through the earth. For electrical resistivity surveys, current is transmitted through surface electrodes whilst in electromagnetic methods, current is induced by utilizing time-varying magnetic fields.

The main advantage offered by the electrical resistivity technique is that, quantitative interpretation is possible using computer software (MacDonald et. al., 2002). Accurate estimates of depth, thickness and resistivity of subsurface layers could be deduced from the resulting models. For groundwater surveys for example, the electrical resistivities of

the subsurface layers could be used to estimate the resistivities of the saturating fluid which has a relation with the total concentration of dissolved solids in the fluid. Another advantage of using this method is its non-destructive nature.

Nevertheless, a few limitations prevail in using the electrical resistivity method. This method is not conducive for use in industrial areas which produce radiations of electrical noise since they reduce the accuracy of the measurements of the resistivity meter. Measurements are also affected by power lines and grounded metallic structures such as metal fences, pipelines and railroad tracks. Any setback has to do with the labour intensive nature of this survey method. Due to the labour involved in physically planting electrodes prior to each measurement, the resistivity survey is usually restricted to relatively small-scale investigations. Hence, this method is not commonly used for reconnaissance exploration (Kearey and Brooks, 2002).

2.2.2.1 Electrical Resistivities of Geological Materials

The ground resistivity is related to various geological parameters such as the mineral and fluid content, porosity and degree of water saturation in the rock (Loke, 1999). Generally, most rock resistivities are roughly equal to that of pore fluids divided by the fractional porosity. Archie's law provides a closer approximation in most cases which is given by:

$$\rho_r = a\emptyset^{-m}S^{-n}\rho_w, \ldots\ldots\ldots\ldots\ldots\ldots\ldots\ldots\ldots\ldots (2.20)$$

where$\emptyset$ is the porosity, S is the fraction of pores containing water and ρ_w is the resistivity of water. a, m, and n are empirically determined constants i.e. ($0.5 < a < 2.5$, $1.3 < m < 2.5$ and $n \sim 2$). Resistivity values of common geological materials are given in Table 2.1 below.

Table 2.1 Resistivity values for some common geological formations (based on Telford et. al. 1990).

Material	Nominal resistivity (Ω-m)
Quartz	3×10^2 - 10^6
Granite	3×10^2 - 10^6
Granite (weathered)	30 – 500
Consolidated shale	20 - 2×10^3
Sandstones	200 – 5000
Sandstone (weathered)	50 – 200
Clays	1 - 10^2
Boulder clay	15 – 35
Clay (very dry)	50 – 150
Gravel (dry)	1400
Gravel (saturated)	100
Lateritic soil	120 – 750
Dry sandy soil	80 – 1050
Sand clay/clayed sand	30 – 215
Sand and gravel (saturated)	30 – 225
Mudstone	20 – 120
Silstone	20 – 150

2.2.2.2 Basic Principles of the Electrical Resistivity method

Ground resistivity is measured by passing an electric current through the ground using two electrodes (C_1 and C_2) and measuring the resultant potential using two or more potential electrodes (P_1 and P_2). Figure 2.4 illustrates this principle of operation. The depth of investigation is often given as a function of the electrode spacing. That is to say that the greater the spacing between the outer current electrodes, the deeper the electrical currents will flow in the Earth, thus the greater the depth of exploration. Therefore, the depth of investigation is normally 20% to 40% of the current electrode spacing depending on the structure of the Earth resistivity.

Ohms law is generally used to calculate the resistance which is then multiplied by a geometric factor (usually called a K factor) to calculate resistivity MacDonald et. al., (2002) as shown in equations (2.21) through to (2.23) below.

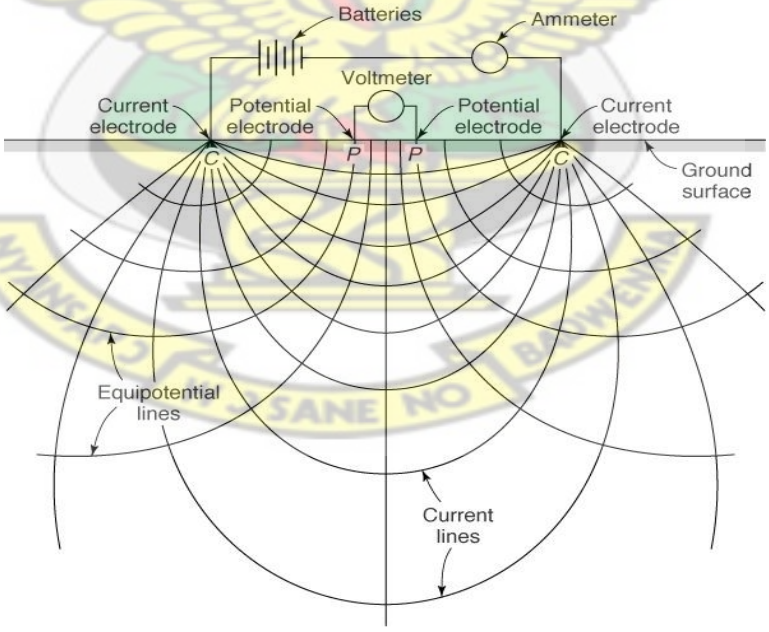

Fig.2.4 Schematic diagram illustrating basic concept of electrical resistivity measurement (Walton, 2010)

Assuming an electrically conductive body lends itself to the description of a one-dimensional body (like a wire), the relationship between the current and potential distribution could be described by Ohm's law as:

$$V = IR, \ldots\ldots\ldots\ldots\ldots\ldots\ldots\ldots\ldots\ldots\ldots\ldots\ldots\ldots\ldots (2.21)$$

where; V = the potential difference (in volts), I = current (in Amperes) and R = resistance (in ohms)

The resistance is therefore given by:

$$R = \frac{V}{I} = \rho\left(\frac{L}{A}\right), \ldots\ldots\ldots\ldots\ldots\ldots\ldots\ldots\ldots\ldots\ldots\ldots\ldots\ldots (2.22)$$

For an area, A ($2\pi r^2$), equation (2.22) could be rewritten in terms of voltage, V as:

$$V = \frac{\rho I}{2\pi r}, \ldots\ldots\ldots\ldots\ldots\ldots\ldots\ldots\ldots\ldots\ldots\ldots\ldots\ldots (2.23)$$

Considering an electrode pair with current I at electrode C_1, and –I at electrode C_2 as shown in Figure 2.4 above, the potential at any point is given by the algebraic sum of the individual contributions. Hence,

$$V = V_{C1} + V_{C2} = \rho I\left(\frac{1}{2\pi r_{C1}} - \frac{1}{2\pi r_{C2}}\right) = \frac{\rho I}{2\pi}\left(\frac{1}{r_{C1}} - \frac{1}{r_{C2}}\right), \ldots\ldots\ldots\ldots\ldots\ldots\ldots\ldots\ldots (2.24)$$

where; r_{C1} and r_{C2}= distances from the point between electrodes C_1 and C_2 respectively

For the potential electrodes, P_1 and P_2 as in Figure 2.4 above, the potential is given as:

$$V = V_{P1} - V_{P2} = \frac{\rho I}{2\pi}\left(\frac{1}{C1P1} - \frac{1}{C2P1} + \frac{1}{C2P2} - \frac{1}{C1P2}\right), \ldots\ldots\ldots\ldots\ldots\ldots\ldots\ldots\ldots (2.25)$$

where; V_{P1} and V_{P2}= potentials at P_1 and P_2

$C1P1$ = distance between C_1 and P_1

$C1P2$ = distance between C_1 and P_2

When we represent $\frac{1}{2\pi}\left(\frac{1}{AM}-\frac{1}{BM}+\frac{1}{BN}-\frac{1}{AN}\right)=\frac{1}{K}$ Equation (2.25) becomes

$$V=\frac{\rho I}{K}, \ldots\ldots\ldots\ldots\ldots\ldots\ldots\ldots\ldots\ldots\ldots\ldots\ldots\ldots (2.26)$$

From which resistivity is calculated i.e.:

$$\rho=\frac{KV}{I}=R_{app}K, \ldots\ldots\ldots\ldots\ldots\ldots\ldots\ldots\ldots\ldots\ldots\ldots\ldots\ldots (2.27)$$

where; ρ = resistivity (in ohm m), R_{app} = apparent resistance (in ohm) and K = geometric factor (in m)

The geometric factor, K varies for different electrode configurations. According to Vogelsang (1994), the geometric factor, K for the Wenner array is $2\pi a$. That of the Schlumberger array is given as; $\frac{\pi}{a}\left[\left(\frac{s}{a}\right)^2-\left(\frac{a}{2}\right)^2\right]$ and the dipole-dipole array is given as $\pi n(n+1)(n+2)a$.

where a = electrode spacing

s = distance

n = dipole length factor

2.2.2.3 Electrode Configurations

Until the 1960s, the Wenner, Lee-Partitioning and the Schlumberger arrays were the most commonly used electrode arrays for resistivity surveys. Now, other electrode arrays have been discovered for several electrical resistivity exploration including the dipole-dipole, pole-dipole, square and the gradient arrays. In more recent years, although the Wenner array is still used, the Schlumberger array has been a generally preferred method for groundwater investigations. Generally, four electrodes are placed at arbitrary locations as

shown in Figure 2.5 below. Each electrode configuration is suitable for a particular geological situation. It is possible for apparent resistivity values observed by the different array types over the same structure to differ. The choice of a particular array depends however on a number of factors which include the geological structures to be delineated, heterogeneities of the subsurface, sensitivity of the resistivity meter, the background noise level and electromagnetic coupling. Other factors which are worth considering are the sensitivity of the array to vertical and lateral variations in the resistivity of the subsurface, its depth of investigation and the horizontal data coverage and signal strength of the array (Ahzegbobor, 2010).

Conventional array systems like the Wenner (alpha) and Schlumberger are comparatively sensitive to vertical variations in the subsurface resistivity below the centre of the array but less sensitive to horizontal variations which is the main limitation of these arrays. Wenner array is preferred for surveys in noisy sites due to its high signal strength; however it is less sensitive to 3D structures (Dahlin and Loke, 1997).

The dipole-dipole array on the other hand, is most sensitive to resistivity variations below the electrodes in each dipole pair and is very sensitive to horizontal variations but relatively insensitive to vertical variations in the subsurface resistivities (Ahzegbobor, 2010). This makes it most preferred for the mapping of vertical structures like cavities and dykes. In addition, it is the most sensitive array to 3D structures among the common arrays (Dahlin and Loke, 1997). One of the limitations to this method is the depth of probing. It comparatively probes to shallower depths. Another limitation has to do with the decrease in signal strength with increasing distance between the dipole pair.

The pole-dipole array is an asymmetrical array with asymmetrical apparent resistivity anomalies in the pseudosections over a symmetrical structure, which could influence the inversion model (Ahzegbobor, 2010). It has a good horizontal coverage and higher signal strength compared to the dipole-dipole array but less signal strength relative to that of the Wenner and Schlumberger arrays. It is however, very sensitive to vertical structures.

The pole-pole array comprises of one current and one potential electrode with the second current and potential electrodes at infinite distances (Ahzegbobor, 2010). The difficulty in using this type of array is in the search for suitable locations for these electrodes in order to satisfy theoretical requirements. Another advantage is its high susceptibility to high amounts of telluric noise which have the ability of degrading the observed data quality. Hence, this array has the poorest resolution. Nevertheless, this array has the widest horizontal coverage and the deepest depth of investigation (Dahlin and Loke, 1997). Where the electrode spacing is small and a good horizontal coverage is required, the pole-pole array is most suitable.

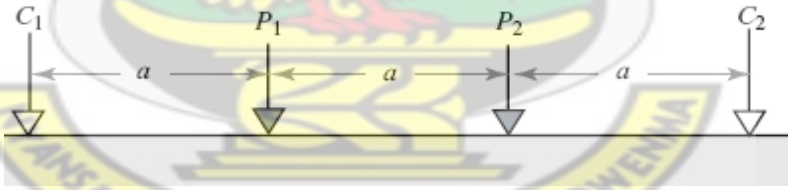

(a) Conventional Wenner array

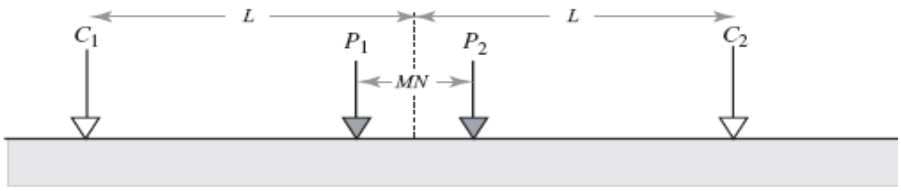

(b) Schlumberger array

(c) Dipole-Dipole array

(d) Pole-Dipole array

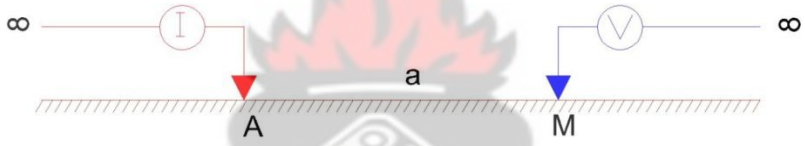

(e) Pole-Pole array

Fig. 2.5 Conventional electrode configurations commonly used in geoelectrical resistivty surveys with their corresponding geometric factors (after (Ahzegbobor, 2010).

2.2.2.4 Applications of Electrical Resistivity Method

Electrical resistivity surveys have been used for many decades in hydrogeological, mining and geotechnical investigations. More recently, it has been used for environmental surveys (Loke, 1999). Electrical resistivity techniques are either used in the profile mode (usually in dipole-dipole surveys) to map lateral changes and detect near-vertical features (eg. fracture zones) or in the sounding mode (usually in Schlumberger soundings) for determining depths to geoelectric horizons (eg. depth to

saline groundwater). Other common applications include: estimating the depths to bedrock, to the water table or to other geoelectric boundaries, delineation of aggregate deposits for quarry operations, measuring resistance for electric grounding circuits or for cathodic protection and mapping of other geologic features.

2.3 Regional Geological and Hydrogeological Settings

Two major formations dominate the geology of Ghana. These include: the basement crystalline rocks associated with the West African Craton which covers 54% of the country and the Palaeozoic consolidated sedimentary formation formed in a depression of the West African Craton which covers 45% of the country. Minor geological formations underlie the remaining 1% of the country which includes the Cenozoic, Mesozoic and Palaeozoic sedimentary strata lying along narrow belts on the coast and Quaternary alluvium lying along the major stream courses (Barry and Obuobie, 2010). These are shown in Figure 2.6 below.

The basement crystalline rocks are of Precambrian age and consist of granite-gneiss-greenstonerocks, phyllite, schist, quartzite, strongly deformed metamorphic rocks and amorogenic intrusions (Key, 1992). The principal tectonics stress orientation generally influences the structural trend in these basement rocks and they therefore follow a northeast-southwest axis (Apambire, 1996). This formation is normally subdivided into the Birimian group (with associated granatoid intrusions), Granite, Tarkwaian group, Dahomeyan formation, Togo formation and Buem formation. The Birimian group covers densely populated areas including most of western, south-central, northeast and northwest

of the country and can be as thick as 15,000 m and therefore is said to be the dominant group of the basement crystalline formation (Key, 1992).

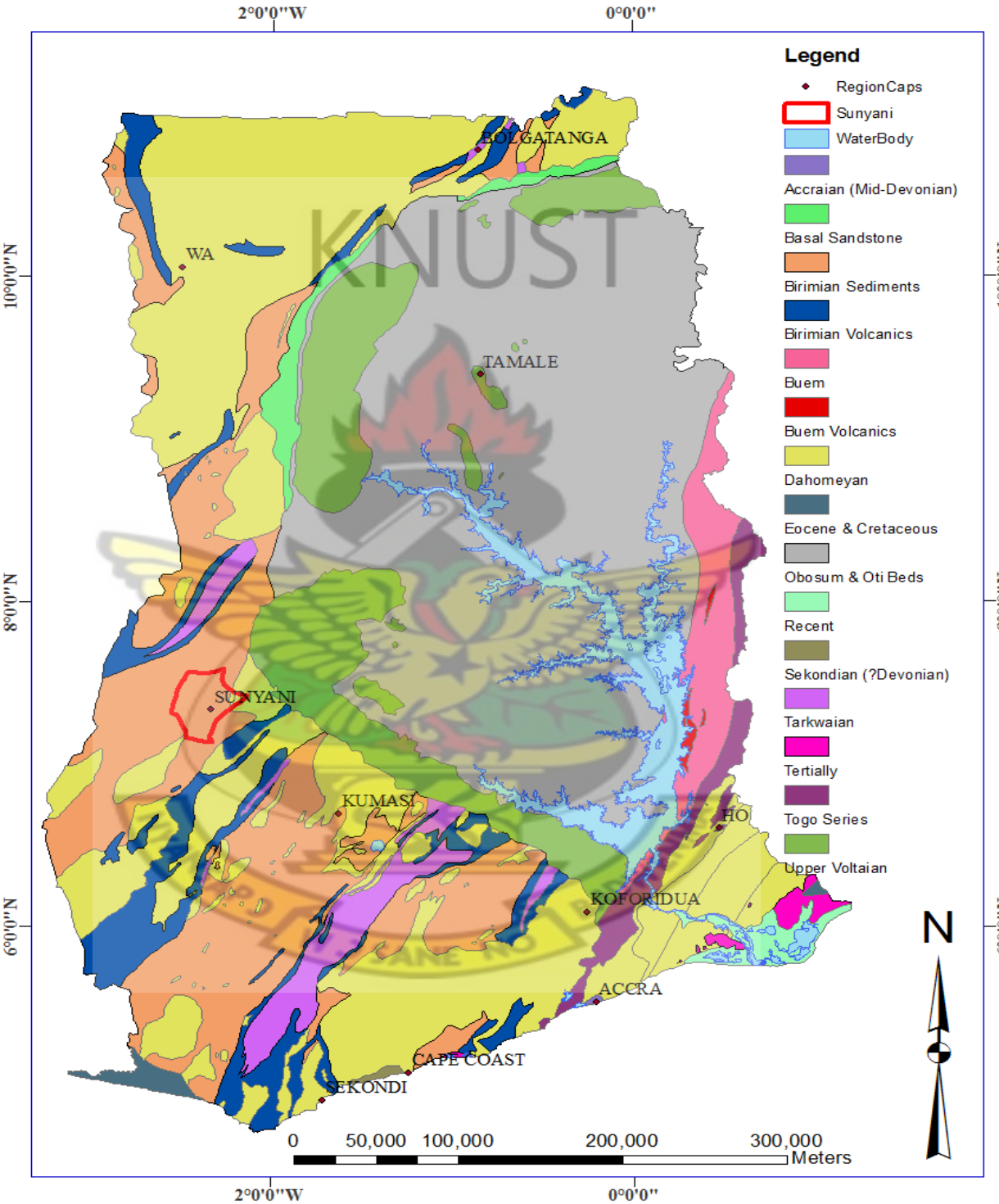

Fig. 2.6 General Geological map of Ghana (After Kesse,1985)

On the other hand, the Palaeozoic consolidated sedimentary formation usually known as the Voltaian formation comprises principally of sandstone, shale, arkose, mudstone, sandy and pebbly beds and limestone (WARM, 1998). On the basis of lithology and field relationships, the Voltaian is further grouped into the upper, middle and lower Voltaian. The first subgroup being the upper Voltaian comprises masses and thin-bedded quartzite sandstones interbeded with shale and mudstone in some areas. The middle Voltaian (usually the Obusum and Oti Beds) consists of shales, sandstones, arkose, mudstones and siltstones whereas the lower Voltaian mainly comprises massive quartzite sandstone and grit (WARM, 1998).

The minor geological formations which include the Cenozoic, Mesozoic and Palaeozoic sedimentary strata are made up of two coastal formations namely, the coastal Block-Fault and the coastal Plain. The coastal Block-Fault comprises a narrow discontinuous belt of Devonian and Jurassic sedimentary rocks that have been parted into numerous fault blocks and are cut across by minor intrusives. Semi-consolidated to unconsolidated sediments underlie the coastal plain formation. These sediments range from Cretaceous to Holocene in age in south-eastern Ghana and in a relatively small isolated area in the extreme southwestern part of the country (WARM, 1998). One other minor formation, the Alluvia, consists of narrow bands of alluvium of Quarternary age, which occurs mainly adjacent to the Volta River and its major tributaries and in the Volta delta (Dapaah- Siakwan and Gyau-Boakye, 2000).

The major geological formations in the country are overlain by the regolith. This regolith is a weathered layer that varies in thickness and lithology (Martin and van de Giesen, 2005). The topography, structural characteristics, vegetation cover, lithology, erosion,

climate, aquifer characteristics are all factors that influence the thickness of this regolith. Unlike in the extreme northwest part of the country where the thickness of the regolith can be up to 140 m, its thickness in the Precambian formation varies widely ranging from 2.7 to 40 m (Apambire et al., 1997; Apambire, 1996; Smedley, 1996). The thickness of the regolith is generally thicker in the Precambian formation than in the Voltaian formation (Acheampong, 1996).

2.3.1 Basement Crystalline Rocks

2.3.1.1 Birimian System

The Birimian System comprises a series of basic volcanic and sedimentary units which hosts most of Ghana's mineral deposits and occupies most of the western, southern and northern parts of the country. One member of the Birimian system called Lower Birimian is basically sedimentary comprising phyllites, tuffs and greywackes (Junner, 1935). The other member which is the Upper Birimian comprises mostly of volcanic and pyroclastic rocks (Junner, 1935). The ages of these Birimian rocks range from 2.195 to 2.166 Ga (Taylor et al., 1988). Birimian rocks derive their name from the Birim River valley in Ghana (Kesse, 1985). This formation comprises of large thickness of isoclinally folded metamorphosed sediments coupled with metamorphosed tuff and lava. Whereas the sediments dominate the lower part of the formation, the tuff and lava are dominant in the upper part. The whole sequence is intruded by lots of granite and gneiss which have partially or fully granitized the Birimian host rocks. It is believed that the argillaceous sediments metamorphosed to schist, slate and phyllite which are normally foliated and jointed and in areas where they lie close to the surface, water is likely to permeate

through the fractures and joints. These rocks have varying amounts of carbonaceous, ferrous, maganiferous or calcareous material (Gill, 1969). Amongst the mafic and silicic composition of the tuff and lava, the mafic type remains the most common. Most of these mafic lavas were extruded underwater. Because the areas of deepest erosion show only the granitized roots of the complex, the base and thickness of the Birrimian is not known.

The granites and gneisses that have intruded the Birimian rocks are of tremendous benefit in the water system of Ghana due to the fact that, they underlie extensive and generally high-populated areas. Both the granites and the gneisses are not usually permeable but they have a secondary permeability acquired as a result of fracturing, chemical weathering, shearing and jointing (WARM, 1998). The occurrence of groundwater in this formation is related to the secondary porosity developed. In areas where there is high precipitation and weathering agents are able to perforate along fracture or joint systems, these granites and gneisses usually erode down to form comparatively low-lying areas. On the contrary, in low precipitation areas, the granites and gneisses occur in poorly jointed systems that ascends above surrounding lands. Such low precipitation areas can be found in the Northern Region and in some parts of the forest zones of Southern Ghana. Usually, major fault zones are favourable locations for groundwater reservoirs (Gill, 1969). In the Upper West Region, the weathered zone (regolith) is as much as 137.16 m thick but it is generally half as thick in the Upper East Region.

Groundwater studies were carried out by (Gill, 1969). The research revealed that out of 328 boreholes drilled in the Upper West and the Northern Regions, 279 were successful. The average yield of successful boreholes was 5.45 m^3/h and ranged from 0.45 m^3/h to 23.86 m^3/h. Also, the depth of boreholes in these regions averaged 35.05 m. Elsewhere in

the Central Region, boreholes appeared to have lower yields in that of the 25 boreholes drilled, 17 were successful averaging to a yield of 0.41 m^3/h. Also, in the Ashanti Region, of the 13 boreholes drilled, 9 were successful with an average yield of 9.42 m^3/h. Boreholes tapping the lower part of Birimian rocks in the Brong-Ahafo region had generally slightly smaller average yield. He stated that, the boreholes yield ranged between 3.18 and 29.1 m^3/h and that those with the highest yields were located between Berekum and Dormaa-Ahenkro. In the upper part of the Birimian rocks in the Western Region, 12 out of the 16 boreholes drilled were considered successful with an average yield of 12.67 m^3/h (Gill, 1969).

Water tapped from the Birimian rocks and its associated gneisses and granites has been found on analysis to have multiple uses. In certain areas, even though temporary hardness exceeds 100 mg/l and iron and manganese concentrations are quite above 0.3 mg/l, these concentrations are not high enough to require water treatment (Kesse, 1985).

2.3.1.2 Granitoids

Granitoids are usually located within the Birimian rocks. They form a very significant portion of the Main Shield which occupies the southernmost part of the West African Craton. The granitoids intruded the Birimian rocks about 2.1 Ga ago during the Eburnean Orogeny (Leube et al., 1990). Down through the years, the Eburnean granitoids have been grouped into the Cape Coast type now known as the Sedimentary-basin granitoids, the Sedimentary granitoids of the Winneba type and the Volcanic-belt granitoids formally known as the Discove type (Junner, 1940; Kesse, 1985). Sedimentary-basin granitoids of the Cape Coast type are completely of different origin from that of the Winneba type

(Taylor et al., 1992). The Cape Coast type are granitoids that have intruded the Birimian system. The potash rich rock of this complex comprises biotite granite, granodiorite ore porphyrblastic biotitic gneiss, muscovite, pegmatite and applite. The complex is usually identified with many enclaves of schists and gneisses (Asklund and Eldvall, 2005). The Winneba Granitoids complex pertains to large granitoid batholiths laid within the sedimentary basin which happen to coincide with the central axis of the basin. They are characterized by granites, tonalities, trondhyemites and quartz diorites. Granites are more common here than in all the other types of granitoids whereas quartz diorites are very uncommon (Nyarko et al., 2012). Unlike the Cape Coast type, the Discove type have intruded both the Birimian and Tarkwaian systems. They are generally characterized by granodiorite changing into hornblende diorite and quartz diorite (Asklund and Eldvall, 2005). Generally rocks in the Granitoid formation have lost their primary porosity so groundwater occurrence here is as a result of the secondary porosity developed by jointing, shearing, chemical weathering and fracturing (WARM, 1998). Average yield of boreholes in the Granitoids is 4.0 m^3/h and depth of boreholes in this formation range between 35m and 55m. Success rate of boreholes in this region is between 68% and 85% (HAP, 2006).

2.3.1.3 Tarkwaian Group

This group is composed of thick series of argillaceous and arenaceous sedimentary rocks which have two zones of auriferous conglomerates in the lower formations (Junner, 1940). Typically, rocks of the Tarkwaian group are confined to Birimian volcanic belts where they are found to exist either as fault-bounded slices or as uncomfortably overlying

sedimentary rocks (O' Donovan and Lacey, 2011). The Tarkwaian group is subdivided into four stratigraphic units namely; the Kaware series, Banket series, Tarkwa series and Huni series (Hirdes and Nunoo, 1994). The Kaware series which is found at the base of the Tarkwaian sediments consists of conglomerates, sandstones, grits, phyllites and quartzites. The thickness of this series ranges between 250 and 700 m. Underlying this stratigraphic unit is the Banket series. This series consists of conglomerates with interbeded local cross-bedded sandstone layers which primarily comprise Birimian quartz pebbles and volcanic clasts. The Banket series is estimated to be between 120 and 160 m thick (Hirdes andNunoo, 1994). This series is overlain by the Tarkwa phyllite series basically made up of chloritic and sericitic phyllites and schists. Its thickness it between 120 and 400 m. The Huni series which is 1370 m thick forms the uppermost part of the Tarkwaian group consisting of sandstones, alternating quartzite beds and phyllites intruded by minor dolerite sills (Pigois et al., 2003). Generally, rocks in this formation comparatively have good potential for groundwater development (Gill, 1969).

2.3.1.4 Dahomeyan Formation

The Dahomeyan system, which underlies the southern part of the main Volta Basin is generally comprised of metamorphic rocks, which includes hornblende and biotite, migmatites, granulites, schists and alternating bands of massive acidic and basic gneisses (Barry et al., 2005). The formation is wholly massive rocks with few joints or fractures. These massive rocks usually weather into clay and clayey sand. Due to the impervious nature of clay, groundwater availability in this formation is limited. Nevertheless, where

there are definite discontinuities, appreciable yield of water could occur in wells penetrating these jointed zones (World Vision International (WVI), 1997).

Darko (2001) conducted studies in the Dahomeyan formation in the Greater Accra Region. The results indicated that, out of the over 300 boreholes drilled, the borehole yields ranged between 1 - 3 m^3/hr with an average of 1.9 m^3/hr and the depths of the boreholes ranged between 45 – 70 m with an average of 55 m. This indicates that borehole success rate is poorest in the Dahomeyan formation with an average value of 36%.

2.3.1.5 Togo Series

Rocks of the Togo series underlie the eastern and southern parts of the main Volta and comprise alternating arenaceous and argillaceous sediments. Other types of rocks found in this formation include quartzite, shales, sandstones, schists, phyllites and some silicified limestone (Barry et al., 2005).

Significant amount of groundwater is gained from boreholes if fracture openings in the Togo Series are wide and are not filled with imperviable material. Borehole yields in this formation ranges from 0.7 – 24 m^3/hr with an average of about 9.5m^3/hr (Agyekum, 2002). The depth of boreholes range between 33 – 55 m. Overall, the borehole success rate in this formation is between 85 – 90% (WRI, 2001).

2.3.1.6 Buem formation

The Buem series is located between the Togo series and the Voltaian system to the east and west respectively. Rock types consist of calcareous, argillaceous, sandstones,

greywacke and agglomerates, tuffs, jaspers, arkose, sandy and ferruginous shales. Similar to other crystalline basement rocks, these also have very small intergranular pore spaces and hence have negligible primary porosity. However, the weathered and fractured rocks that occur at the surface possess secondary porosity. The weathered layers and fractures within the bedrock are the main avenues of groundwater supply to the rocks (Barry et al., 2005). Borehole yields usually range between 0.7 – 24 m^3/hr and the depths range between 30 – 45 m in this formation. On the whole, borehole success rates are between 85 – 90 % (WRI, 2001).

2.3.2 Paleozoic Consolidated Sedimentary Formation

This formation is popularly known as the Voltaian Formation. It forms a Neoproterozoic to Early Paleozoic, largely clastic sedimentary fill in an intracontinental basin and underlies 45% of the total landmass of Ghana (Carney et al., 2008). Three main lithostratigraphical units divide this formation from the oldest to the youngest namely, the Kwahu/Bombouaka, Oti/Pendjari and Obosum/Tamale groups all separated by unconformities. The two upper groups, Oti/Pendjari and Obosum/Tamale represent foreland to the Pan-African Dahomeyide orogen in Eastern Ghana and Togo. The lowermost group which differs in history is rather older (Carney et al., 2008).

From history, the Voltaian Basin strata are divided into three hydro-geological sub provinces which are the Upper Voltaian, Middle Voltaian and Lower Voltaian (Annan-Yorke, 1971). The Upper Voltaian sub province consists of massive, cross-bedded quartzite sandstones interbedded with shale and mudstone in some areas (Unihydro, 2002). This sub province belongs to the Upper Ordovician to Lower Carboniferous age

(Kesse, 1985). The Middle Voltaian is made up of basically argillaceous Obosum beds and arenaceous Oti beds. The Obosum beds consists of siltstone, mudstone, shale and minor sandstone whilst the Oti beds consists of conglomerate, arkose, shale, grit and minor limestone (Unihydro, 2002). The age of these rocks lie within the Lower Vendian and Lower Ordovician (Kesse, 1985). The Lower Voltaian comprises massive quartzite with minor grit (Unihydro, 2002) and it belongs to the Late Middle Riphaean to the Upper Riphaean age (Jones, 1978). According to Ghana's geological survey, the age of the Voltaian system generally ranges from upper Proterozoic to Paleozoic which are about 620-1000 million years (Kesse, 1985).

Hydro-geologically, groundwater flow and storage in unweathered rocks normally occurs in fractured zones. Unfortunately, the unweathered rocks of the Voltaian Basin are well-cemented and possess little primary porosity therefore rocks found here have very low aquifer productivity and hence low groundwater potential (Ó Dochartaigh et al., 2011). Success rates of boreholes drilled in this Basin are not more than 70% even in the highest productivity aquifer and could be as low as 20% in the lowest productivity aquifer. On the whole, rates of successful boreholes range between 40 and 60% in this region (Ó Dochartaigh et al., 2011). Records have shown that the average borehole depth in the Voltaian is 48.1m and the maximum borehole depth usually occurs at about 90 m (Akudago et al., 2009).

2.3.3 Minor Geological Formation

The minor geological formation is made up of the Cenozoic, Mesozoic and Paleozoic sedimentary strata located in the extreme southeastern and western parts. Rock types

found in this geological formation include a thick section of marine sands, shale, clay, limestone, sandstone and some gravels which underlie more recent sediments in the coastal areas (Junner and Bates, 1945).

Three aquifers occur in this formation with the first being the unconfined which occurs in the recent sand close to the coast, the next is the semi-confined or confined which occurs in the continental deposits of sandy clay and gravels and the third is the limestone aquifer (WARM, 1998). The occurrence of groundwater in this province is controlled by matrix flow. Borehole yields range between 0.7 – 27.5 m^3/hr and average borehole depth in the province is 52 m.

2.4 Local Geological and Hydrogeological Settings

The Sunyani Municipality is geologically underlain by Precambian rocks of Birimian and Dahomeyan formations. Extensive masses of granite predominantly those of the Cape Coast Granite Complex are associated with the Birimian formations in the Municipality. The geologically map of the study area is shown in Figure 2.7 below.

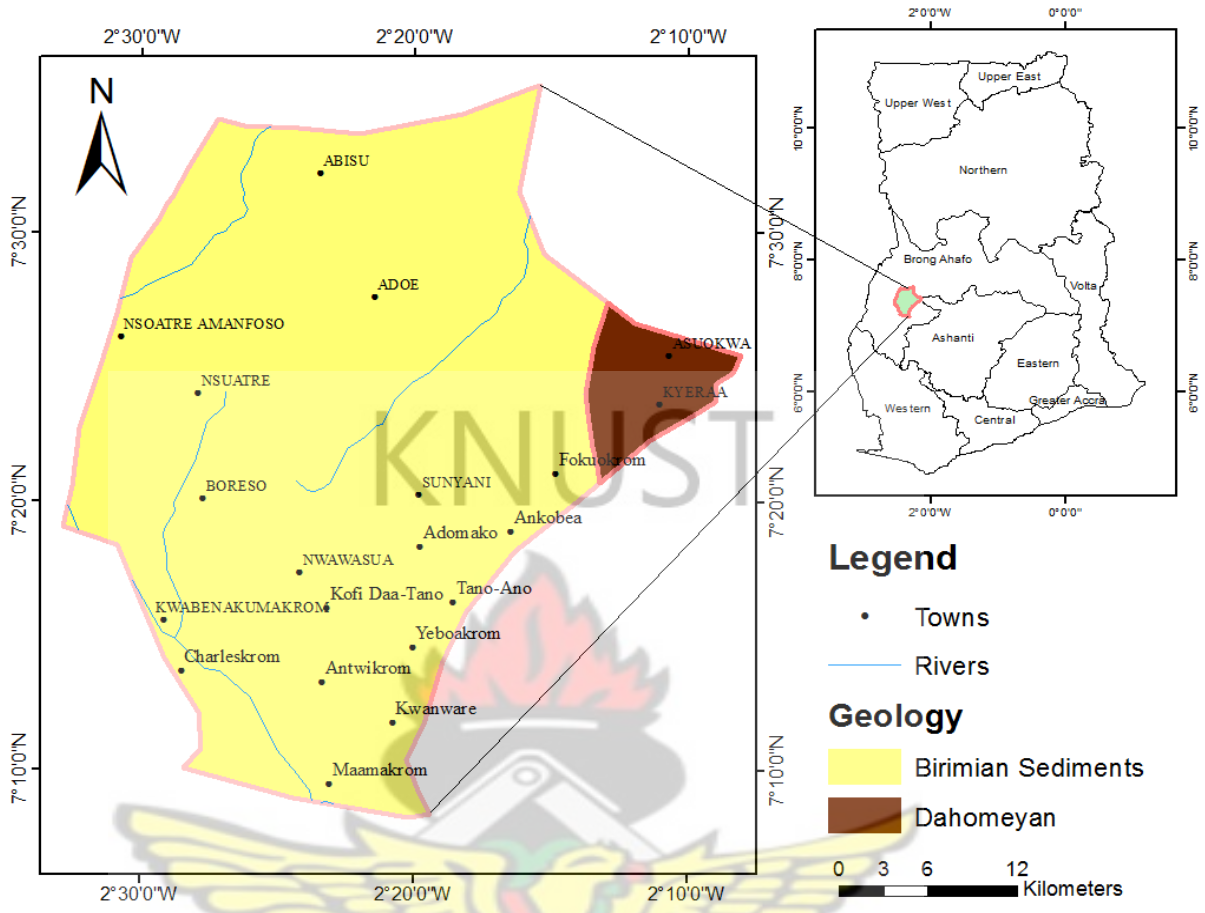

Fig. 2.7 Geology map of the Sunyani Municipality

The Birimian and its associated granites as well as the Dahomeyan belong to the basement crystalline rock which is one of the two major formations dominant in the geology of Ghana making up 54% of the land area of the country. The basement crystalline rocks are of Precambian age comprising gneiss, granite-gneiss, phyllite, schist, quartzite and migmatite. Other subdivisions of this basement complex include the Togo, Buem and Tarkwaian rock formations (Key, 1992).

The Birimian Supergroup is a series of basic volcanic and sedimentary units consisting of two members namely, the Lower Birimian and Upper Birimian. The Lower Birimian consists of tuffs, greywackes and phyllites whilst the Upper Birimian comprises mainly

of volcanic and pyroclastic rocks (Junner, 1935). The Birimian rocks are believed to have undergone changes during active tectonics during the Eburnean event between 2150 and 1850 Ma. The rocks are folded, metamorphosed and intruded by granitoids as a result. The tectonic sequence of the Eburnean event are contributing factors to the structure in the Birimian Supergroup even though the beginning of the Eburnean is not fully understood. This is also because there are no basement rocks to show the underlying materials upon which the initial Birimian rocks were laid (Leube et al., 1990). Three phases of felsic intrusives intruded the Birimian Supergroup during this Eburnean event. The first phase being the Birimian sedimentary rocks were intruded by the Cape Coast granitoids which are considered to be syn-tectonic intrusions because of the presence of well-developed foliations (Milesi et al., 1990). The second phase which is the Birimian volcanic rocks were intruded by the Dixcove granitoids according to Kesse (1985) and are considered to be post-tectonic intrusion, because of the absence of foliation (Milesi et al., 1990). The third phase found within the metasedimentary basins consists of K-rich granitoids also known as the Winneba granitoids (Leube et al., 1990). For economic purposes, the Birimian makes up the most important geologic group (Cudjoe, 1961).

Rocks of the Birimian Supergroup are not permeable so groundwater occurrence in this formation is associated with the development of secondary porosity which results from chemical weathering and fracturing. Hence, groundwater occurrence is found in these fractured zones. Since the amount of rainfall determines borehole yields in these fractured zones, groundwater potential is very low in areas where there are no fractures and the amount of rainfall is comparatively less. (Gyau-Boakye and Dapaah-Siakwan, 2000). Generally, borehole yields range between 0.41 m^3/hr and 29.8m^3/hr and the

depths also range between 16m and 187 m in this formation. Borehole success rate is about 76% (Darko, 2001).

The Dahomeyan similar to the Birimian formation, belongs to the basement crystalline rocks system. Rocks of this formation are usually metamorphic in nature. Rock types include: magmatites, crystalline gneisses, quartz schists and biotite schists. The crystalline gneisses are the dominant rock types in this formation. They have few fractures and generally occur in two types the silicic and mafic gneisses. The silicic gneisses later weather into slightly permeable clay sand whilst the mafic gneisses weather into nearly impermeable calcareous clay. Due to the very low permeability of these rocks, borehole success rate is poorest in this formation. The average success rate of boreholes is about 36% (Dapaah-Siakwan and Gyau-Boakye, 2000). Depth of boreholes range between 22 m and 122 m and borehole yields range between 1 m^3/hr and 3 m^3/hr (Darko, 2001).

2.4.1 The Sunyani Municipal District

The area of concern as far as this project is concerned is the Sunyani municipal district. Sunyani is the capital of Brong-Ahafo Region located in the middle belt of Ghana. The region shares local borders with the Northern, Volta, Ashanti and Western Regions. It shares a common border internationally with La Cote D'Ivoire.

2.4.2 Location and size

The Sunyani Municipality is one of the twenty-two administrative districts in the Brong-Ahafo Region of Ghana. The district shares borders with the Sunyani West, Dormaa East, Asutifi and Tano-North Districts. The Sunyani West District lies to the north, Asutifi District lies to the South, Tano-North District lies to the East and Dormaa East District lies to the West of the Sunyani Municipality. The area lies between latitudes 7^0 55'N and 7^0 35'N and longitudes 2^0W and 2^0 30'W. The total land area of the Municipality is 2,488 square kilometres with about one-third of this area uninhabited providing lands for future investments (Arthur, 2006). The Municipality is home to about 248,496 people as of the 2012 census. Groundwater exploration was carried out in thirteen out of twenty-three communities in the Sunyani Municipality. Figure 2.8 is a map of the study area showing some selected communities.

2.4.3.1 Topography and Drainage

The Sunyani Municipality falls within the middle belt of Ghana with heights ranging from 229 m to 376 m above sea level and it is characterized by a moderately flat topography. Due to this, building and road construction cost is minimal. Large scale agricultural mechanization is best suited in this area. The drainage in the municipality is dendritic with several streams and rivers. Some of these water bodies include: the Kankam, Amoma, Benu, Bisi, Yaya and Tano rivers. These surface waters are seasonal hence, water shortage is paramount during harsh (dry) seasons. (Sunyani Municipal Assembly (SMA), 2010).

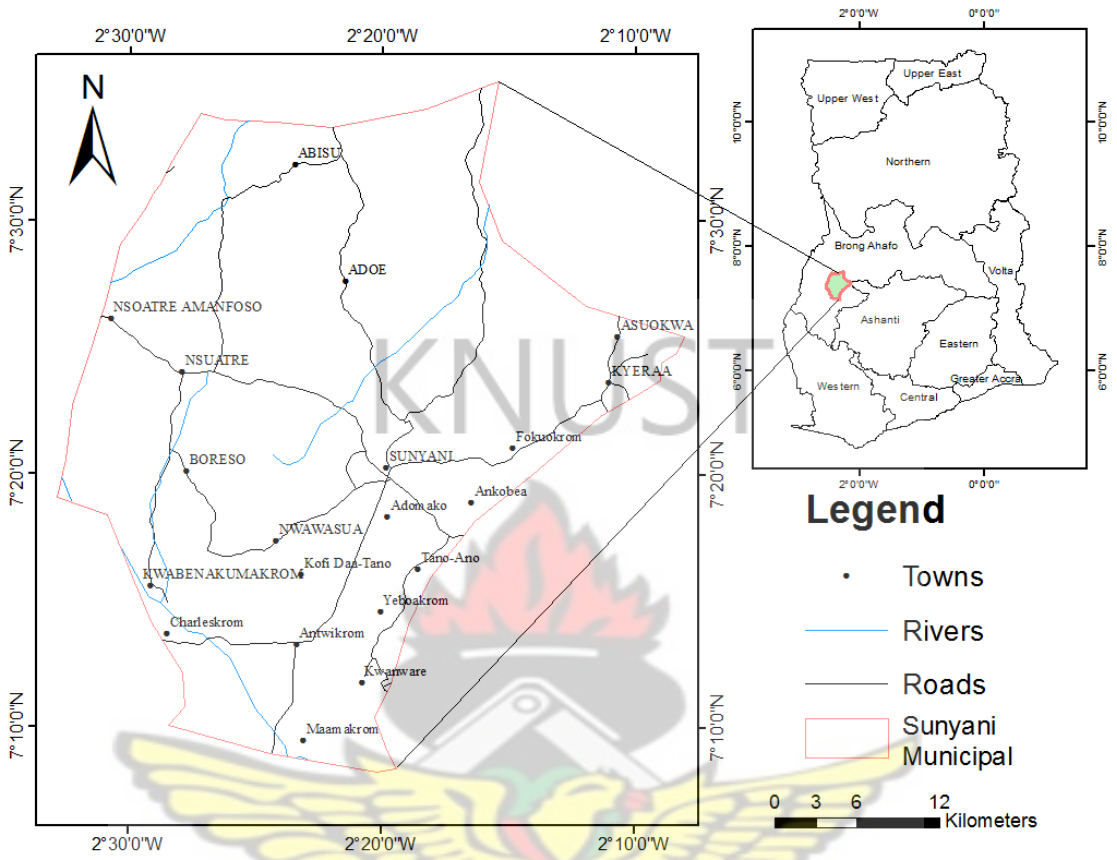

Fig. 2.8 A map of the study area

2.4.3.2 Climate and Rainfall

The Sunyani Municipality lies within the wet Semi-Equatorial Climatic Zone of Ghana. The monthly temperature variations range from 23^{o}C to 33^{o}C with the lowest occuring in August and the highest around March and April. Relative humidity variations over the year usually ranges between 75 to 80% in the rainy season and between 70 to 80% in the dry seasons which are very idle for vegetative growth (SMA, 2010).

Rainfall patterns vary across the country. Sunyani experiences double maxima rainfall patterns with the primary rainy season occurring between March and September and the

minor between October and December. Over the years however, this rainfall pattern has been observed to be changing due to deforestation and depletion of water bodies (SMA, 2010).

2.4.3.3 Vegetation

The municipality lies within the Moist Semi-Deciduous Forest Vegetation Zone with most of its principal vegetation found in small patches around the south, east and north-western parts. Notable forests include the Amama and Yaya reserves. Due to the vegetation cover, timber and cash crops like cocoa and citrus, flourish very well in this zone. Nevertheless, bad farming practices have degraded a greater portion of these forest areas and so efforts are now being made in the sphere of reforestation to reverse this trend (SMA, 2010).

2.4.4 Socio-Economic Activities

The economy of the Sunyani Municipality is predominantly based on agriculture. About 48% of the populace are into agriculture production, 24% are employed in the service sector (Government workers, communication workers, hairdressers, seamstresses, financial institutions, etc), 15% are into commerce and the remaining 13% are in the industry (timber related industries, construction workers, bricks and block laying). The district obtains its electricity from the Volta River Authority (VRA). Sunyani is notable for high-quality water supply with rain water, water from rivers, streams and springs being the districts main sources of water. Since these water sources are not reliable all-

year long, there's great difficulty in accessing water during severe harmattan conditions (Sunyani West District Assembly (SWDA), 2010).

2.4.5 Water-related Diseases

Due to the high dependency rate of the populace in the Sunyani Municipality on surface water bodies as their main source of water for domestic and agricultural purposes, they are exposed to a number of water-borne diseases. The major water-borne disease in the area is guinea worm infection. Apart from the Sunyani Municipality, there are ten other endemic districts. Cholera outbreaks are also prevalent amongst households in the municipality. In 2001 for example, there were reports of 8.6% of indigens dying of the cholera disease. Finally, the buruli ulcer disease is found to affect many people living in communities along the Tano River.

CHAPTER 3

INSTRUMENTATION ANDFIELD PROCEDURE

3.1 Introduction

This research involved the use of two integrated geophysical methods namely, the electromagnetic and electrical resistivity methods. Electromagnetic method was used for reconnaissance survey (for profiling) whereas the electrical method was employed in further probing. Specifically, the vertical electrical depth sounding (VES) method was applied. Many instruments are used for both electromagnetic and resistivity methods but for purposes of this project, the Geonics EM34-3 and ABEM SAS 1000C terrameter equipment were used respectively.

3.1.1 Equipment for the Electromagnetic (EM) Profiling

EM profiling generally refers to a method of translating the Transmitter (Tx) and Receiver (Rx) coils along a profile line keeping the frequency and coil spacing constant (Liopis and Simms, 1994). Electromagnetic (EM) traverses were done using the Geonics model EM34-3 conductivity meter in this study. The method provides a direct reading of apparent electrical conductivity of the earth and allows for rapid surveying to be done (MacDonald et. al., 2002). The equipment is a two-person portable system which comprises a separate transmitter and receiver consoles and transmitter and receiver coils (loop antenna), reference cables and power supply (usually rechargeable dry cells). The transmitter coil is energized with an alternating current at an audio frequency in order to give rise to a time-varying magnetic field which subsequently induces small eddy

currents in the ground. Secondary magnetic fields are further generated by these currents which are detected together with the primary field by the receiver coil. The units of conductivity are millimhos per meter (mmhos/m). In areas where conductivities range between 1 and 100 mmho/m, the EM34-3 equipment is calibrated to take readings directly (Liopis and Simms, 1994). The transmitter of the EM34-3 equipment functions at switch selectable, controlled frequencies of 6.4, 1.6 and 0.4 KHz, with each frequency keyed to transmitter-receiver (Tx-Rx) spacings of 10, 20 and 40 respectively. It gives variable depths of exploration down to 60 m. The conductivity meter could be used in both horizontal and vertical dipole modes. The coils could be oriented either vertically or horizontally (MacDonald et. al., 2002). The kind of orientation used determines the direction of the inducing field and what the instrument is sensitive to.

In the horizontal dipole mode (where coils are aligned vertically), the reading gives a good estimate of electrical conductivity and the instrument is not affected by misalignment of the coils. However, as the current moves deeper from the surface, the response reduces. The average depth of penetration when using this coil system is about (0.5 – 0.7) × the coil spacing. In the horizontal dipole mode (where Tx-Rx coils vertically and co-planar), 30% of the response at the surface is due to material deeper than 0.75 times the Tx-Rx coil separation. A general rule of thumb for the horizontal dipole mode is that, the depth of investigation is approximately 0.75 times the Tx-Rx coil separation.

The vertical dipole mode (where coils are aligned horizontally) is on the contrary not reliable for giving good estimates of electrical conductivity especially beyond 30 mmhos/m even though readings can be made up to about 65 mmhos/m. It is however advantageous in detecting vertical conductors like vertical fractures which are often good

targets for groundwater. When it is made to pass over a vertical anomaly, a negative response is given and in some cases gives readings less than zero. Horizontal coils are also very sensitive to misalignment of the coils.

The vertical dipole mode has a greater depth of penetration than that of the horizontal dipole mode. So where the conductivity of the vertical dipole exceeds the horizontal dipole conductivity, the primary contribution to the conductivity of the ground is coming from depths over 39% of the spacing between the coils. This makes the equipment efficient for quantitatively interpreting the variation of ground conductivity with depth (Paine, 2000). The depths of exploration for the Geonics EM 34-3 equipment at different intercoil spacing are shown in Table 3.1 below.

Table 3.1 Exploration depths for Geonics EM 34-3 equipment at various intercoil spacing (McNeil & Snelgrove, 1995).

Intercoil spacing (meters)	Exploration Depths (meters)	
	Horizontal Dipoles	Vertical Dipoles
10	7.5	15
20	15	30
40	30	60

3.1.2 Electromagnetic Data Acquisition

Before setting up the equipment for a geophysical survey (groundwater exploration), the terrain was evaluated. Care was taken in order to avoid areas that are prohibited such as cemeteries, toilets and refuse dumps.

After demarcating suitable sites for the survey, the equipment was set up for use. Coils and transmitter and receiver consoles were connected. A 20 m coil separation was chosen for all the profiles. Both horizontal and vertical dipole measurements were taken at each position with the receiver trailing the transmitter always. A total of 18 profiles were traversed in all the 13 communities where the survey was conducted. Measurements were made at 10 m station interval. Constantly, daily checks on both the transmitter and receiver batteries were made. The receiver batteries should read more than 4.5 volts in the battery + and – position. Potential groundwater bearing sites were identified for further VES investigation to be done.

3.1.3 Electromagnetic Data Processing

The Grapher 8 software was used to plot the data acquired from each of the profiles. Graphs of station intervals (in meters) against the apparent conductivities (in mmhos/m) were obtained. Points where the vertical dipole (VD) conductivities exceeded the horizontal dipole (HD) conductivities were noted for VES investigation. Other points were also selected for VES investigation based on experience.

3.1.4 Equipment for VES Survey

As aforementioned, vertical electrical sounding (VES) followed the electromagnetic profiling. The ABEM terrameter SAS 1000C equipment was employed for the sounding. In all, forty vertical electrical soundings were conducted using the symmetrical-

schlumberger electrode spread technique at each of the selected points. Due to the rugged and robust nature of the ABEM terrameter SAS 1000C equipment, it could be used for demanding field work and has been well proven over the years in all parts of the world. This equipment comprises a powerful built-in constant current transmitter (that runs on either a clip-on battery pack or an external power source), high resolution receiver (which provides an excellent dynamic range), an intuitive user interface and other accessories like cable sets and steel electrodes.

The fundamental principle of operation of the terrameter is to determine the variation of the subsurface resistivity with depth by measuring the resistance of the ground. From this, the apparent resistivities were computed.

3.1.5 VES Data Acquisition

The ABEM terrameter SAS 1000C equipment was setup, ensuring that the batteries were fully charged and that, electrodes were well hammered into the ground. Cables connected both current and potential electrodes to their appropriate terminals. The schlumberger protocol was chosen. Artificially generated direct current was introduced into the ground through the current electrodes and the resulting potential difference measured by another pair of potential electrodes in the region of the current flow. Expanding the electrode system varied the depth of investigation. The resistivity values of each of the VES sites were read directly from the terrameter. These values were multiplied by the geometric factor of the array give apparent resistivity values as shown in Appendix 2.

3.1.6 VES Data Processing

A third party software package, RES1DINV was used for the resistivity data processing. Before processing with the RES1DINV software, the data was converted into .dat file extension with surfer software. This conversion was done to enable the RES1DINV software read the VES data. In the RES1DINV software platform, each of the apparent resistivity data files were read and inverted with user model. The inverted data was printed and saved as BMP file format. The output is a log-log plot of apparent resistivity versus electrode separation which is referred to as the sounding curve. Additional information on number of layers, the resistivity of the layers as well as their thicknesses was generated from the software to make interpretation less ambiguous.

CHAPTER 4

DATA ANALYSIS, INTERPRETATION& DISCUSSION OF RESULTS

Groundwater is expected to be found in the weathered zone or fractured bedrock (Ndlovu et. al., 2010) in the area of study. In light of this, traverses were made to help locate zones of fracturing or contact zones, which are potential areas for the storage of large quantities of groundwater. Data from the EM 34-3 equipment were qualitatively analysed to detect adequate conductive zones which were priority areas for further probing with the vertical electrical sounding method. The Schlumberger depths sounding were performed to model the thickness of the different underlying layers and their corresponding resistivities. Generally, electrical methods reflect variations in ground resistivity. The electrical resistivity contrasts between lithological sequences in the subsurface are usually adequate to enable the delineation of aquiferous or non-aquiferous layers (Schwarz, 1988; Lashkaripour, 2003).

It is the primary aim of collecting any geophysical data to interpret it in terms of a geologically identifiable condition. It is evident that in some cases, the interpreted situation may differ slightly from the actual geologic situation. Nevertheless, it is the best that approximates the true geological situation. Two forms of interpretation of geophysical data exists which are, qualitative and quantitative interpretations (Shehu, 1998).Qualitative interpretation which was employed in this study involves explanation of an anomaly based on observations. Normally, this kind of interpretation demands, on one hand, considerable practical experience with the method and, on the other, a sound knowledge of the geology of the region under consideration (Ameloko and Rotimi,

2010). All the available information on the geological framework of the project areas was taken into consideration to constrain the interpretations.

In all the thirteen communities, a total of eighteen (18) EM profiles were run. The resulting VES was also carried out at forty (40) stations to aid in selecting appropriate sites for the drilling. Unfortunately, it should be noted that, drilling had not yet been commenced at the time of the completion of this report. The thirteen communities considered in this study included, Adomako, Ankobea, Antwikrom, Atesim Zongo, Charleskrom, Domsesre, Fokuokrom, Kofi Daa-Tano, Kwanware, Maamakrom, Nkranketewa (No. 3), Tano-Ano and Yeboakrom all in the Sunyani Municipal District. The results which evolved from the electromagnetic (EM) and vertical electrical sounding (VES) data are presented.

4.1 Presentation of Results

The electromagnetic data are presented as profiles of apparent conductivity against distance traversed. The data obtained from the vertical electrical sounding are plotted on a logarithmic scale. Samples of these results are shown in Appendices 1 and 2. The community by community interpretation of both the EM and VES data are given below:

4.1.1 Adomako

In this community, only one electromagnetic traverse was run and three sites were located for VES based on the electromagnetic traverse data. It should be noted that, a spot sounding was conducted upon request of the indegens of the community. A sketch of the layout of the traverse line at Adomako is shown in Figure 4.1.

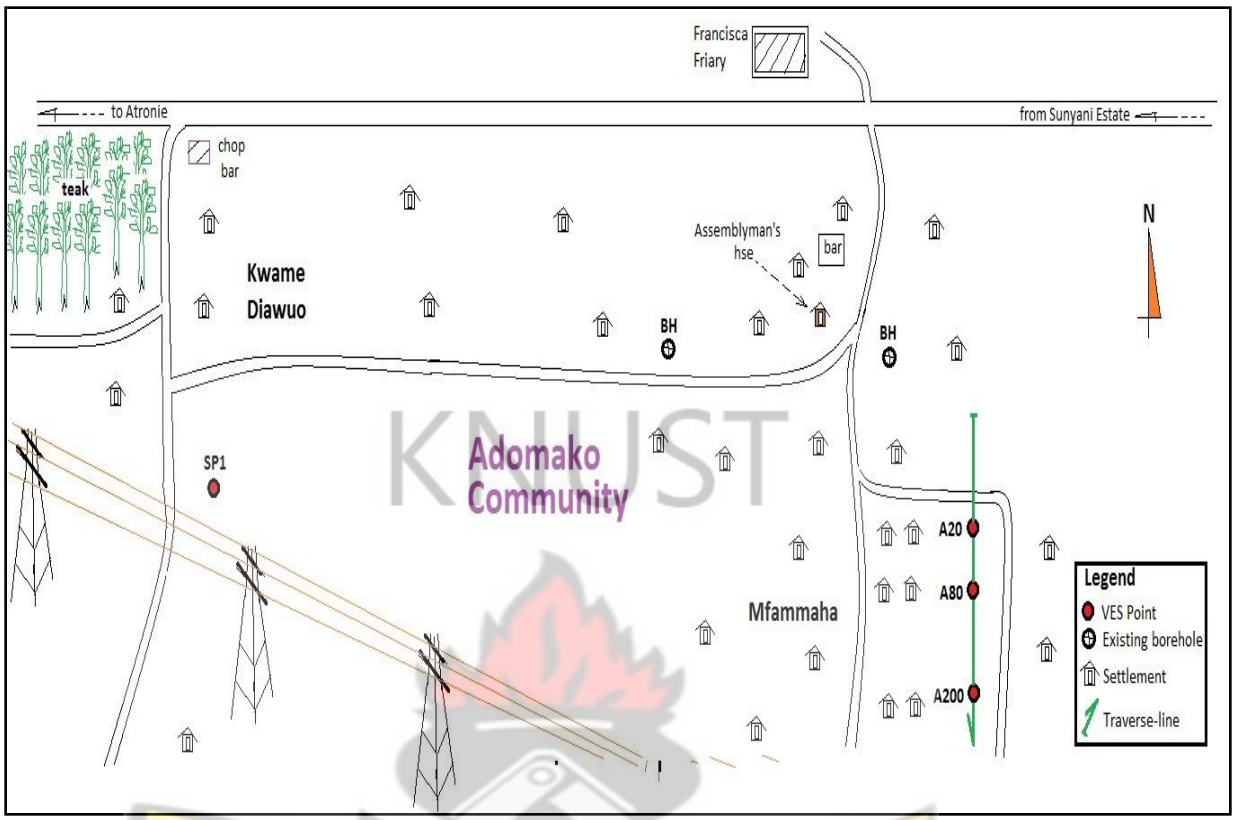

Fig. 4.1 A sketch of the layout of Adomako community (Not to scale)

The EM traverse was carried out on a profile length of 210 m and on a bearing of $151^0$from the True North on the layout at the 20 m coil spacing. From the graph as shown in Figure 4.2, it is observed that the curves of both the HD and VD dipole mode behave erratically. However, the results of the VD mode show higher conductivities than that of the HD mode almost along the whole of the profile except between 100 m and 125 m along the profile. Altogether, four VES stations were selected in this community, three of them (A20, A80 and A200) along the profile, which were at the 20 m, 80 m and 200 m points respectively and the fourth (SP1) being the spot sounding station. The apparent conductivity of the community ranges between 4 – 15 m mhos/m with an average value of 11.7 m mhos/m.

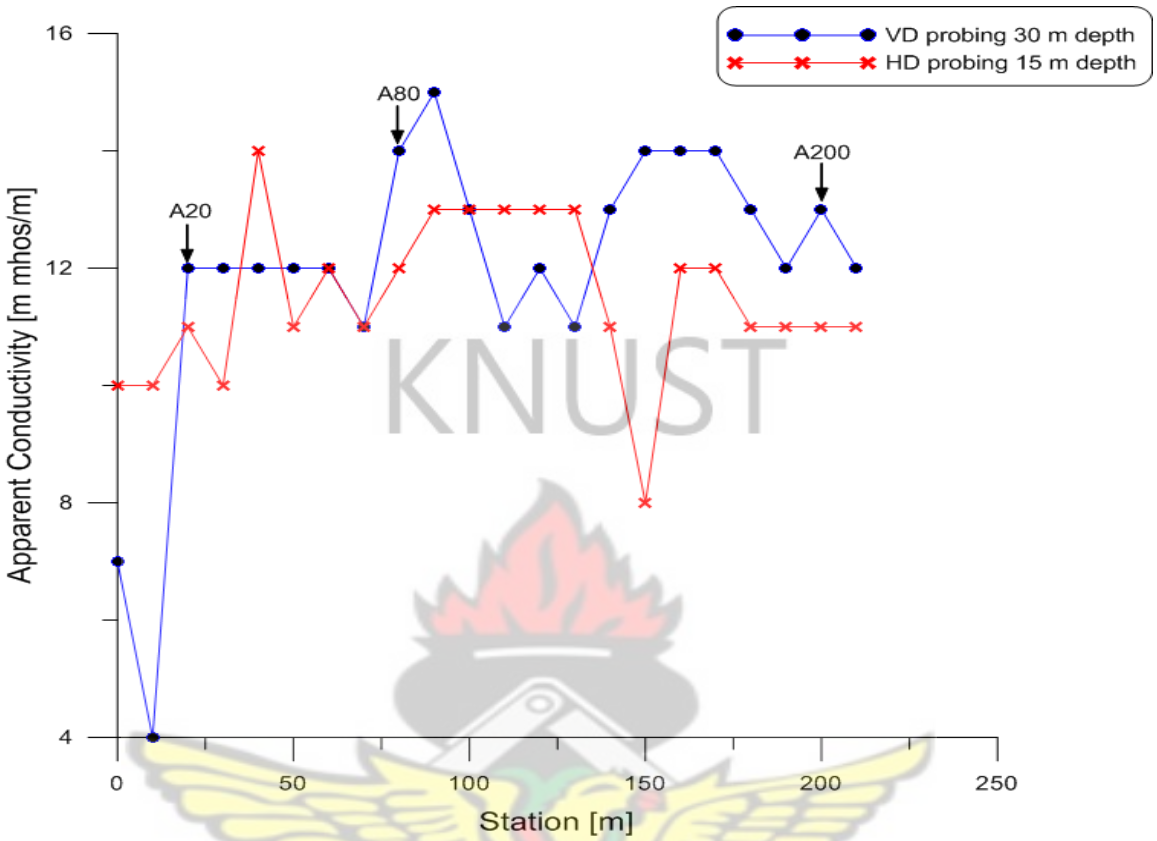

Fig. 4.2 EM terrain conductivity measurements along a profile at Adomako

VES for A20

The apparent resistivity model curve for A20 reveals a three-layer subsurface structure with resistivity varying between 42 Ωm and 495 Ωm as shown in Figure 4.3. The topsoil was 0.7 m thick and had a resistivity of 42 Ωm whereas the second layer had a thickness of 10.9 m with a resistivity of 495 Ωm. The resistivity of the third layer is 140 Ωm. Deductions made from the results suggest a slightly weathered layer sandwiched between fairly weathered first and third layers. The resistivity drop from the second to the third

layer depicts that the fairly weathered bedrock could be a potential zone for groundwater accumulation.

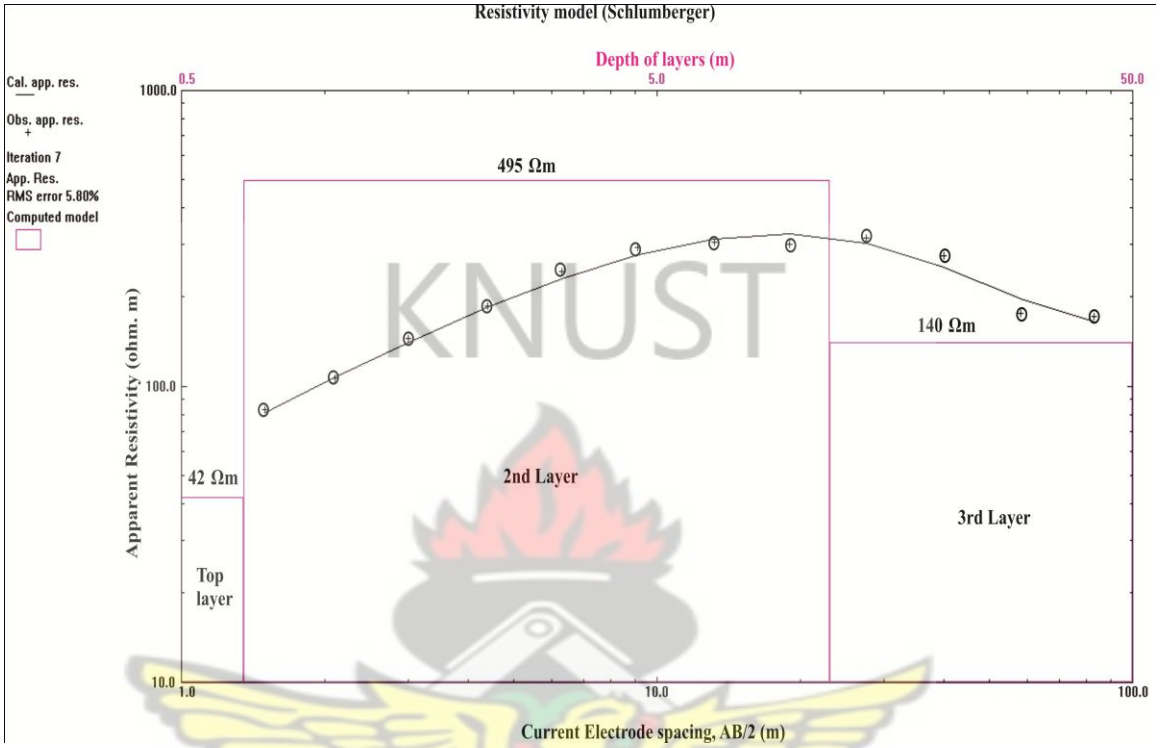

Fig. 4.3 VES curve at station A20 at Adomako

VES for A80

The geological section at station A80, suggests that the subsurface is made up of three layers as shown in Figure 4.4with apparent resistivity values ranging between 46 Ωm and 384 Ωm. The upper layer which has an apparent resistivity of 46 Ωm is 0.9 m thick followed beneath it by a second layer of resistivity, 384 Ωm and thickness, 12.7 m. The third layer, which is the deepest layer, has an apparent resistivity of 266 Ωm. It is inferred from these results that, the top layer is highly weathered and is underlain by slightly weathered layers. These might not host sufficient quantities of groundwater and hence, not worth considering in the drilling of boreholes.

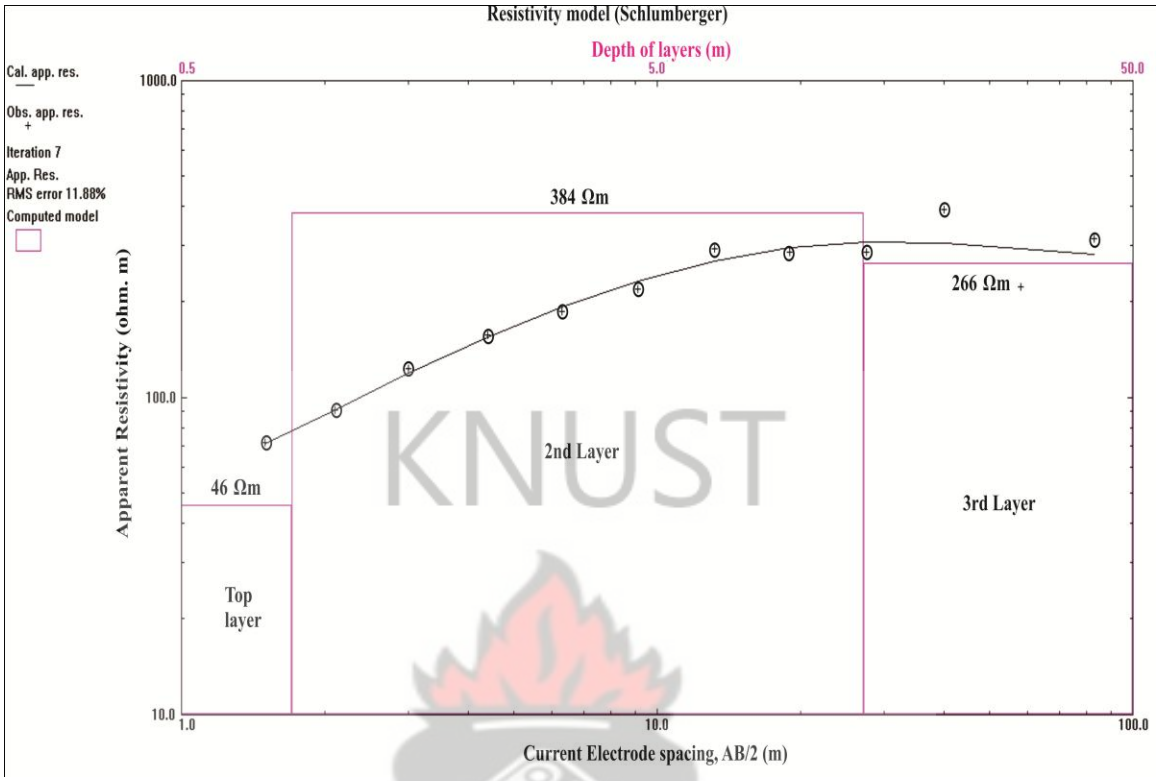

Fig. 4.4 VES curve at station A80 at Adomako

VES for A200

From the VES curve of station A200, the subsurface consists of three layers as shown in Figure 4.5. The apparent resistivity values range from 200 Ωm to 755 Ωm. The thickness and apparent resistivity of the first layer are 2.9 m and 212 Ωm. The second layer is 10.7 m thick and has a resistivity of 755 Ωm. The third layer however has the lowest apparent resistivity of 200 Ωm. It is apparent that the top layer might be moderately weathered and is underlain by a slightly weathered second layer. The resistivity of the deepest layer suggests a moderately weathered formation and could be a potential zone for water accumulation.

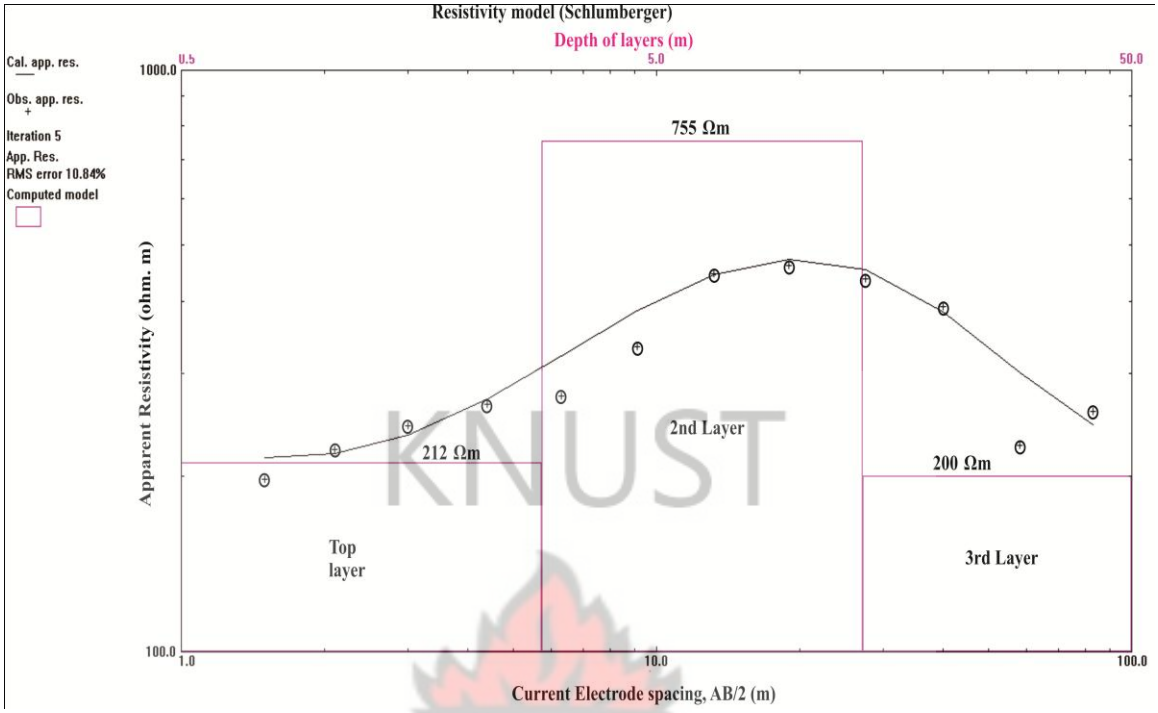

Fig. 4.5 VES curve at station A200 at Adomako

VES for SP1

The subsurface structure at station SP1 is made up of three layers of apparent resistivities ranging between 51 Ωm and 527 Ωm as shown in Figure 4.6. The results reveal that the topsoil has an apparent resistivity of 106 Ωm and is 1.4 m thick. The second layer with a thickness of 37.8 m has an apparent resistivity of 527 Ωm and is underlain by a third layer of resistivity 51 Ωm. The analysis of these results reveal a fairly weathered upper layer, a slightly weathered second layer and a moderately weathered third layer which could be a good zone for groundwater storage.

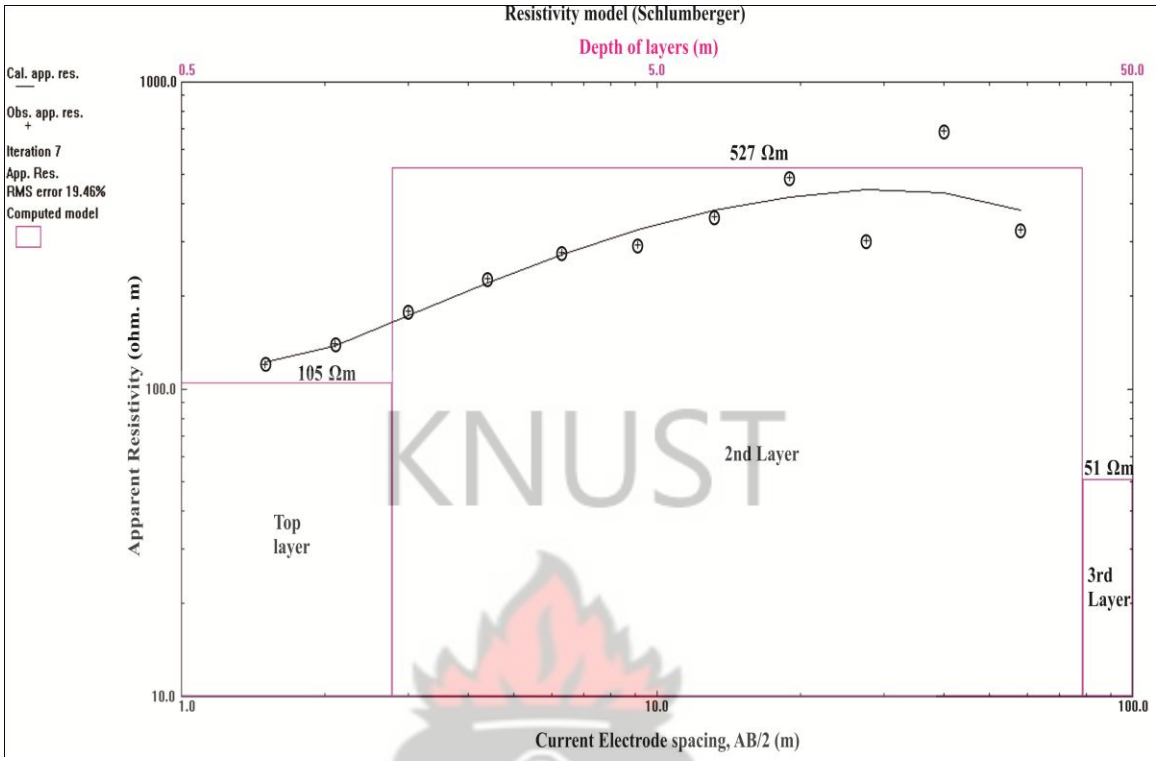

Fig. 4.6 VES curve at station SP1 at Adomako

On a whole, the results of the depth soundings conducted at Adomako reveal that there are three lithological layers and that the bedrock is moderately-fractured. Hence, groundwater potential is anticipated to be moderate in this area. The ranking of the various VES stations for test drilling based on their apparent resistivity values, thicknesses and depths are provided in Table 4.1 below. The best recommended station worth considering for test drilling in the community is A20, followed by A200, SP1 and A80 in order of importance. The results of the VES measurement are also presented in Appendix 2.

Table 4.1 Ranked VES points for test drilling at Adomako

Community	VES Point	Layer	Apparent Resistivity (Ωm)	Thickness (m)	Depth (m)	Rank
Adomako	A20	1 2 3	42 495 140	0.7 10.9 -	0.7 11.6 -	1
	A200	1 2 3	212 755 200	2.9 10.7 -	2.2 13.6 -	2
	SP1	1 2 3	105 527 51	1.4 37.8 -	1.4 39.2 -	3
	A80	1 2 3	46 384 266	0.8 12.7 -	0.8 13.5 -	4

4.1.2 Ankobea

One EM traverse of length 230 m was run in this community using the 20 m coil spacing. Three VES stations were also established including a spot sounding, which was chosen based on the nature of the geological settings of the area. The layout of the community is sketched and shown in Figure 4.7.

The profile was run on a bearing of 010^0 from the True North. Both curves of the HD mode and VD mode move erratically along the profile. From the graph as shown in Figure 5.8 below, it can be observed that the terrain conductivities of the VD mode were generally higher than that of the VD mode almost along the whole of the traverse. However, two significant cross over points (A20 and A230) at the 20 m and 230 m stations were chosen respectively for further investigation using the VES technique. Generally, the range of apparent conductivities measured in this community varied between 5 to 19 m mhos/m with an average value of 9.9 m mhos/m.

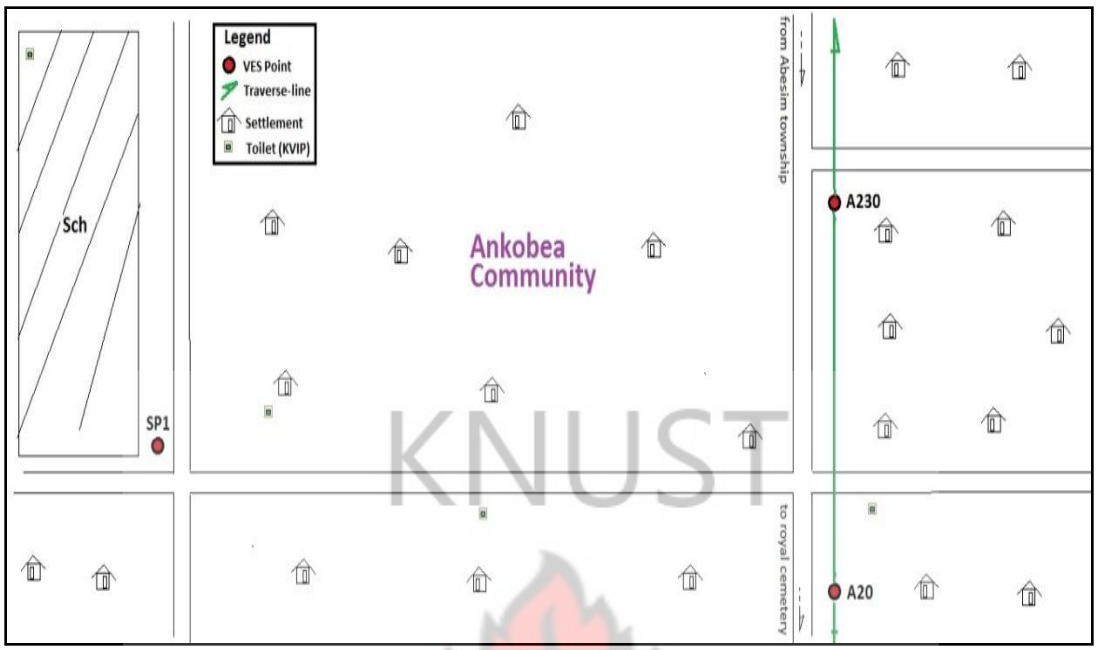

Fig. 4.7 A sketch of the layout of Ankobea community (Not to scale)

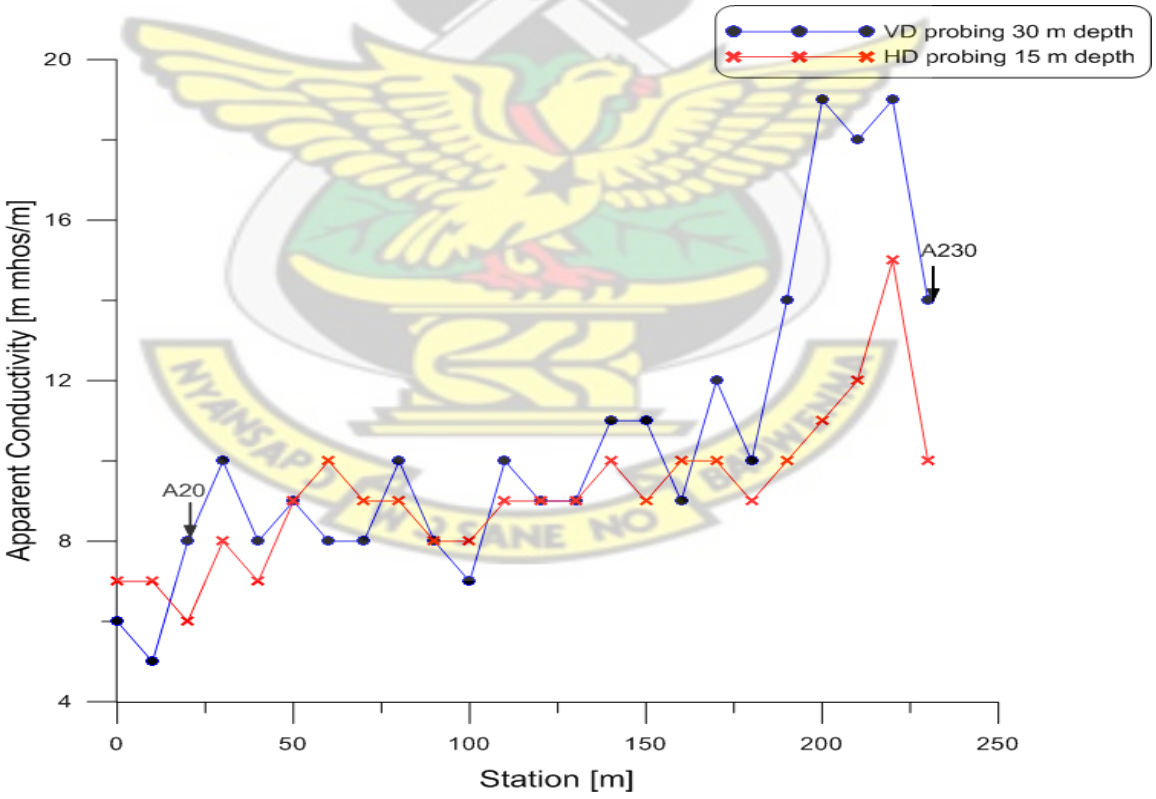

Fig. 4.8 EM terrain conductivity measurements along a profile at Ankobea

As previously mentioned, three VES stations were established at A20, A230 and SP1. The VES plots of the apparent resistivities with depth at these stations are shown in Figures 4.9 – 4.11.

VES for A20

The geological section at station A20 reveals that the subsurface structure consists of three layers with apparent resistivity values ranging between 56 Ωm and 3758 Ωm as shown in Figure 4.9. The upper layer has thickness and apparent resistivity values of 2.8 m and 149 Ωm and respectively whilst the second layer has a thickness of 9.5 m and a resistivity of 3758 Ωm. The third layer which is the deepest layer has an apparent resistivity of 56 Ωm. Analysis of these results reveal that the top layer is probably fairly weathered and underlain by a very resistive second layer. The deepest layer, which is most likely to be highly weathered in view of its low apparent resistivity value, could contain appreciable quantity of groundwater. Hence, it's considered to be a good borehole drilling point.

VES for A230

From the VES curve at station A230, it is observed that three lithological layers exist in the subsurface as shown in Figure 4.10. Apparent resistivity values generally range between 81 Ωm and 672 Ωm. The topsoil which is moderately weathered has apparent resistivity of 81 Ωm and thickness of 2.7 m. Below this layer is a second layer of apparent resistivity and thickness of 672 Ωm and 9.4 m and a third layer of resistivity 116

Ωm. The third layer may be fairly weathered and may probably host moderate amount of groundwater.

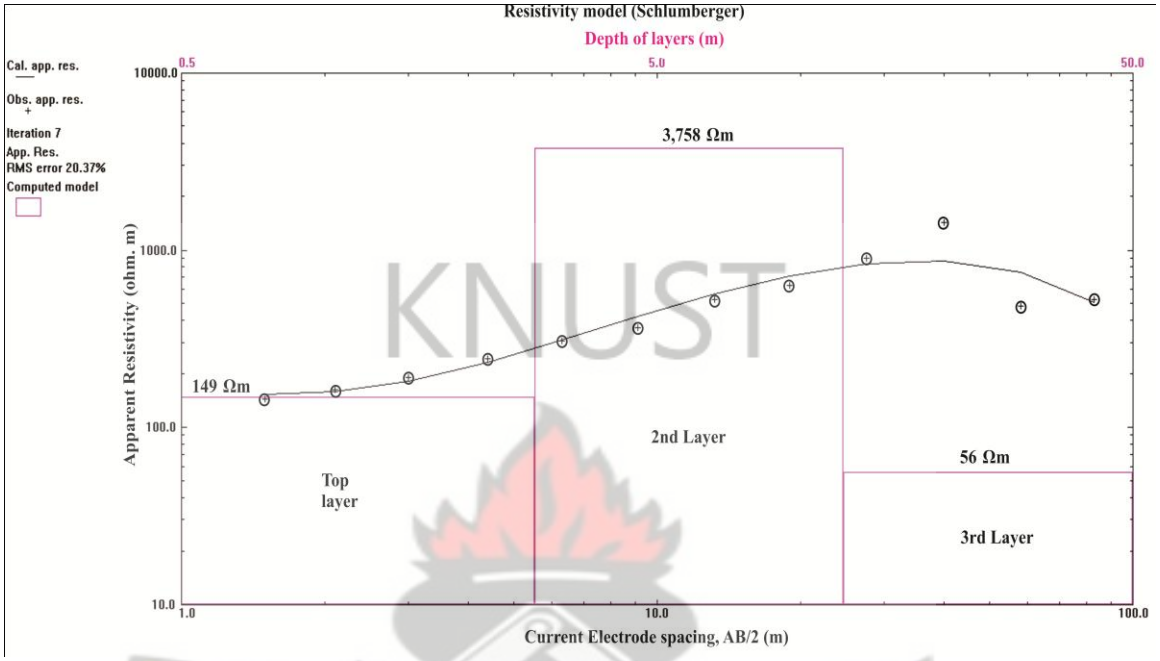

Fig. 4.9 VES curve of at station A20 at Ankobea

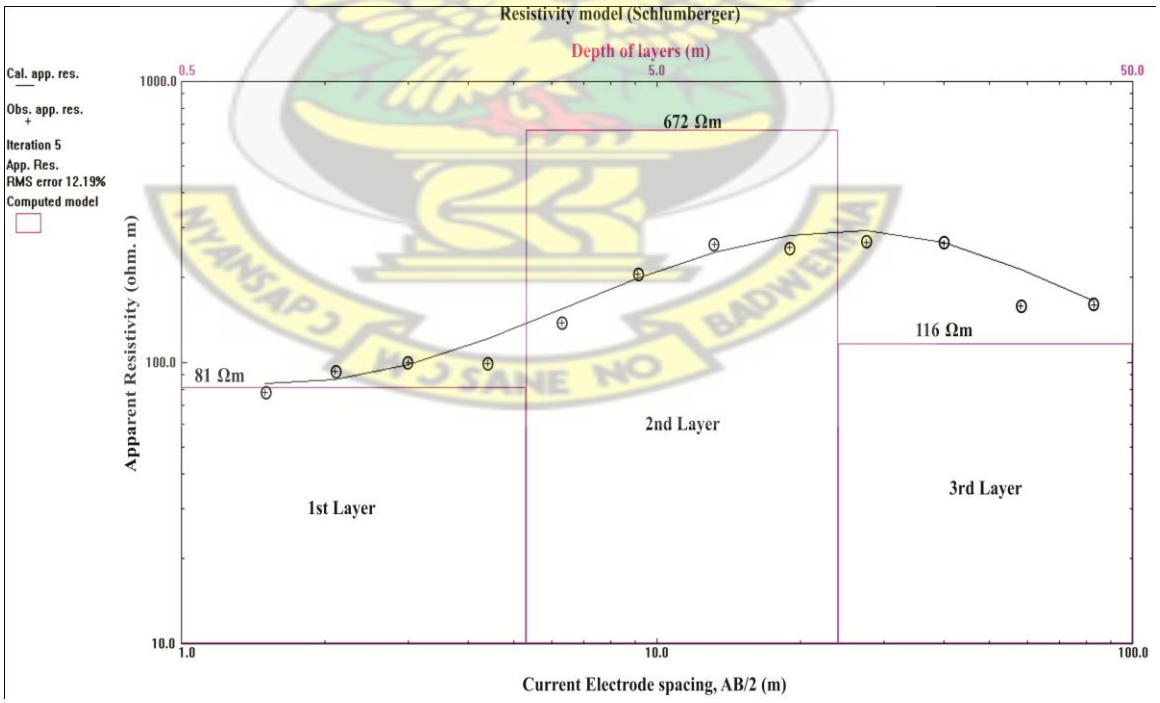

Fig. 4.10 VES curve at station A230 at Ankobea

VES for SP1

As shown in Figure 4.11, it is evident that the subsurface structure at station SP1 consists of three layers with apparent resistivity values ranging between 135 Ωm and 737 Ωm. The topsoil, which is 1.8 m thick has an apparent resistivity of 144 Ωm whereas the second layer has thickness and resistivity values of 18.9 m and 737 Ωm respectively. The third layer has apparent resistivity of 135 Ωm. These results depict that a slightly weathered second layer is sandwiched between two moderately weathered first and third layers. The third layer could probably host limited quantity of groundwater and hence, might not be reliable for borehole drilling.

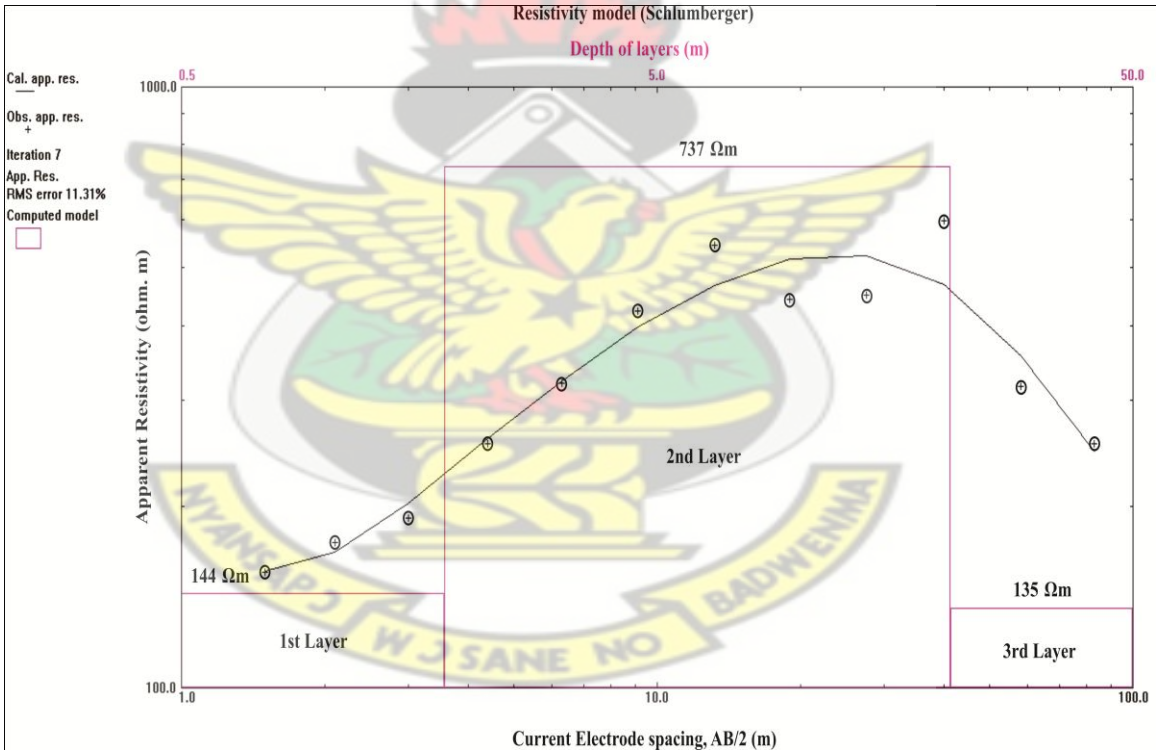

Fig. 4.11 VES curve at station SP1 at Ankobea

The apparent resistivity values obtained for this community reveals that the subsurface comprises three lithological units. Analysis also suggests that the bedrock is moderately

fractured and groundwater potential is expected to be moderate. The various stations are however ranked in order of the highest expected groundwater potential to the least and are shown in Table 4.2. From the Table, VES station A20 was considered the most suitable site for test drilling and station A230 was an alternate site.

Table 4.2 Ranked VES points for test drilling at Ankobea

Community	VES Point	Layer	Apparent Resistivity (Ωm)	Thickness (m)	Depth (m)	Rank
Ankobea	A20	1	149	2.8	2.8	1
		2	3,758	9.5	12.3	
		3	56	-	-	
	A230	1	81	2.7	2.7	2
		2	672	9.3	12	
		3	116	-	-	
	SP1	1	144	1.8	1.8	3
		2	737	18.9	20.7	
		3	135	-	-	

4.1.3 Antwikrom

Electromagnetic (EM) profiling was carried out along one traverse of length 70 m using 20 m coil spacing in this community. Three stations were chosen for further probing by the vertical electrical sounding (VES) method including one spot sounding. A schematic layout of the community showing the location of the traverse lines and the selected VES points is shown in Figure 4.12.

The EM traverse was run on a bearing of 134^0 from the True North. The results for the HD mode indicate that there is a decrease in terrain conductivity along the traverse up to the 20 m point with a value of 7 m mhos/m where a neck is obtained. The terrain conductivity then increases steadily up to 50 m point with a value of 10 m mhos/m and

then it finally decreases to a conductivity of 8 m mhos/m at the 70 m point. The curve of the VD mode indicates an increase in terrain conductivity up to the 10 m point with a value of 10 m mhos/m and then decrease to a conductivity of 7 m mhos/m at the 20 m point where there is a crossover point. The conductivity remains constant afterwards until it reached the 40 m point where it increased again to a conductivity value of 8 m mhos/m at the 60 m point. We obtained a crossover point between the HD and VD curve at this point hence, it was one of the points chosen for VES investigation. The terrain conductivity finally reduces at the end of the profile with a value of 8 m mhos/m. The range of conductivities in this community was generally between 7 and 25 m mhos/m. From the graph shown in Figure 4.13, two stations (A20 and A60) where we obtained an anomaly were selected for further VES probing.

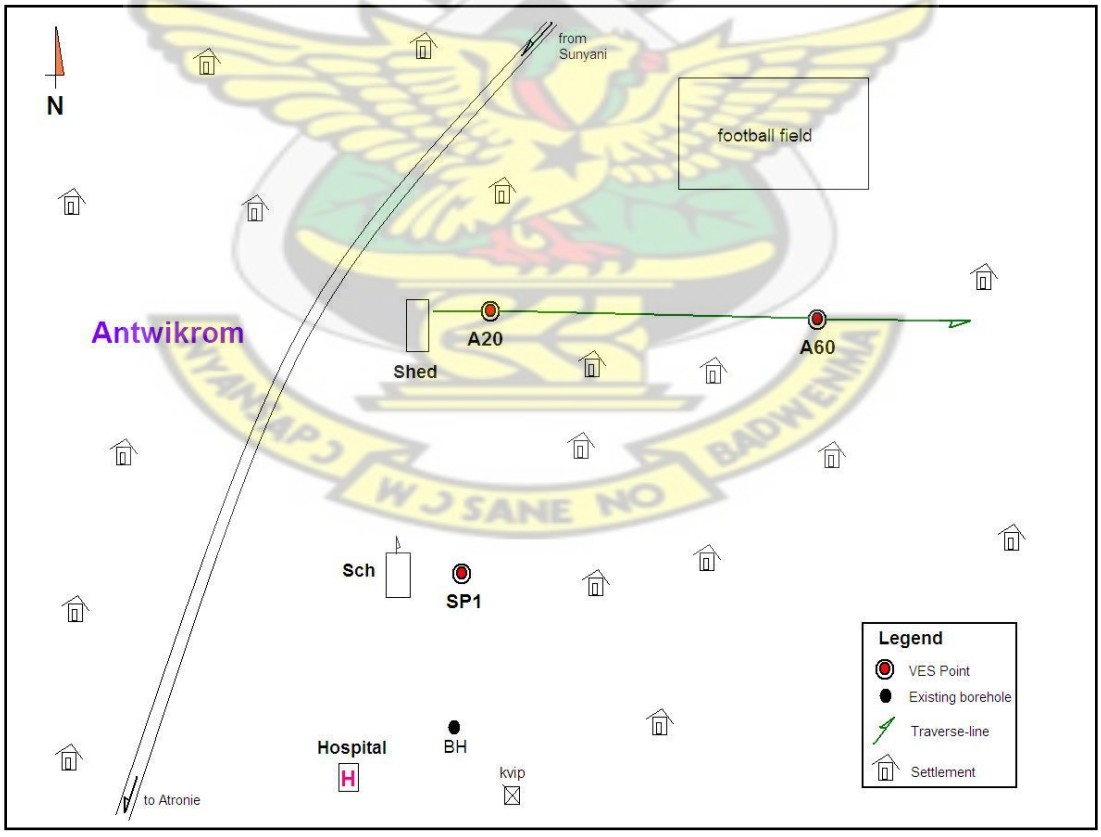

Fig. 4.12 A sketch of the layout of Antwikrom community (Not to scale)

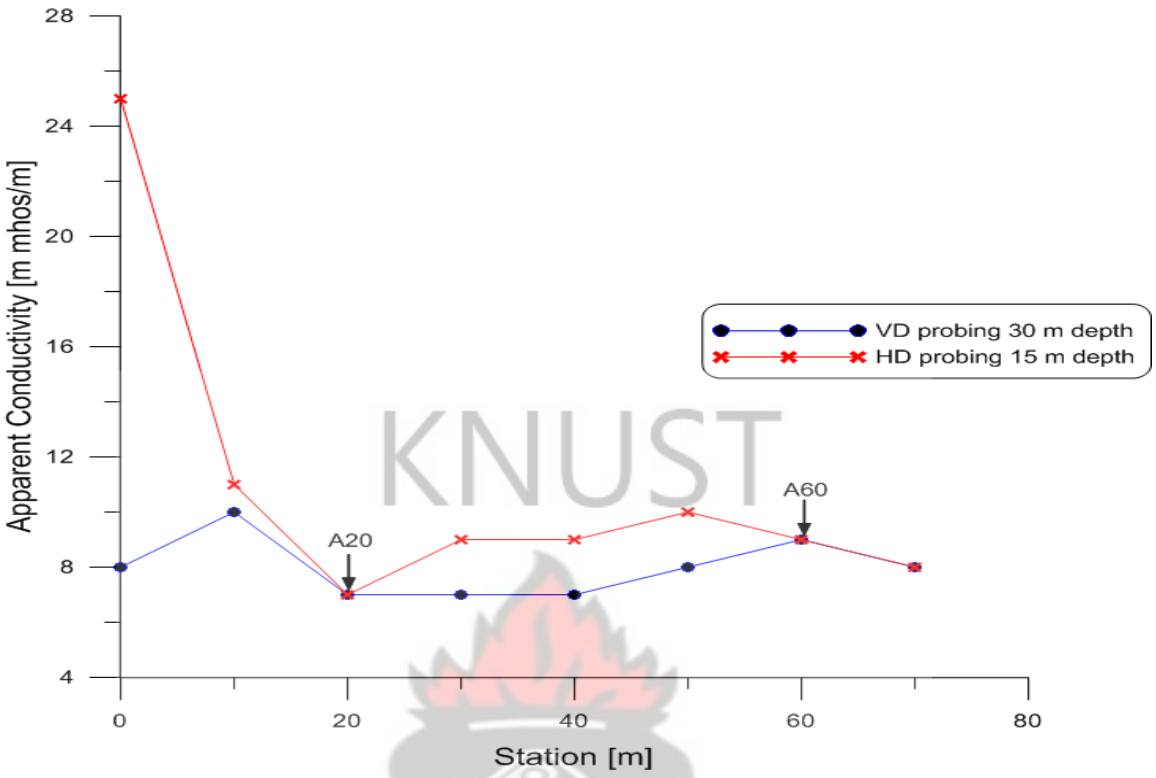

Fig. 4.13 EM terrain conductivity measurements along a profile at Antwikrom

VES for A20

The VES plots of apparent resistivity against depth at the three stations selected (A20, A60 and SP1) are shown in Figures 4.14 – 4.16.

Results from the VES curve at station A20 as shown in Figure 4.14reveals three layers in the subsurface with the top layer having an apparent resistivity of 15 Ωm and a thickness of 0.5 m. The second layer, which is 9.6 m thick has an apparent resistivity of 121 Ωm and is underlain by a third layer of resistivity 1058 Ωm. Deductions made from these results suggests that the topsoil is highly weathered and it is underlain by a moderately weathered second layer which could be a good zone for water accumulation. It is apparently underlain by a very high resistive rock.

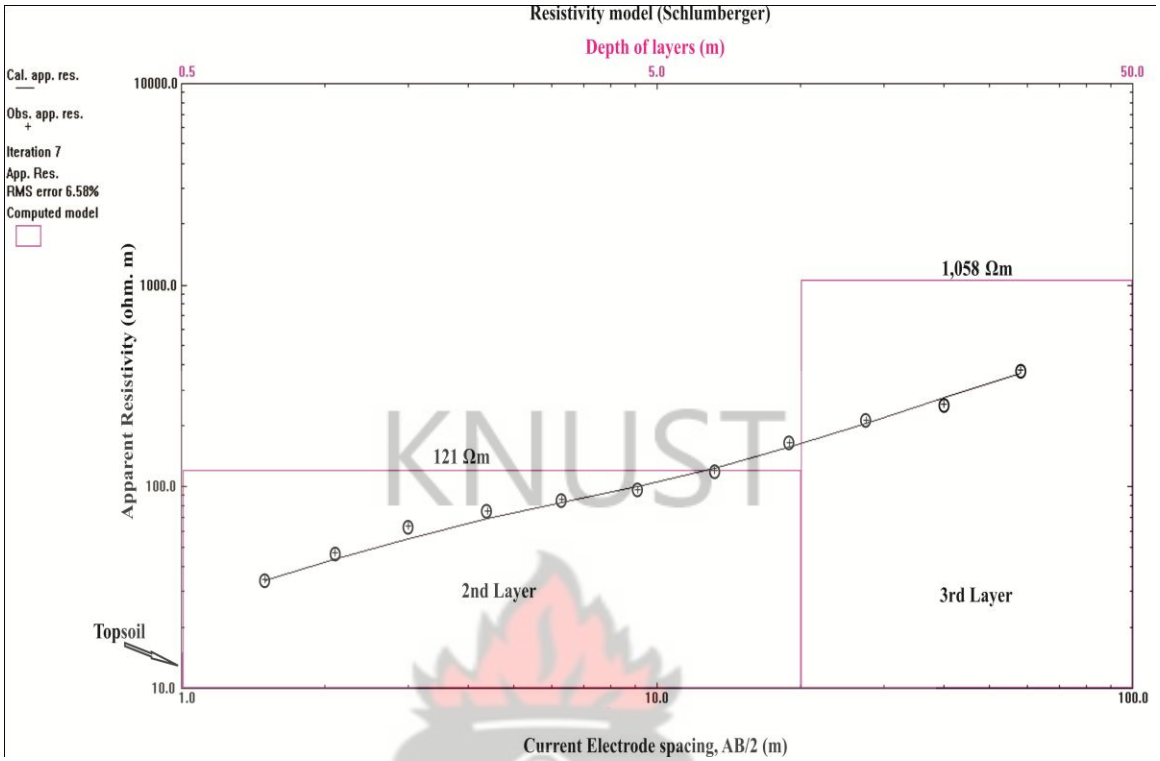

Fig. 4.14 VES curve at station A20 at Antwikrom

VES for A60

VES curve analysis at station A60 revealed a three layered structure as shown in Figure 4.15. The apparent resistivity values range between 76 Ωm and 1376 Ωm. The upper layer, indicative of an apparently weathered formation has a resistivity of 76 Ωm and is 2.2 m thick. Underlying this is a presumably highly resistive second layer with resistivity of 1376 Ωm and a thickness of 12.6 m whilst the deepest layer has an apparent resistivity of 378 Ωm. This is suggestive of a moderately weathered formation and the extent of resistivity variation from the second to the third layer indicates that this layer could host sufficient amount of groundwater. This site could be good for borehole drilling.

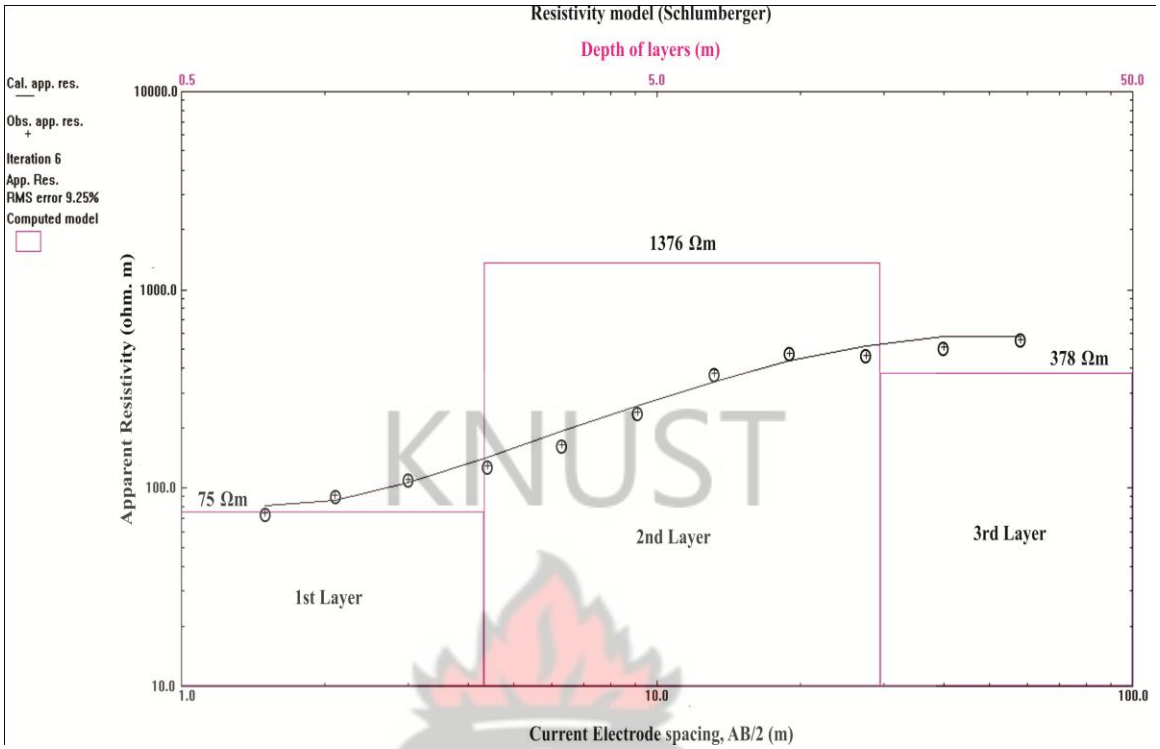

Fig. 4.15 VES curve at station A60 at Antwikrom

VES for SP1

Analysis of the spot sounding at station SP1 depict that the subsurface consists of four layers with apparent resistivity values ranging between 72 Ωm and 1566 Ωm as shown in Figure 4.16. The topsoil, which depicts a fairly weathered formation has apparent resistivity and thickness of 101 Ωm and 1.1 m respectively and has a weathered layer beneath it of resistivity 72 Ωm and thickness of 0.9 m. The third layer is 23.4 m thick and has an apparent resistivity of 368 Ωm. This layer is likely to be moderately weathered and could possibly host some amount of groundwater. The last layer is highly resistive.

The results of the geophysical investigation indicate three lithological units underlying the points except the spot sounding station, SP1 which comprise four geological units. The bedrock is slightly weathered. The aquifer is expected to be intercepted in the

overburden. The ranking of the various stations based on these results are shown in Table 4.3. The best ranked site for test drilling was at station A60.

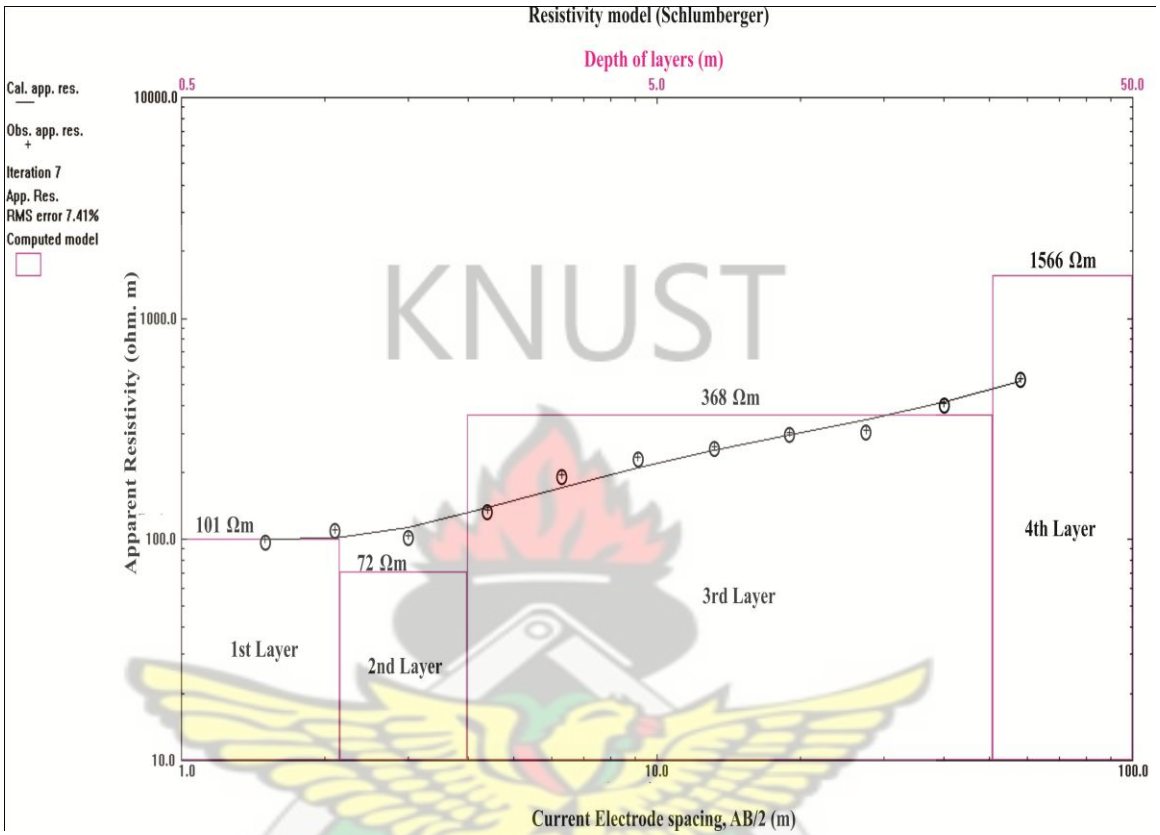

Fig. 4.16 VES curve at station SP1 at Antwikrom

Table 4.3 Ranked VES points for test drilling at Antwikrom

Community	VES Point	Layer	Apparent Resistivity (Ωm)	Thickness (m)	Depth (m)	Rank
Antwikrom	A60	1 2 3	75 1376 378	2.1 12.6 -	2.1 14.7 -	1
	A20	1 2 3	15 121 1058	0.5 9.6 -	0.5 10.1 -	2
	SP1	1 2 3 4	101 72 368 1566	1.1 0.9 23.4 -	1.1 2 25.4 -	3

4.1.4 Abesim Zongo

Electromagnetic profiling was conducted along a profile of length 210 m in this community. In addition to the two vertical electrical depth soundings established based on the results of EM traverse, a spot sounding was also conducted. The schematic layout of the community showing the traverse and the VES points is shown in Figure 4.17.

The EM profiling was conducted on a bearing of $046^0$from the True North using 20 m coil spacing. As shown in Figure 4.18, the results of the EM traverse revealed that apparent conductivities generally varied between 7 – 25 m mhos/m with an average value of 10.3 m mhos/m. The curve of the VD mode showed very high conductivities up to the 90 m point with a conductivity of 25 m mhos/m as compared to that of the HD mode. However, the apparent conductivity reduced drastically to 10 m mhos/m at the 100 m point. Apparent conductivities remained lower than that of the HD mode from this point until an anomaly is obtained at point 190 m with conductivity reaching 10 m mhos. The conductivity then reduced to 9 m mhos/m and then increased up at 10 m mhos/m again at the end of the profile. Conductivities were generally lower in the HD mode. From the HD mode curve, apparent conductivities were constant until the 60 m point with a value of 9 m mhos/m and then increased to a value of 12 m mhos/m at the 90 m point. Apparent conductivity then decreased to 10 m mhos/m at the 110 m point after which it remained constant up to the 160 m point. The curve then became erratic till the end of the profile with a conductivity value of 9 m mhos/m. Two stations A10 and A90 were chosen along this profile for investigation by the VES techinique.

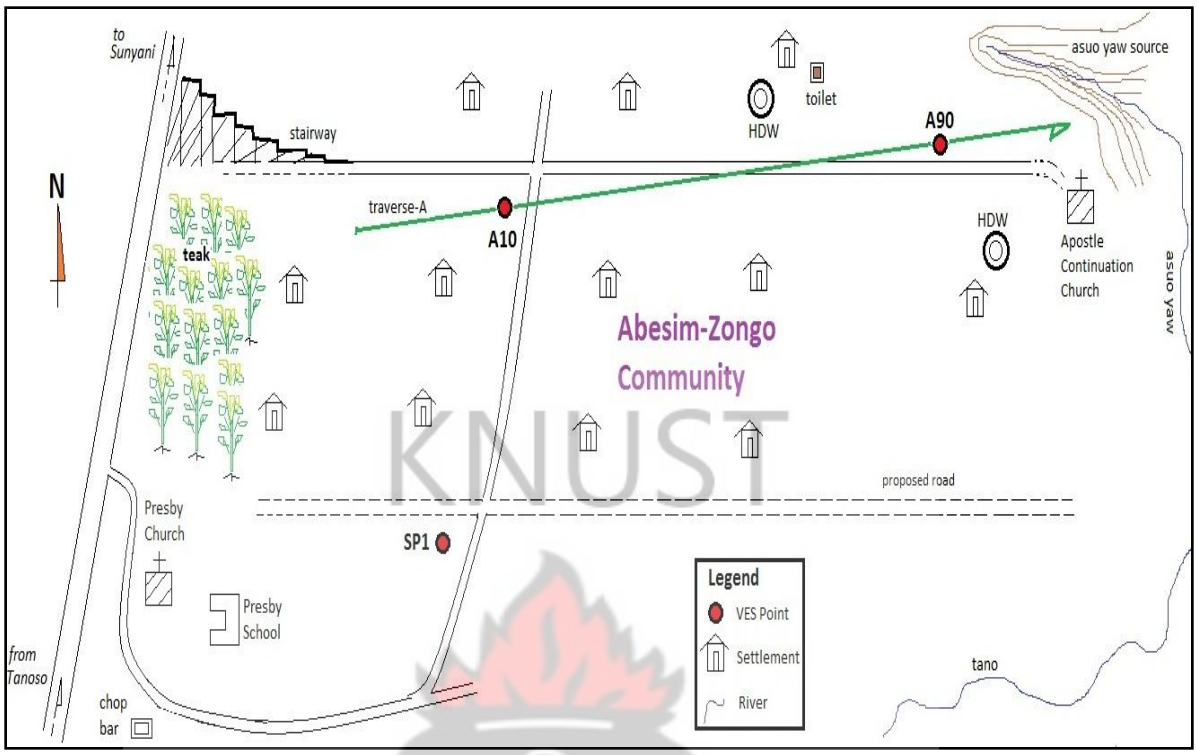

Fig. 4.17 A sketch of the layout of Abesim Zongo community (Not to scale)

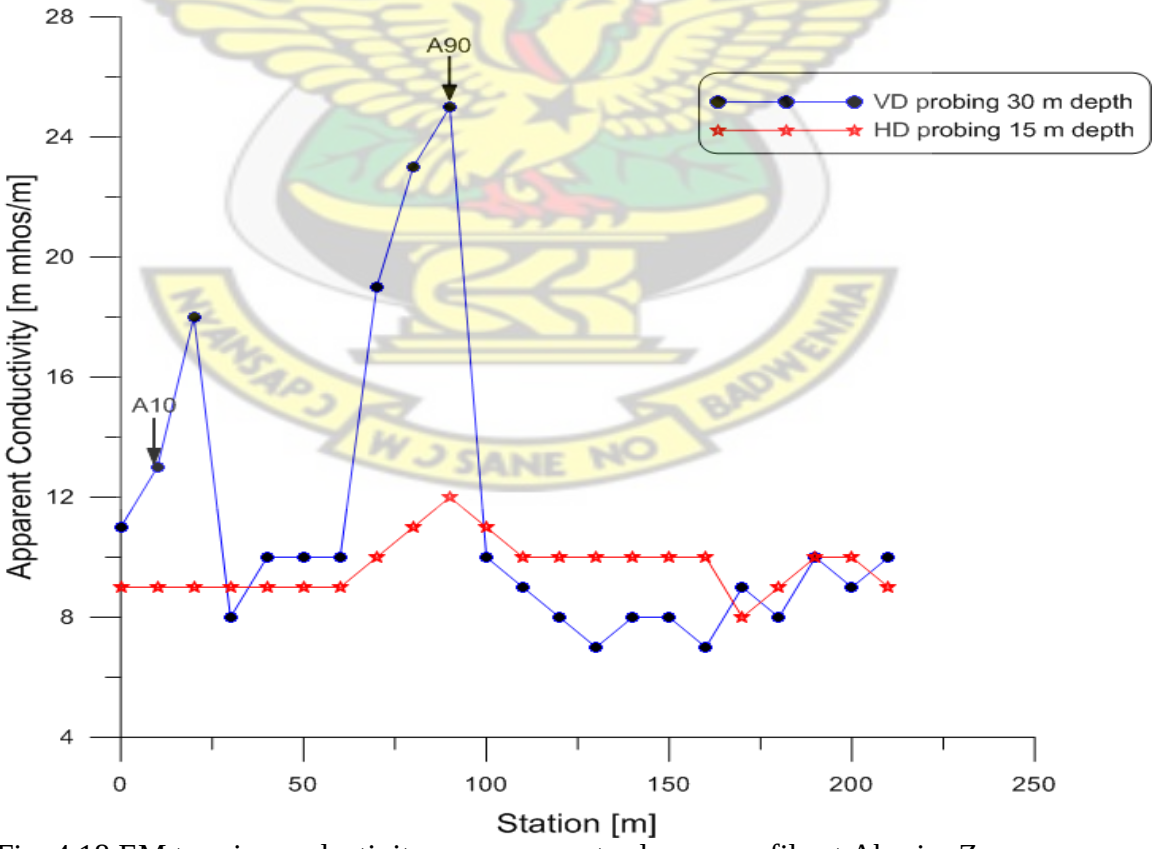

Fig. 4.18 EM terrain conductivity measurements along a profile at Abesim Zongo

Three stations A10, A90 and SP1 were selected and probed further to assess their groundwater potential using the VES method as shown in Figures 4.19 – 4.21.

VES for A10

As shown in the VES graph (Figure 4.19), three layers exist in the subsurface of station A10. Apparent resistivities were in the range of 87 Ωm to 293 Ωm with the first layer resistivity and thickness of 87 Ωm and 2m. The second layer resistivity and thickness was 293 Ωm and 16.2 m whilst the third layer had an apparent resistivity value of 153 Ωm. Analysis of these results indicate that the topsoil is weathered and underlain by moderately weathered second and third layers, which could contain sufficient amount of groundwater.

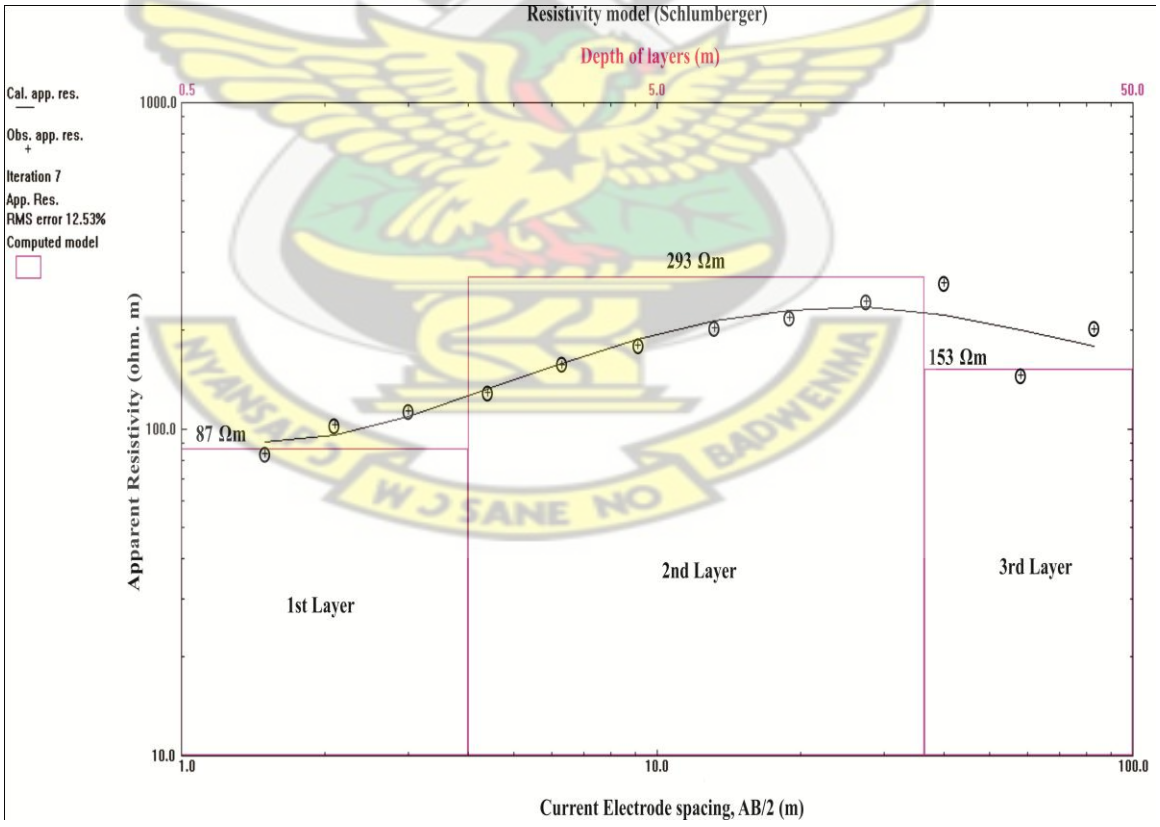

Fig.4.19 VES curve at station A10 at Abesim Zongo

VES for A90

VES curve analysis at station A90 (Figure 4.20) similarly revealed three subsurface layers. Apparent resistivities varied between 28 Ωm at the upper layer with 0.9 m thickness to 370 Ωm at the bedrock. The second layer is 7.1 m thick and 112 Ωm. From the results of the sounding at this station, it is inferred that the topsoil is highly weathered and the second layer which is fairly weathered could be a zone for adequate water accumulation.

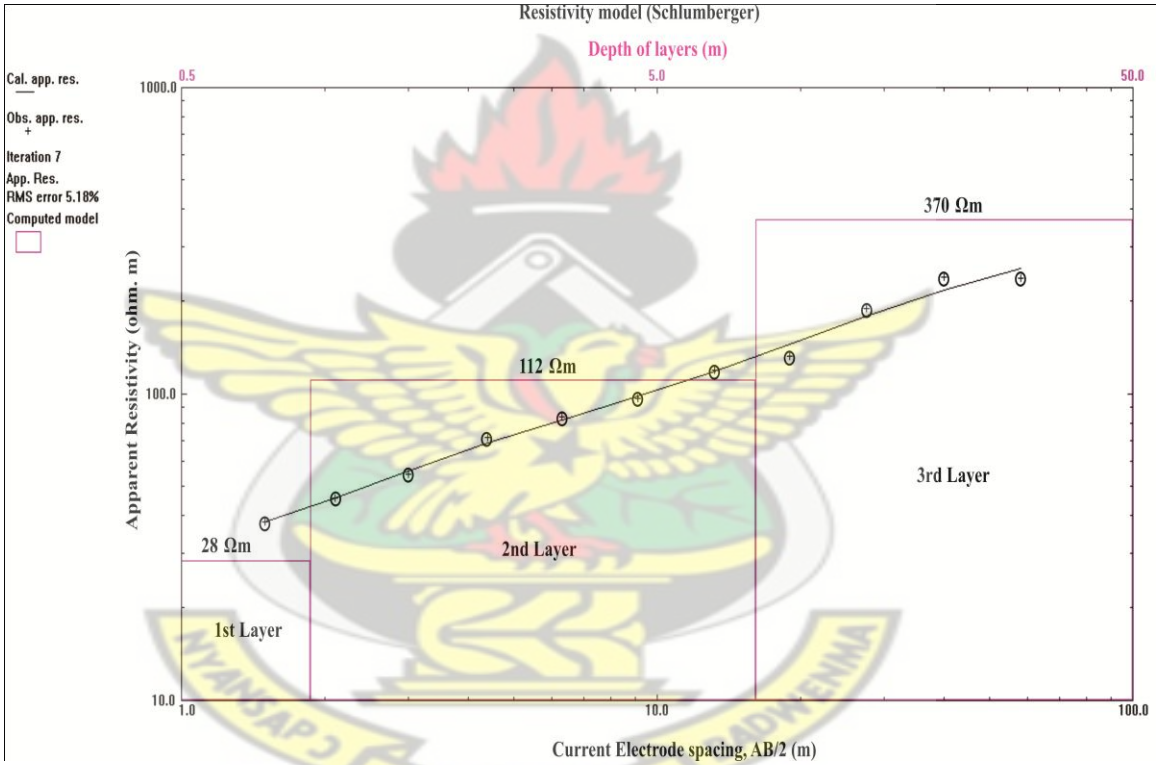

Fig. 4.20 VES curve at station A90 at Abesim Zongo

VES for SP1

Analysis of the VES curve at station SP1 as shown in Figure 4.21 reveals a four-layered structure at the subsurface. Apparent resistivities range between 54 Ωm at the upper layer with a thickness of 0.8 m to 1138 Ωm at the last layer. The second layer is 3.6 m thick

and has an apparent resistivity of 859 Ωm whilst the third layer has thickness and apparent resistivity of 43.7 m and 204 Ωm respectively. Deductions made from these results indicate that the topsoil is highly weathered and underlain by a slightly weathered second layer. Beneath this layer is a probably moderately weathered third layer where the aquifer is expected to be located. The deepest layer is characteristic of a very high resistive rock.

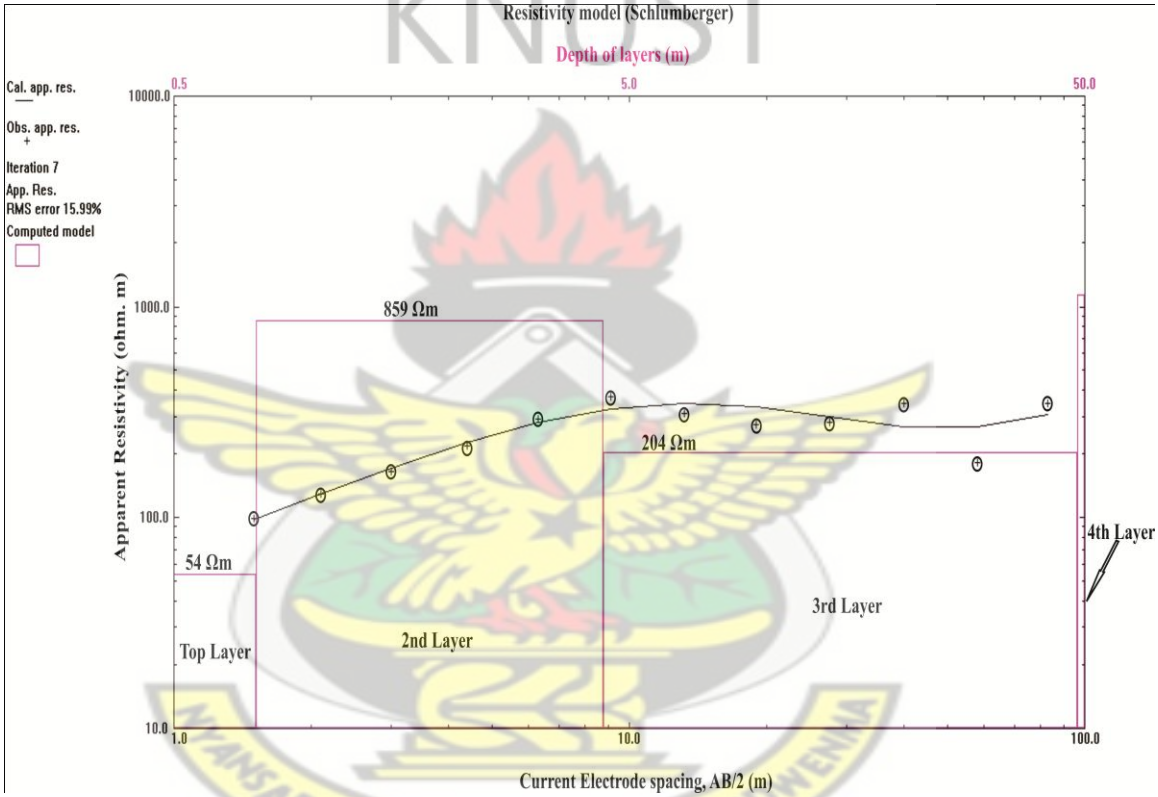

Fig. 4.21 VES curve at station SP1 at Abesim Zongo

From the apparent resistivity values obtained, it can be inferred that the bedrock is moderately fractured and the groundwater potential in this community is expected to be moderate. Ranking for the test drilling based on the groundwater prospects at the various

sounding stations are compiled and presented in Table 4.4. Station A10 was rated the best site for borehole drilling and station A90 unsuitable.

Table 4.4 Ranked VES points for test drilling at Abesim Zongo

Community	VES Point	Layer	Apparent Resistivity (Ωm)	Thickness (m)	Depth (m)	Rank
Abesim Zongo	A10	1	87	2.0	2.0	1
		2	293	16.2	18.2	
		3	153	-	-	
	SP1	1	54	0.8	0.8	2
		2	859	3.6	4.4	
		3	204	43.7	48.1	
		4	1138	-	-	
	A90	1	28	0.9	0.9	3
		2	112	7.1	8	
		3	370	-	-	

4.1.5 Charleskrom

Two EM traverses (one of length 80 m and the other 90 m) were run with the inter-coil spacing of 20 m in this community. Three sounding points were selected for VES as shown in Figure 5.25 – 5.27. VES point A70 was established on profile A, VES point B60 was established on profile B and VES point SP1 was a spot sounding. The schematic layout of the traverse lines and the VES points in this community is shown in Figure 4.22 below.

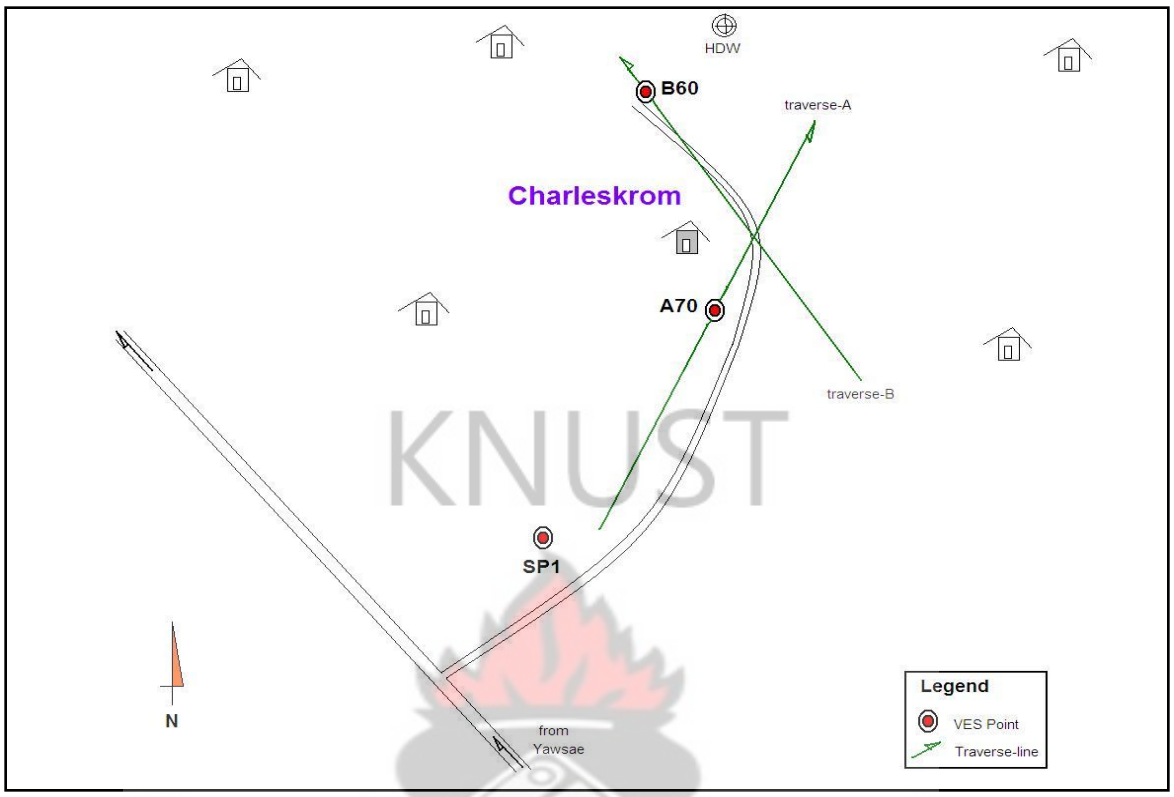

Fig. 4.22 A sketch of the layout of Charleskrom community showing the traverse lines and VES points (Not to scale)

The EM traverse on profile A of length 80 m was run on a bearing of 016^0 from the True North. Figure 4.23 shows higher conductivities for the HD values than the VD values along most of the profile indicating a general decrease in weathering with depth along the profile. From the HD curve, the apparent conductivity remained constant at 6 m mhos/m along the profile except at the 40 m and 70 m marks where conductivities changed to 5 m mhos/m and 7 m mhos/m respectively. The graph of the VD mode was erratic. However, conductivities were constant at 3 m mhos/m between the 10 m and 30 m points and also between the 60 m and 80 m points with conductivity of 7 m mhos/m. One VES station

was selected along this profile at the 70 m mark where both HD and VD values were the same.

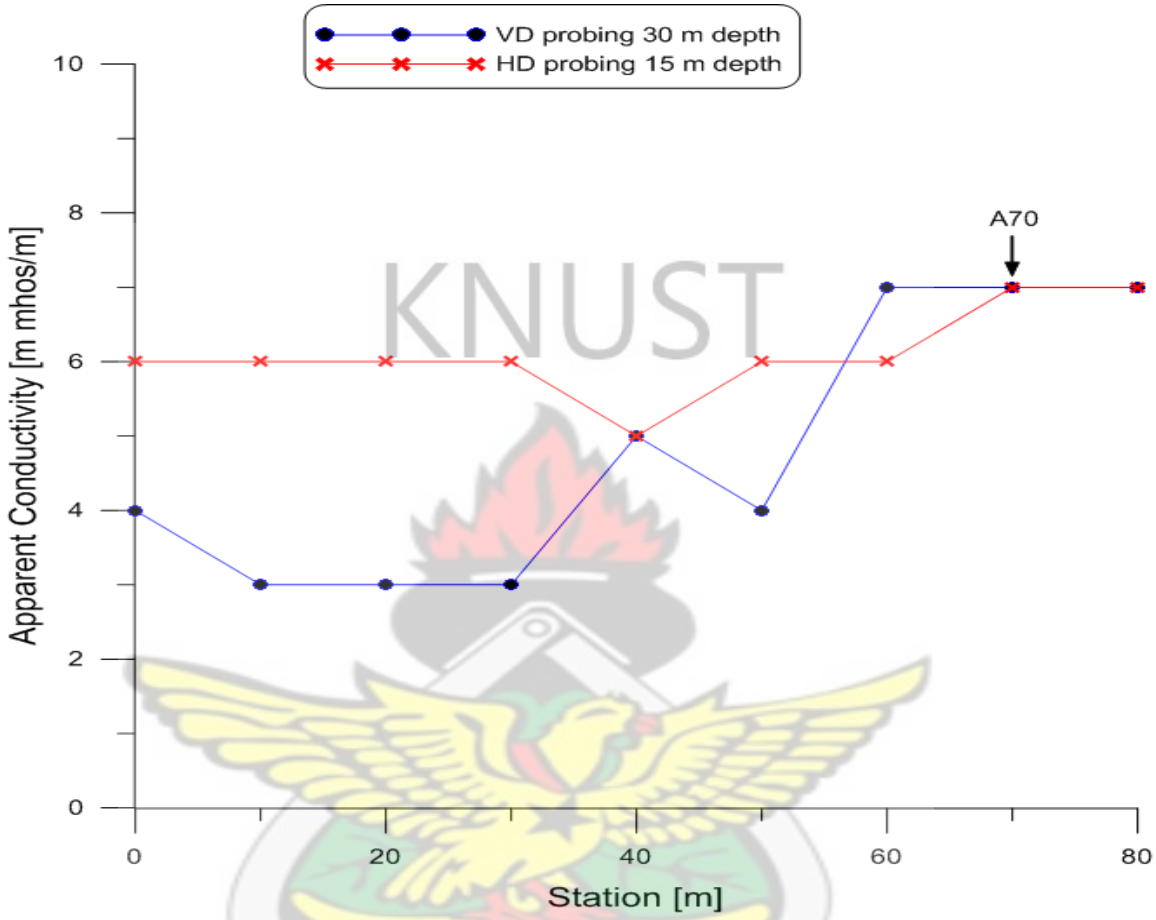

Fig. 4.23 EM terrain conductivity measurements along profile A at Charleskrom

The EM traverse on profile B of length 90 m was run on a bearing of 332^0. Apparent conductivity values varied from 3 –9 m mhos/m. As presented in Figure 4.24, HD values were generally higher than the VD values again confirming the decrease in weathering with depth along the profile. Nevertheless, higher conductivities were observed for the VD curve from the 60 m to 70 m points, hence, station B60 was chosen for further probing using the VES technique.

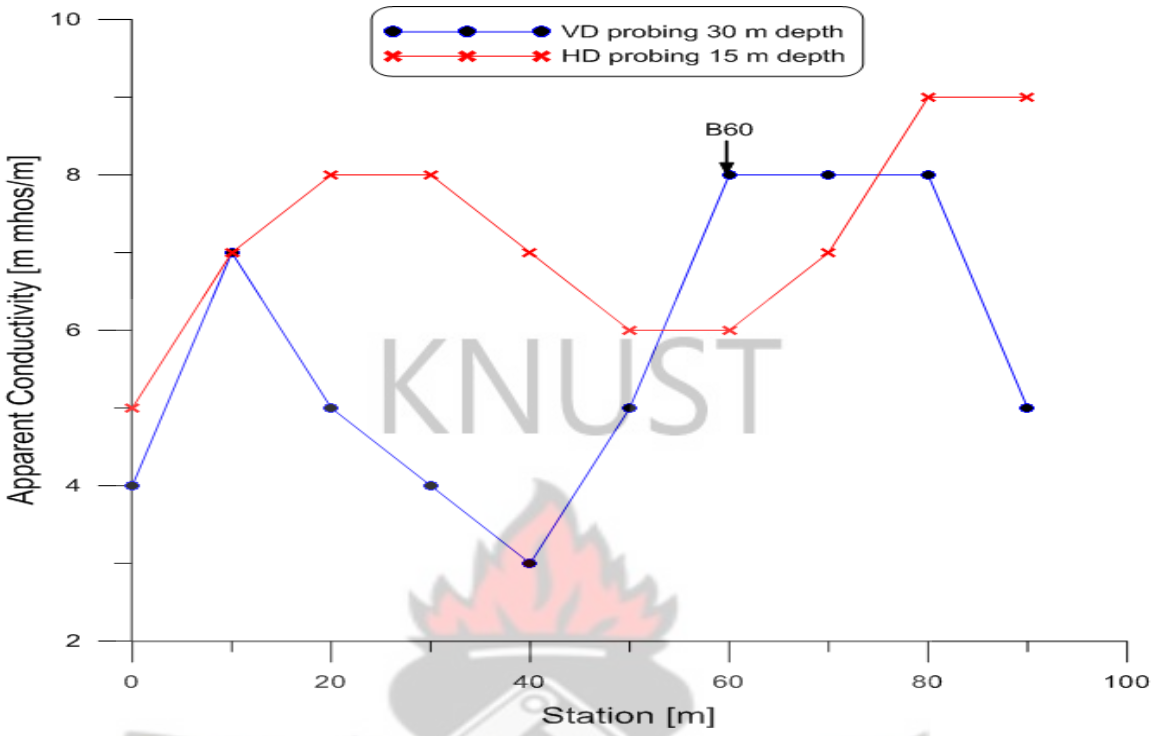

Fig. 4.24 EM terrain conductivity measurements along profile B at Charleskrom

VES for A70

Four subsurface layers exist at the VES point A70 as shown in Figure 4.25. Results obtained showed low to high resistivity, varying from 5 Ωm to 3627 Ωm. The topsoil may be fairly weathered with 274 Ωm resistivity and 2.4 m thickness. Below this layer is a possibly weathered second layer which is 0.8 m thick and has an apparent resistivity of 94 Ωm, and it is underlain by a very resistive third layer characterized by an apparent resistivity and thickness of 3627 Ωm and 5.2 m respectively. The bedrock is inferred to be highly weathered in view of the very low resistivity of 5 Ωm. This layer could contain very high amount of groundwater and it could have good prospect for borehole drilling.

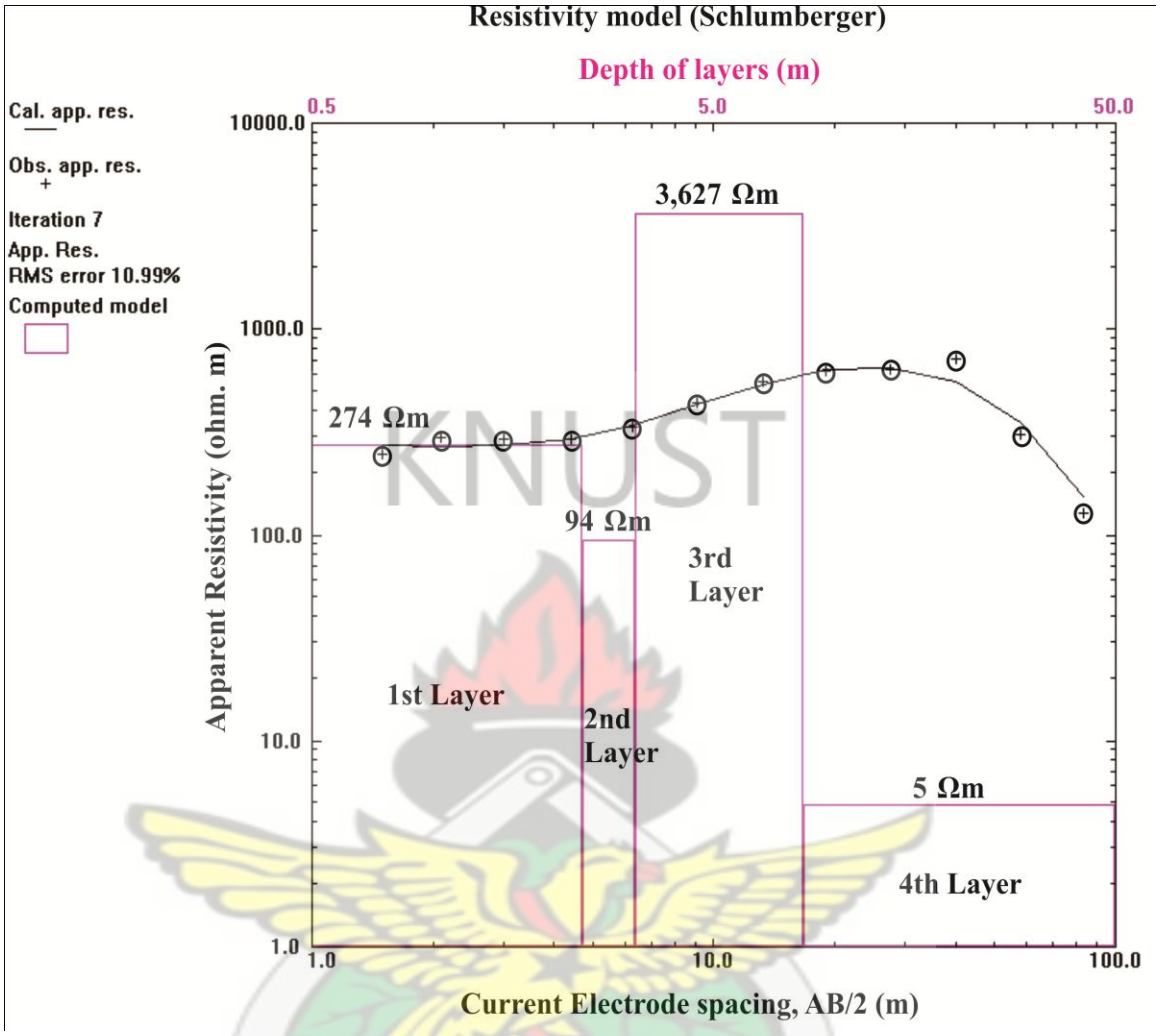

Fig. 4.25 VES curve at station A70 at Charleskrom

VES for B60

Results obtained from VES station B60 similarly indicated a four-layered subsurface structure with apparent resistivities varying from low to very high values (59 Ωm – 32189 Ωm) as shown in Figure 4.26. The upper layer, which is 0.5 m thick, has resistivity of 78 Ωm and it is characteristic of a weathered formation. It is underlain by a more resistive second layer of thickness and resistivity of 1 m and 2618 Ωm. The third layer is

4 m thick and has a resistivity of 59 Ωm whilst the bedrock resistivity is 32189 Ωm. The aquifer is expected to be intercepted in the third layer.

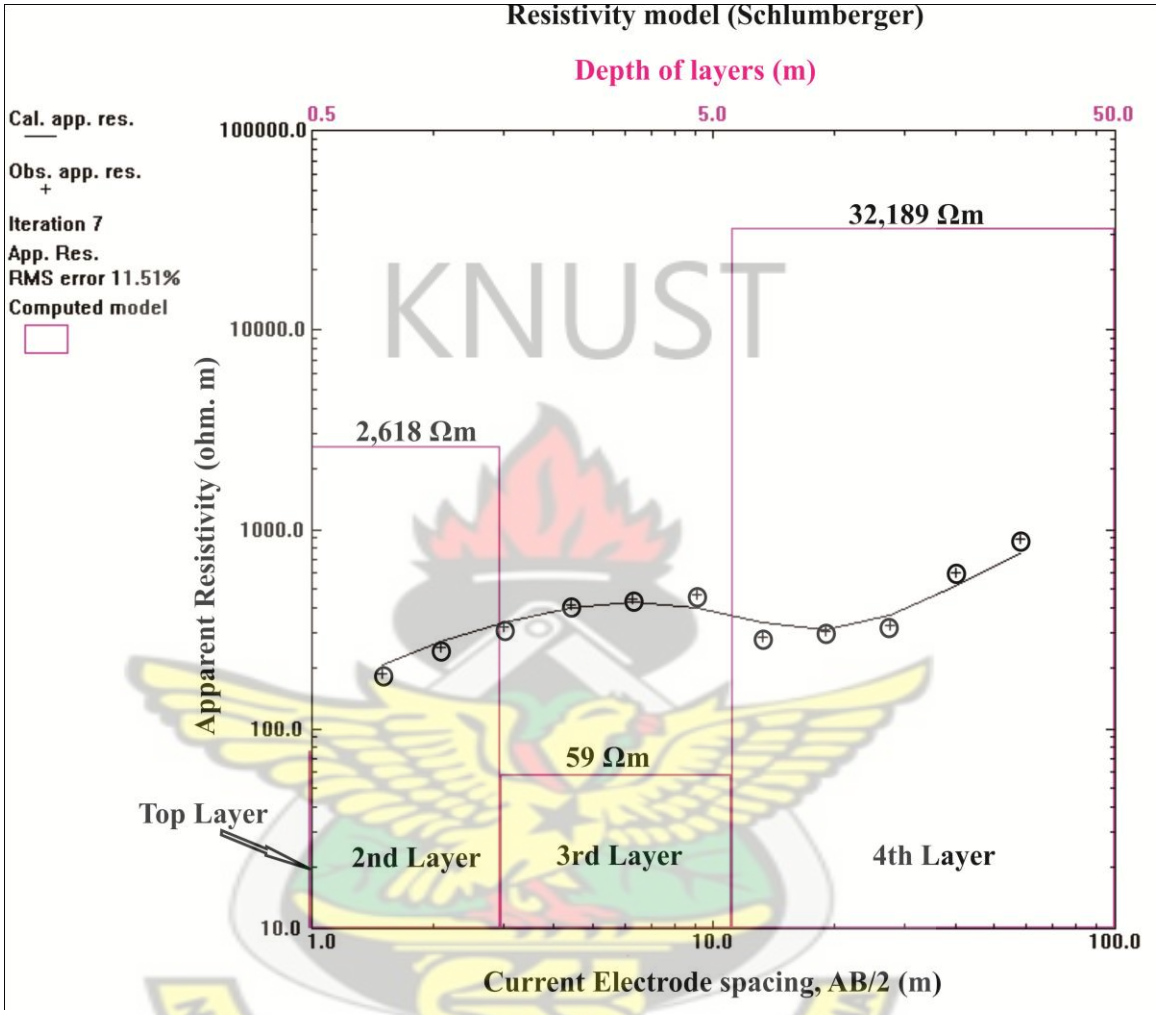

Fig. 4.26 VES curve at station B60 at Charleskrom

VES for SP1

Results obtained from the VES at station SP1 shows that three layers exist in the subsurface as shown in Figure 4.27 below. Apparent resistivities were in the range of 222 Ωm to 4416 Ωm. The resistivity values of the layers indicate high resistive rock sandwiched between moderately weathered first and third layers. Appreciable quantity of

water is expected in the third layer. The apparent resistivities and thicknesses of the layers from the first to the third are 239 Ωm and 2 m, 4416 Ωm and 4.4 m and 222 Ωm respectively.

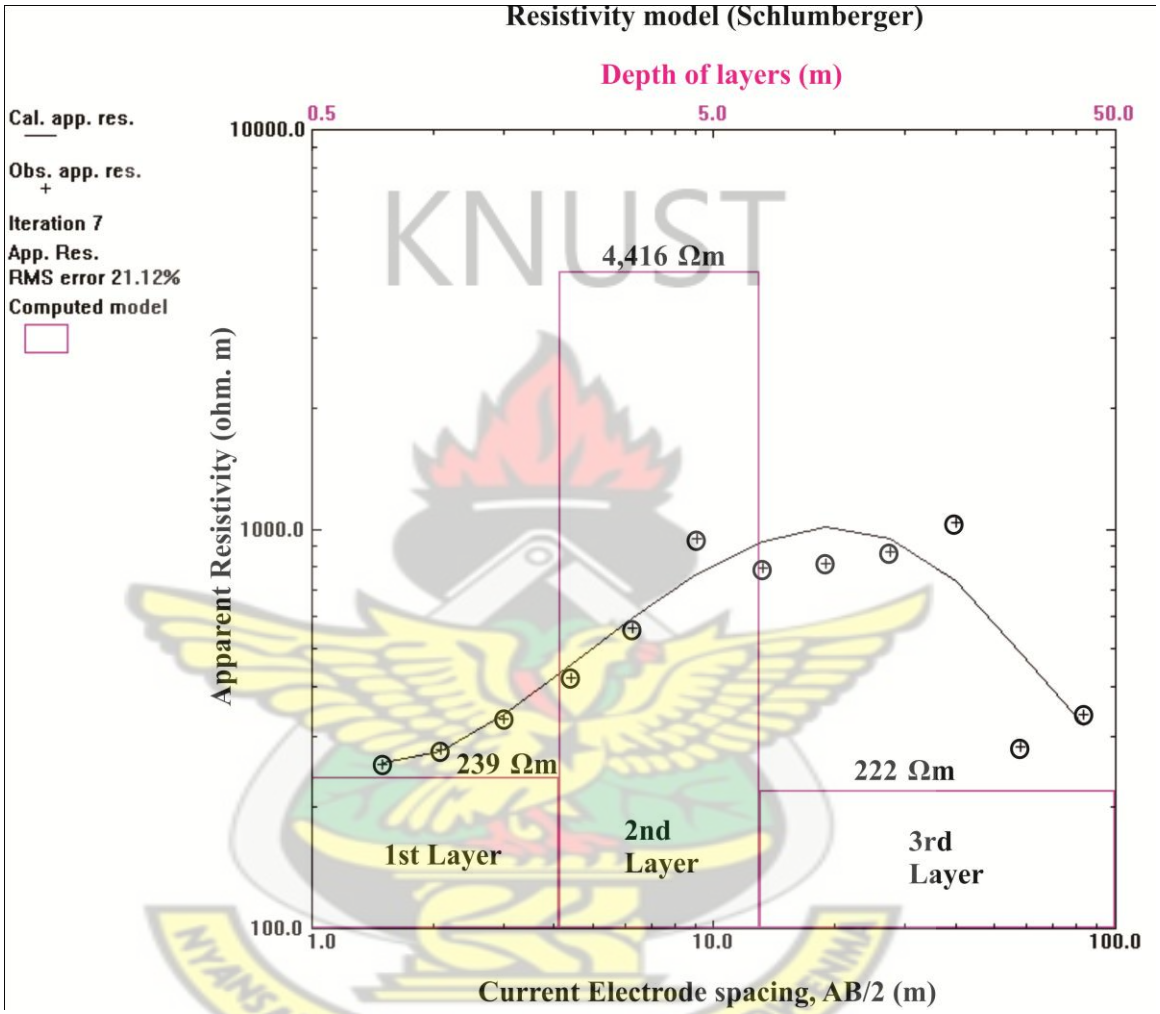

Fig. 4.27 VES curve at station SP1 at Charleskrom

Generally, this community is underlain by four subsurface geological layers except at station SP1 which has three lithological layers. The results indicate moderately fractured rocks in the third layer. From the sounding results, the stations were ranked in order of

their groundwater potentials. Table 4.5 gives information on the recommended drilling sites. The main test drilling point is A70 and SP1 is the alternative drilling point.

Table 4.5 Ranked VES points for test drilling at Charleskrom

Community	VES Point	Layer	Apparent Resistivity (Ωm)	Thickness (m)	Depth (m)	Rank
Charleskrom	A70	1	274	2.4	2.4	1
		2	94	0.8	3.2	
		3	3,627	5.2	8.4	
		4	5	-	-	
	SP1	1	239	2.1	2.1	2
		2	4,416	4.4	6.5	
		3	222	-	-	
	B60	1	78	0.5	0.5	3
		2	2,618	1.0	1.5	
		3	59	4.1	5.6	
		4	32,189	-	-	

4.1.6 Domsesre

In this community, two orthogonal EM traverses were conducted and three potential groundwater points (A120, A230, and B220) were chosen for VES. VES points A120 and A230 were selected along profile A, whilst B220 was selected along profile B. The schematic layout of this community showing the profile lines and VES points are shown in Figure 4.28.

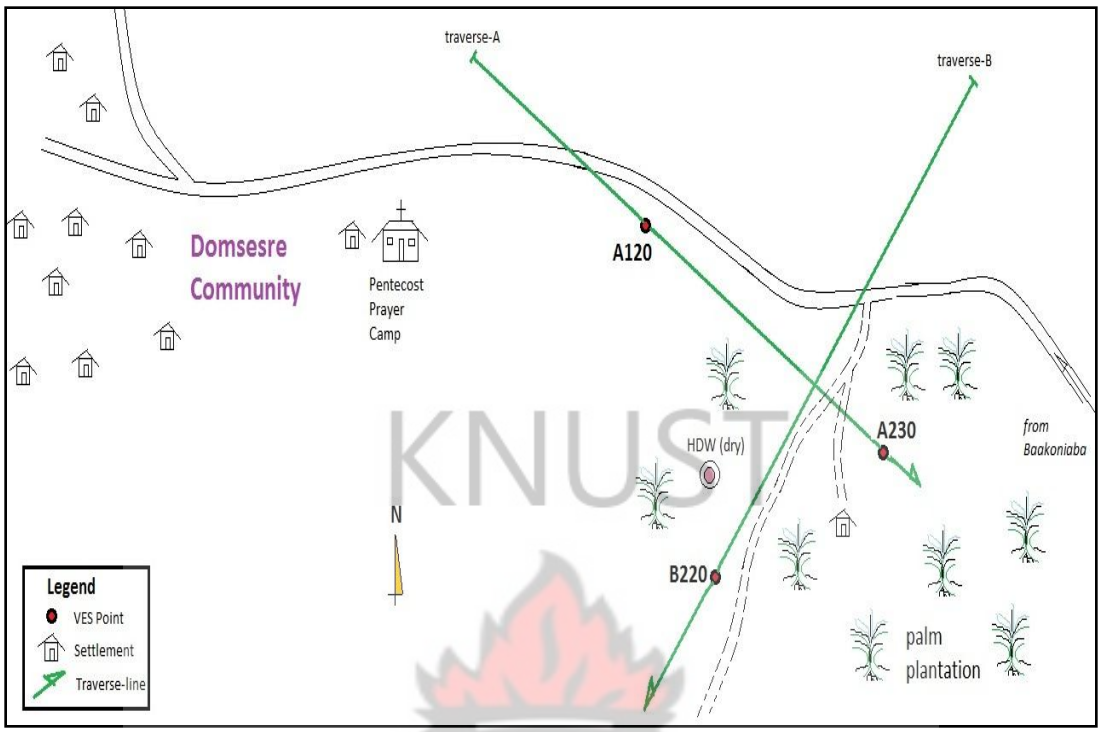

Fig. 4.28 A sketch of the layout of Domsesre community (Not to scale)

EM traverse along profile A of length 260 m was run on a bearing of 094^0 from the True North. As displayed in Figure 4.29, the HD values were higher than the VD values along the whole profile except at points where we obtained anomalies. From the HD curve, the conductivities started off constantly until the 40 m at 4 m mhos/m where it increased up to 6 m mhos/m at the 70 m point. The conductivity was constant again till it reached the 100 m point and then decreased until we obtained an anomaly at 5 m mhos/m at the 110 m point. The conductivity profile was erratic afterwards and then became constant after the 170 m point at 7 m mhos/m until another anomaly is obtained at the 230 m point. The VD curve moved in a similar pattern as the HD curve but it had lower apparent conductivities except at points where the anomalies were obtained (i.e. between the 110

m and 120 m points and also between the 210 m and 220 m points). These positions were selected along the profile for VES.

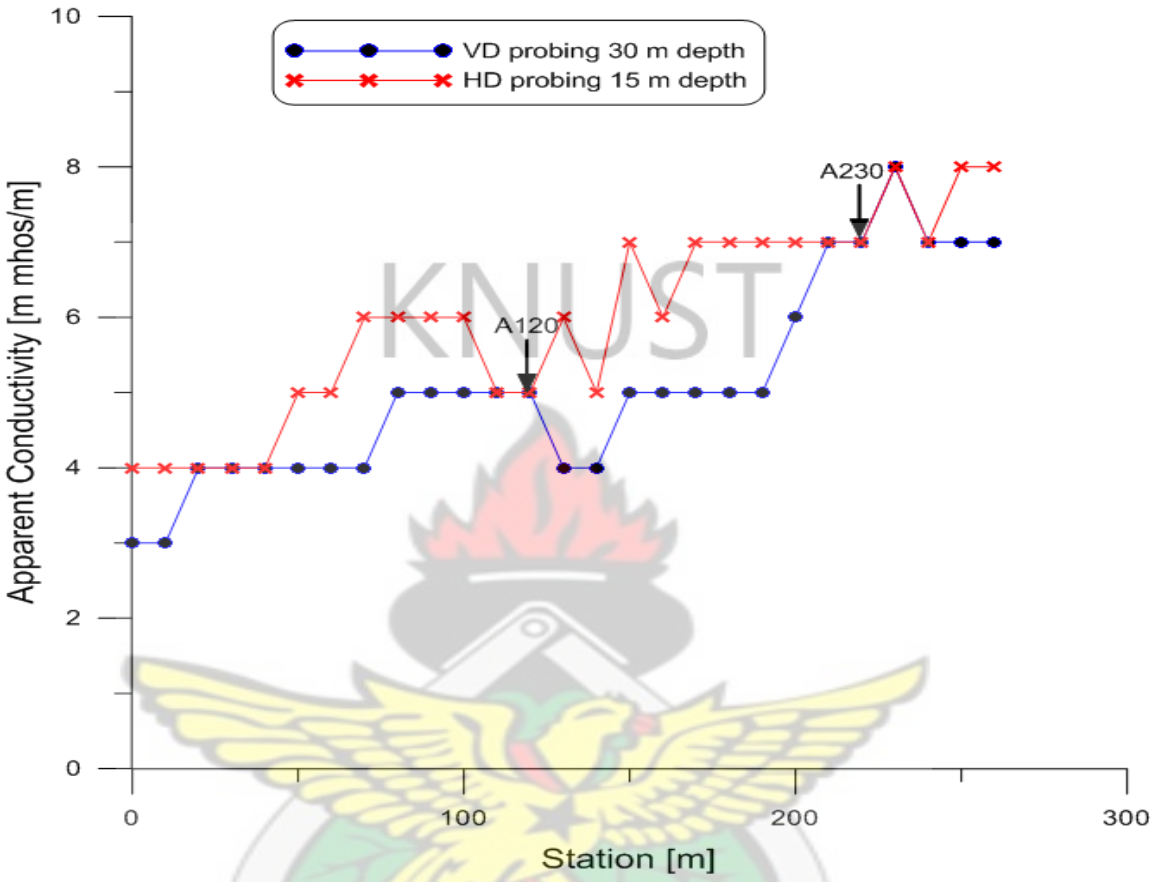

Fig. 4.29 EM terrain conductivity measurements along profile A at Domsesre

EM traverse along profile B of length 290 m was selected on a bearing of 136^0 from the True North. Conductivities ranged between 4 and 19 m mhos/m. As shown in Figure 4.30, both the HD and VD curves behaved erratically along the profile. However, the graph showed higher values of the HD mode than the VD mode except beyond the 210 m point where there was a crossover. Station B220 was selected for VES.

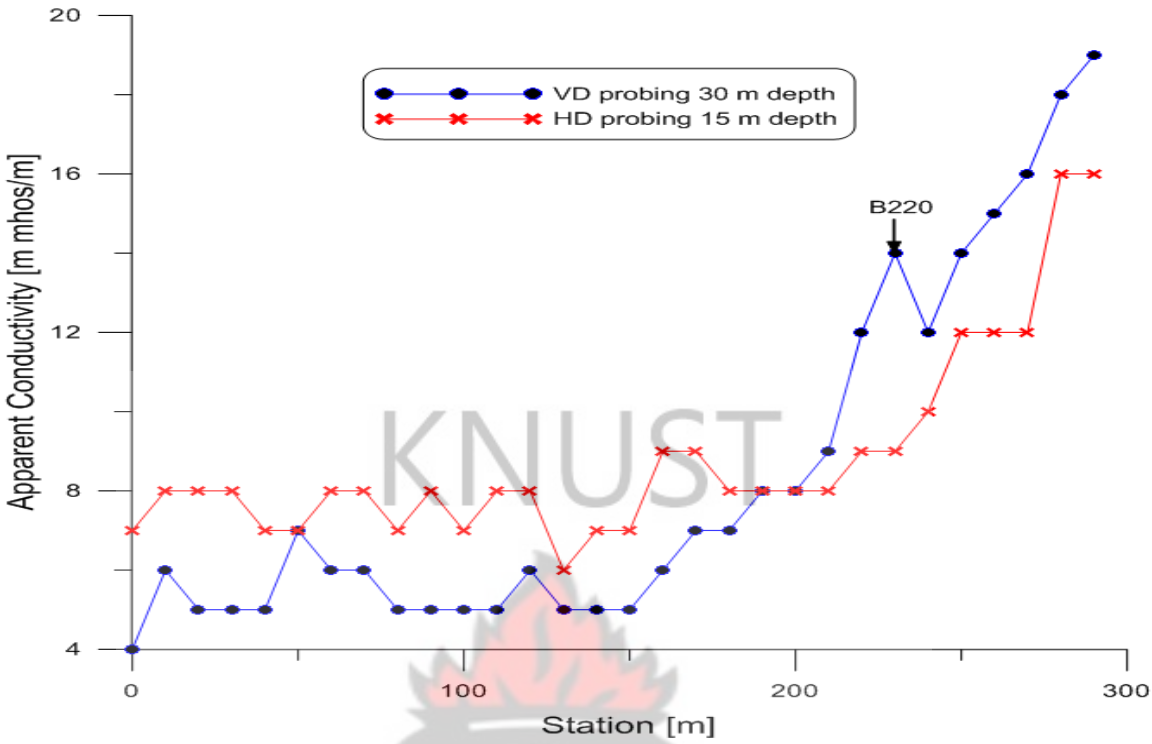

Fig. 4.30 EM terrain conductivity measurements along profile B at Domsesre

The three stations selected for VES to access their groundwater potential were A120, A230 and B220 and are displayed in Figures 4.31 – 4.33.

VES for A120

Figure 4.31 revealed that, three layers exist at the subsurface at station A120. The values of apparent resistivity varied between 245 Ωm and 1526 Ωm. Layer one has apparent resistivity and thickness of 245 Ωm and 1.1 m whilst the second layer, which is 40.3 m thick has a resistivity of 720 Ωm. The apparent resistivity of the third layer is 1526 Ωm. Analysis of the results suggests that layer one and two are moderately fractured and are underlain by a very high resistive rock. This station is not likely to have high prospects for groundwater.

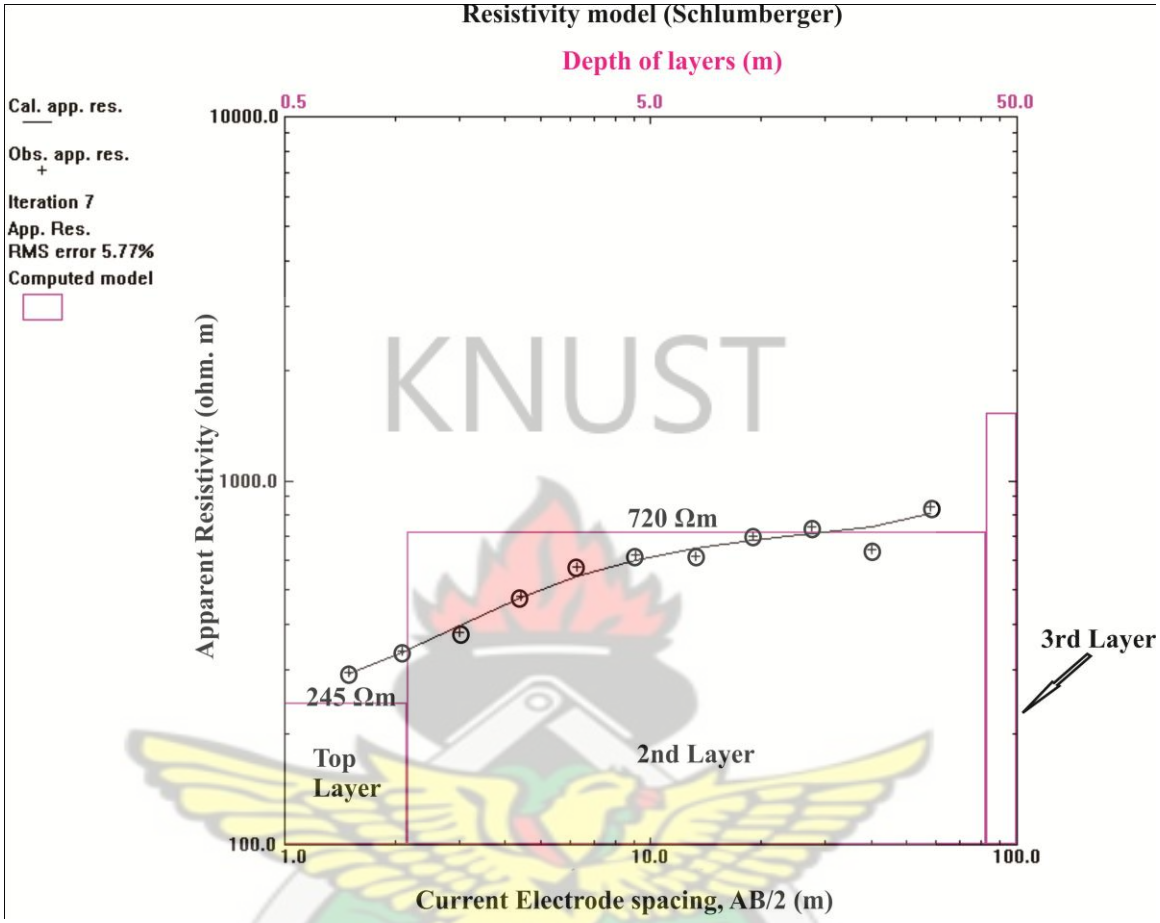

Fig. 4.31 VES curve at station A120 at Domsesre

VES for A230

Results from the VES carried out at station A230 similarly revealed three subsurface structures as shown in Figure 4.32. Resistivity values ranged from 15 Ωm to 521 Ωm with the topsoil being 1.4 m thick with apparent resistivity of 238 Ωm. The second layer had thickness and apparent resistivity values of 22.4 m and 521 Ωm; whereas the deepest layer is 15 Ωm. Deductions made from these results indicate that the first and second layers may be moderately fractured, and underlying these is a probably highly weathered

layer, which could have high groundwater potential. Therefore, this area has very high prospects for groundwater and hence was selected as test drilling point.

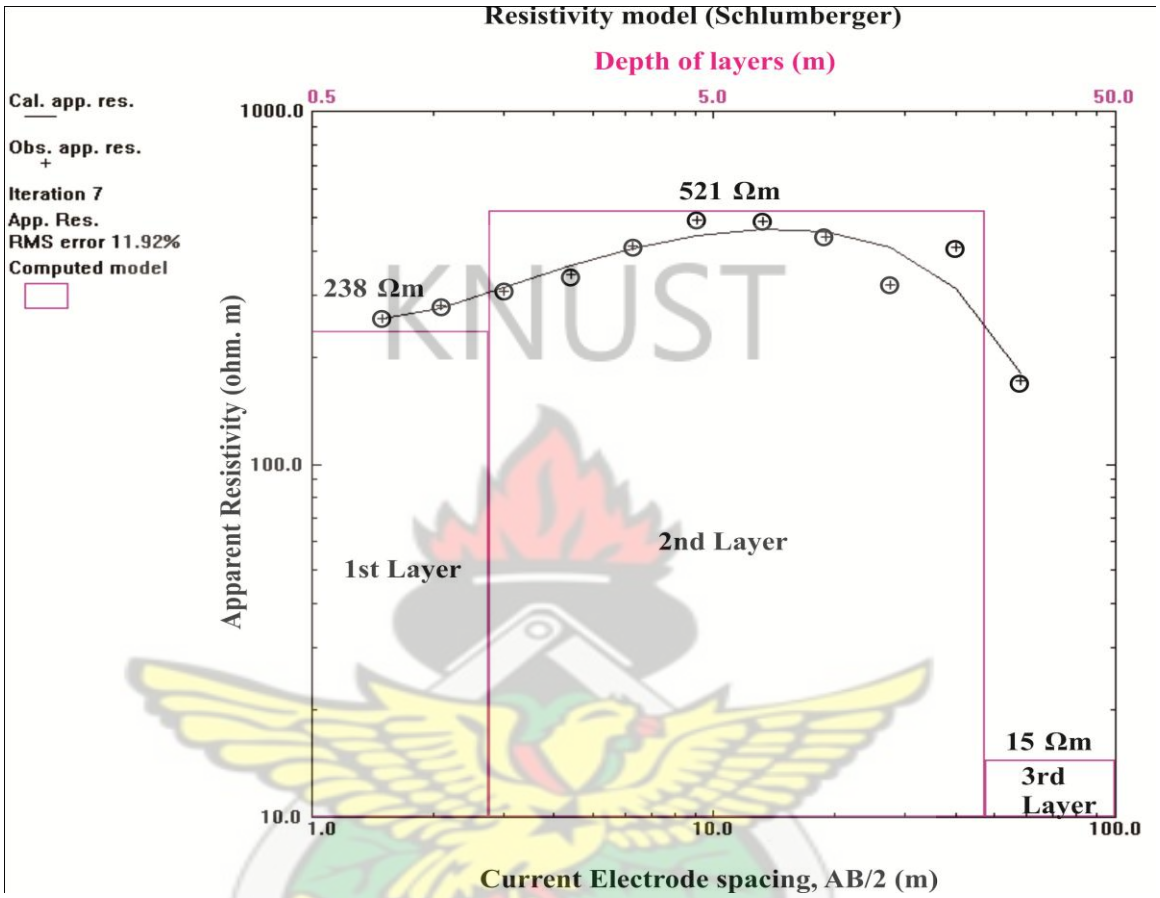

Fig. 4.32 VES curve at station A230 at Domsesre

VES for B220

Analysis of the VES at station B220 showed that four layers exist in the subsurface as is displayed in Figure 4.33 with apparent resistivities ranging from low (131 Ωm) to high (2008 Ωm). The topsoil, which may be fairly weathered, has a characteristic resistivity and thickness of 131 Ωm and 0.7 m whereas the slightly weathered second layer is 1.2 m thick and has a resistivity value of 877 Ωm. This is directly underlain by a moderately weathered layer, which has a resistivity of 290 Ωm and a thickness of 58.7 m. The aquifer

is expected to be intercepted in this zone. The bedrock is most likely to be made up of a very high resistive rock in view of its resistivity of 2008 Ωm.

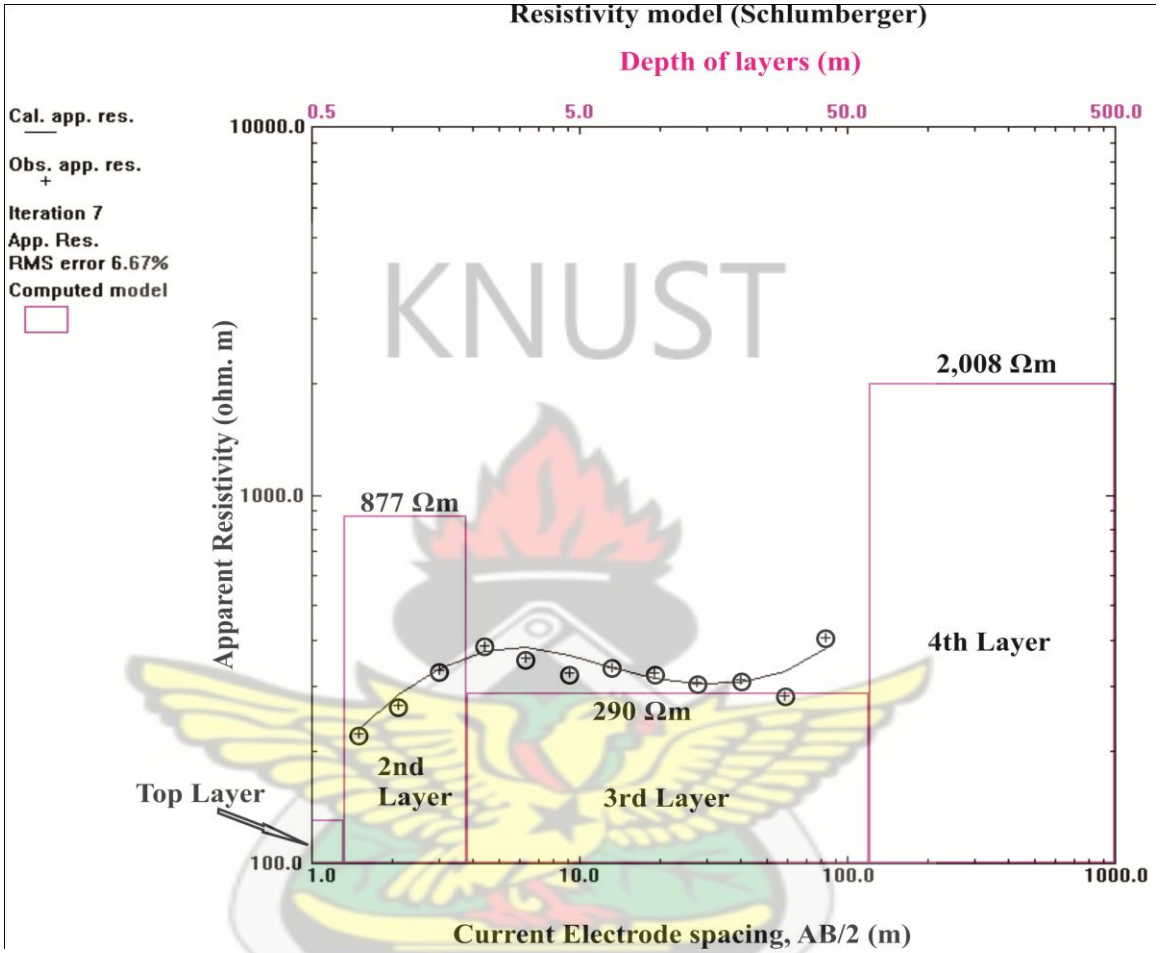

Fig. 4.33 VES curve at station B220 at Domsesre

Results from all the soundings suggest that the area is underlain by either three or four subsurface lithological areas with the bedrock slightly fractured. The aquifer is expected to be intercepted within the bedrock. Table 4.6 displays the ranks of the three sounding points. From the table, station A230 is recommended for test drilling and B220 should be the alternative drilling point.

Table 4.6 Ranked VES points for test drilling at Domsesre

Community	VES Point	Layer	Apparent Resistivity (Ωm)	Thickness (m)	Depth (m)	Rank
Domsesre	A230	1	238	1.4	1.4	1
		2	521	22.4	23.8	
		3	15	-	-	
	B220	1	131	0.7	0.7	2
		2	877	1.2	1.2	
		3	290	58.7	60.6	
		4	2,008	-	-	
	A120	1	245	1.1	1.1	3
		2	720	40.2	41.3	
		3	1,526	-	-	

4.1.7 Fokuokrom

Only one EM traverse was run in this community, and three sounding points were selected for further probing using the VES technique. Station A70 was chosen along the profile and two other spot soundings, SP1 and SP2 were also chosen for VES. Figure 4.34 displays a schematic layout of EM profiling and VES points selected in the Fokuokrom community.

As Figure 4.35 shows, the EM traverse was conducted on a profile length of 100 m and on a bearing of 017^0. From the HD curve, the conductivity values increased steadily from 5 m mhos/m from the beginning of the profile to 10 m mhos/m at the 90 m point where it dropped slightly to 7 m mhos/m at the end of the profile. Unlike the HD curve, the VD curve was undulating. It started off at a conductivity value of 8 m mhos/m and decreased to 3 m mhos/m at the 10 m point where it continued to increase until it became constant

at 9 m mhos/m at the 60 m point. It then decreased to 4 m mhos/m at the 90 m point and increased slightly to 6 m mhos/m at the end of the profile. One of the crossover points (A70) was selected to investigate the groundwater potential with the VES method.

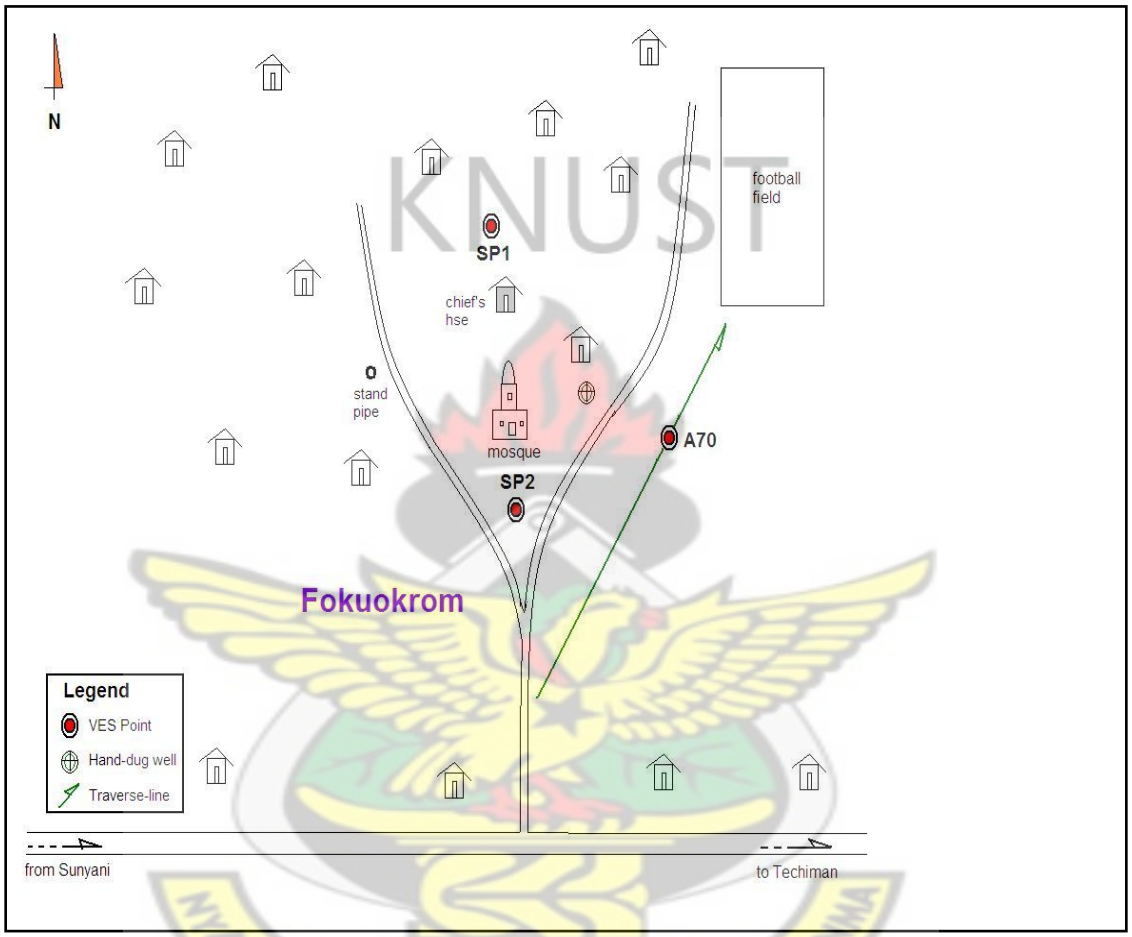

Fig. 4.34 A sketch of the layout of Fokuokrom community (Not to scale)

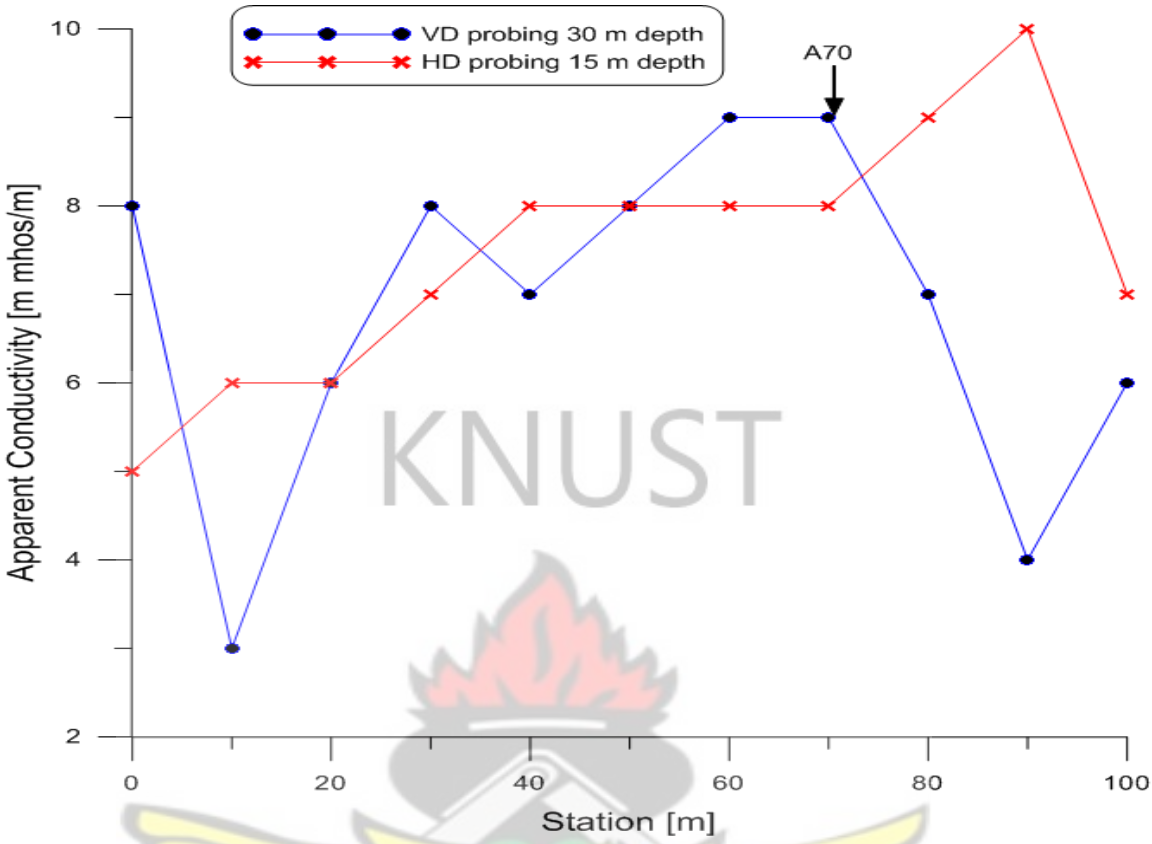

Fig. 4.35 EM terrain conductivity measurements along a profile at Fokuokrom

VES for A70

Results of the vertical electrical sounding conducted at station A70 shows that there are four geological layers in the subsurface. From Figure 4.36, the topsoil, which is likely to be moderately weathered has a resistivity of 145 Ωm and thickness of 0.7 m. Underlying this is a slightly weathered second layer, which is 5.9 m thick and has an apparent resistivity of 241 Ωm. The third layer is 11.1 m thick and has a resistivity value of 676 Ωm whilst the bedrock resistivity is 187 Ωm. The resistivity of the bedrock is diagnostic of a moderately fractured formation and therefore expected to host sufficient amount of groundwater. This could be a very good site for test drilling.

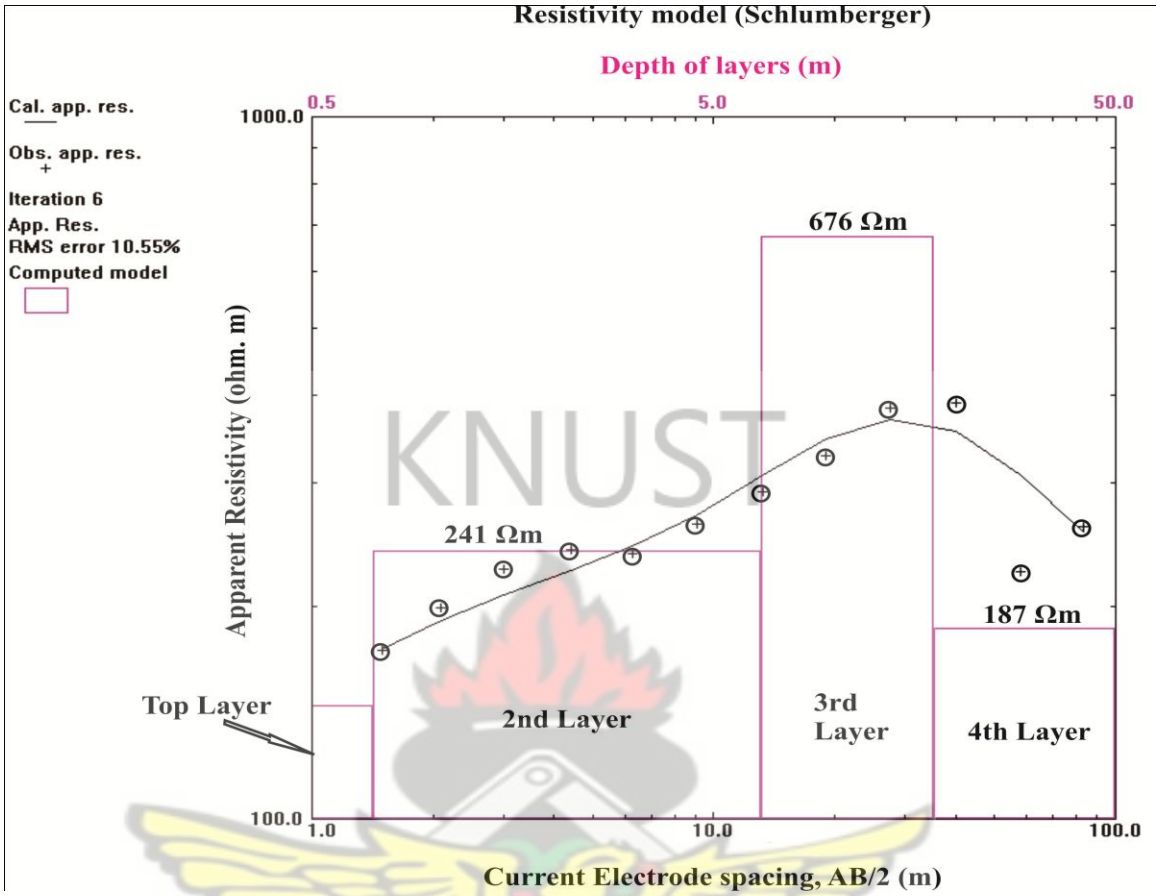

Fig. 4.36 VES curve at station A70 at Fokuokrom

VES for SP1

It is evident from the VES carried out at station SP1 that the subsurface is made up of three layers. From Figure 4.37, the first and second layers presumed to be highly weathered, have thicknesses and apparent resistivity values of 0.9 m and 56 Ωm, 2.8 m and 27.2 Ωm respectively. The deepest layer may be only slightly weathered and not much water is expected to be accumulated in this zone. Therefore, this area is not worth considering for groundwater exploration.

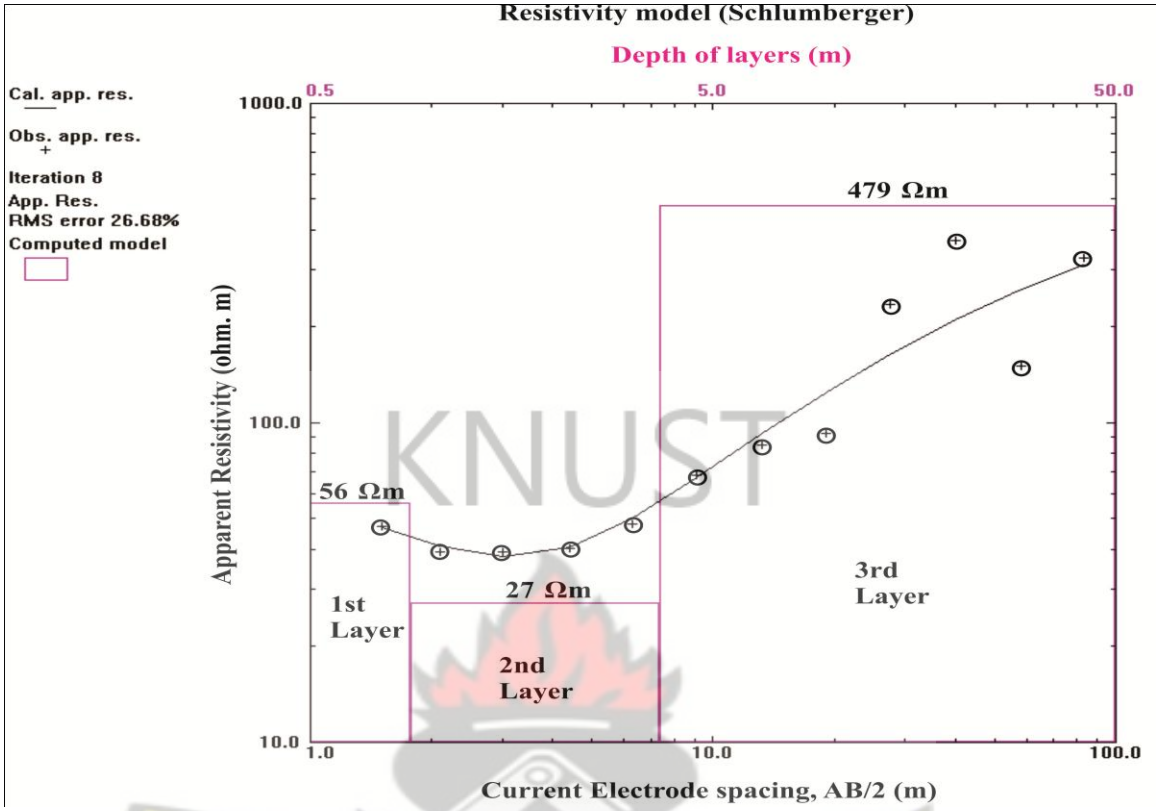

Fig. 4. 37 VES curve at station SP1 at Fokuokrom

VES for SP2

The spot sounding conducted at station SP1 as shown in Figure 4.38 indicates that there are three lithological layers in the subsurface. The topsoil presumed to be fairly weathered is 3.2 m thick and has an apparent resistivity of 193 Ωm. Beneath this is a highly weathered second layer by virtue of its low resistivity of 49 Ωm resistivity and 2.1 m thickness. Groundwater is expected to be accumulated in this zone. The deep seated layer could be slightly weathered and has an apparent resistivity of 625 Ωm.

Results from the vertical electrical soundings reveal that three or four lithological layers underlie the community and the aquifer is expected to be located in the bedrock. Information on the recommended drilling points are compiled and displayed in Table 4.7.

From this table, station A70 is the first ranked site for test drilling followed by station SP2.

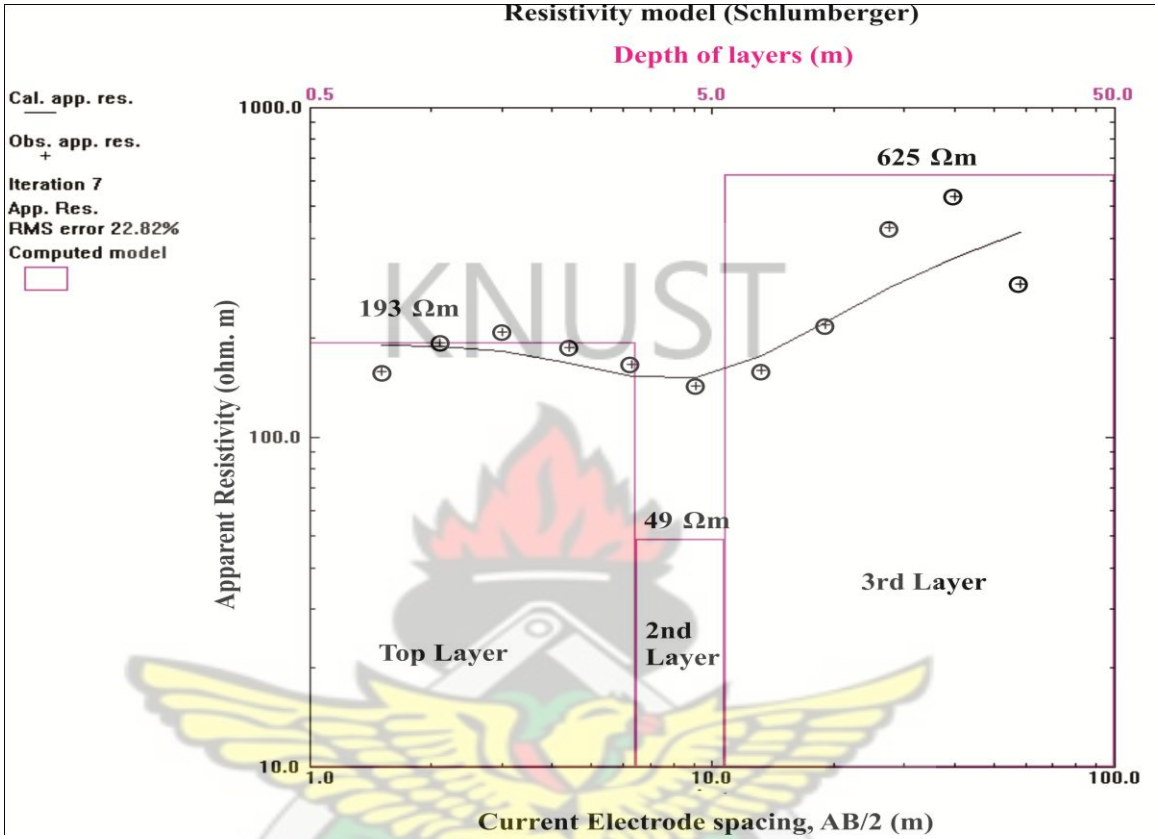

Fig. 4.38 VES curve at station SP2 at Fokuokrom

Table 4.7 Ranked VES points for test drilling at Fokuokrom

Community	VES Point	Layer	Apparent Resistivity (Ωm)	Thickness (m)	Depth (m)	Rank
Fokuokrom	A70	1	145	0.7	0.7	1
		2	241	5.9	6.6	
		3	676	11.1	17.7	
		4	187	-	-	
	SP2	1	193	3.2	3.2	2
		2	49	2.1	5.3	
		3	625	-	-	
	SP1	1	56	0.9	0.9	3
		2	27	2.8	3.7	
		3	479	-	-	

4.1.8 Kofi Daa-Tano

In Kofi Daa-Tano community, an EM profiling was conducted on a traverse line of length 120 m out of which three potential points A20, A40 and A80 were chosen for further investigation using the VES method. The schematic layout of the community is shown in Figure 5.39 below.

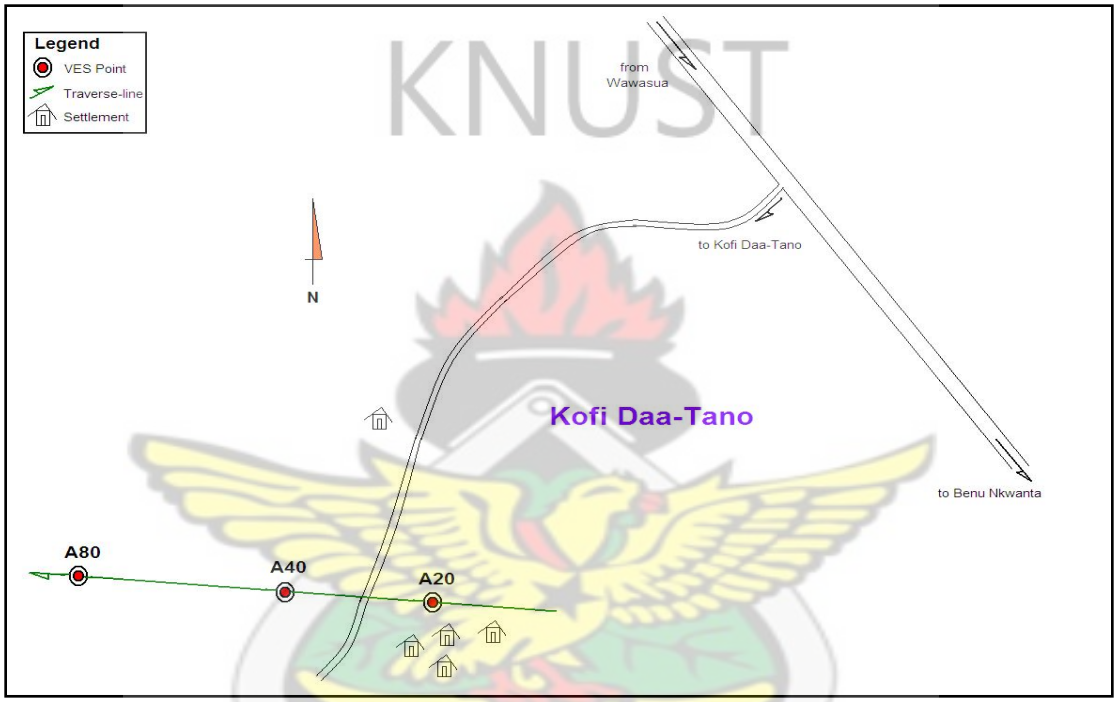

Fig. 4.39 A sketch of the layout of Kofi Daa-Tano community (Not to scale)

The EM profiling was carried out on a bearing of 334^0 from the True North. From the results, the apparent conductivity of the area ranges between 7 and 25 m mhos/m with an average of 17.3 m mhos/m. As shown in Figure 4.40, the graph of conductivity variation with distance, there is a steady decline in the HD values along the profile up to the 80 m point with conductivity of 16 m mhos/m. Then, it increased gradually till it reached the end of the profile. The VD mode showed an erratic graph with apparent conductivity values increasing and decreasing along the profile. Even though the VD values were

generally lower than the HD values, there were a few cross-over points. Three of these points (A20, A40 and A80) were selected for sounding to investigate their groundwater potential.

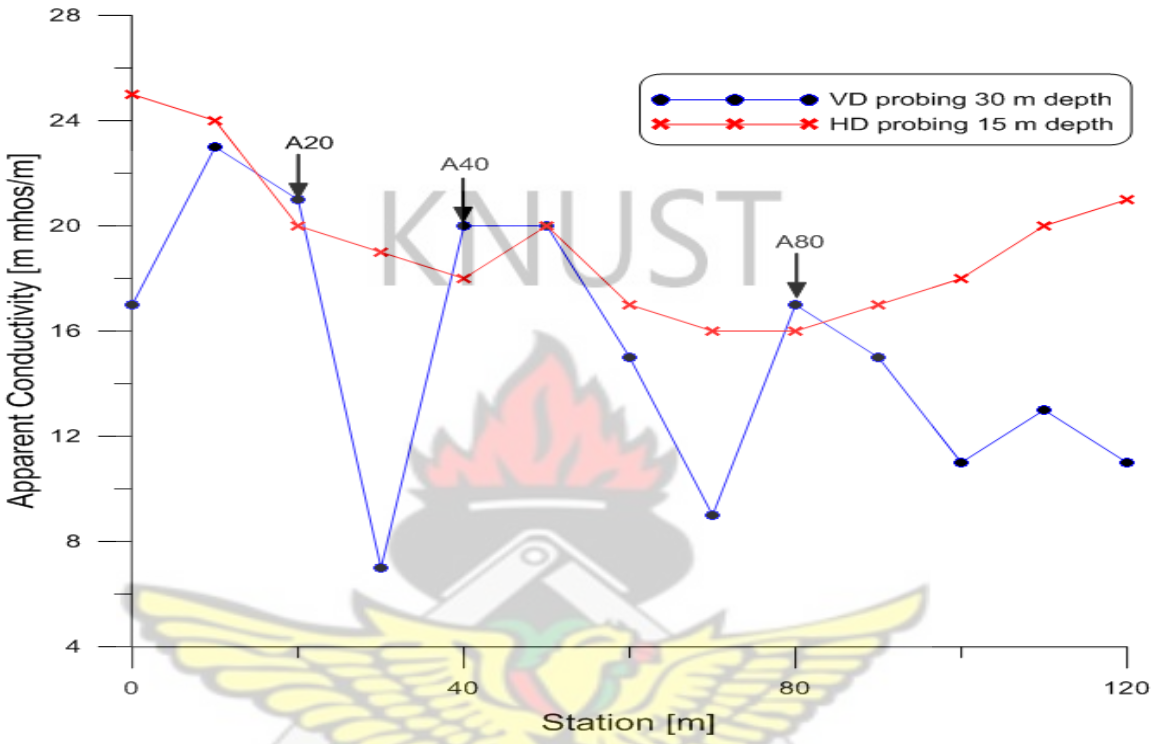

Fig. 4.40 EM terrain conductivity measurements along a profile at Kofi Daa-Tano

VES for A20

The sounding results from station A20 indicated that the subsurface comprised three geological layers. The apparent resistivity values ranged between 18 Ωm and 1594 Ωm as shown in Figure 4.41. Analyses show that, the first and second layers may be highly weathered and are possibly underlain by a deep-seated high resistive rock. The first layer is 4.3 m thick and has an apparent resistivity of 49 Ωm and the second layer has thickness and resistivity of 12.2 m and 18 Ωm respectively. The bedrock had an apparent resistivity of 1594 Ωm.

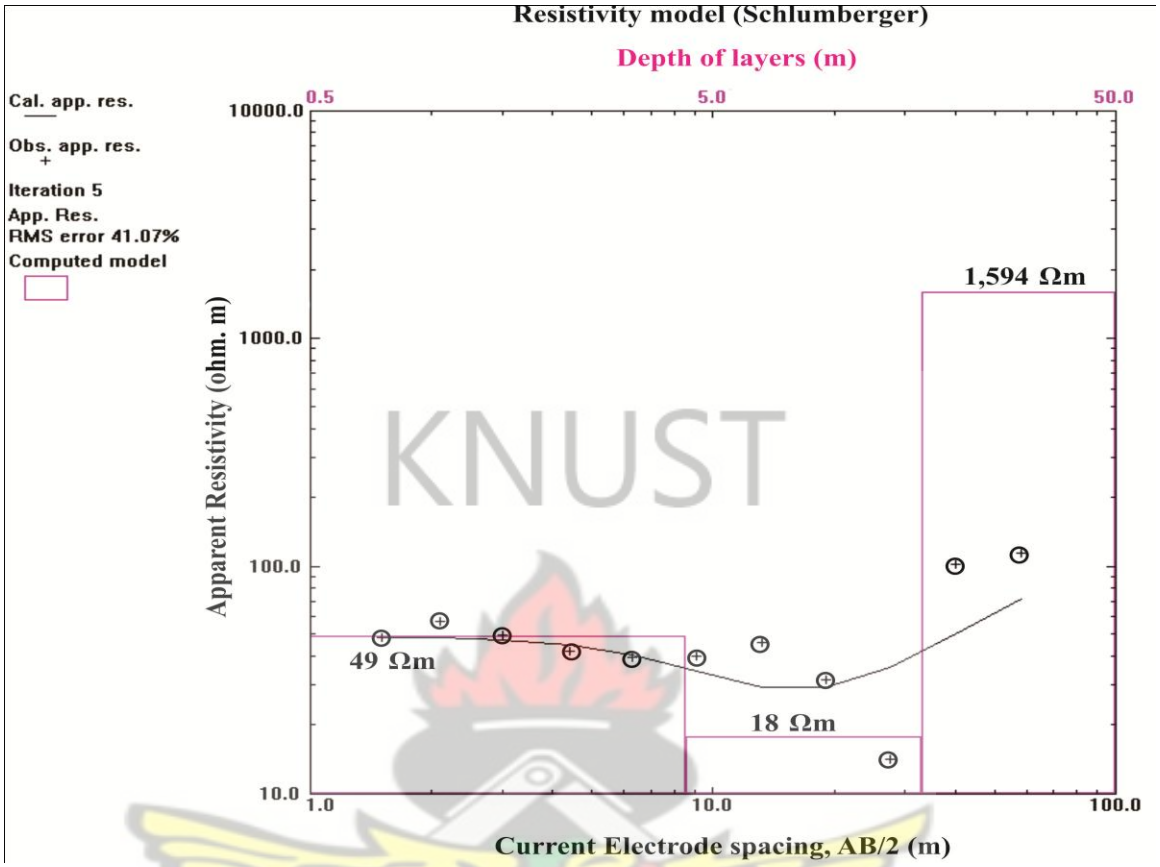

Fig. 4.41 VES curve at station A20 at Kofi Daa-Tano

VES for A40

From Figure 4.42, it is apparent that three layers exist in the subsurface at the VES point A40. The topsoil has apparent resistivity and thickness of 153 Ωm and 1.2 m whereas the second layer which is 8.8 m thick has 53 Ωm resistivity. The third layer has apparent resistivity of 274 Ωm. Deductions made from these results indicate that the subsurface resistivity is characteristic of a highly weathered formation sandwiched between moderately weathered first and third layers. This could be a very good point for borehole drilling since sufficient amount of water is expected to be accumulated both in the second and third layers.

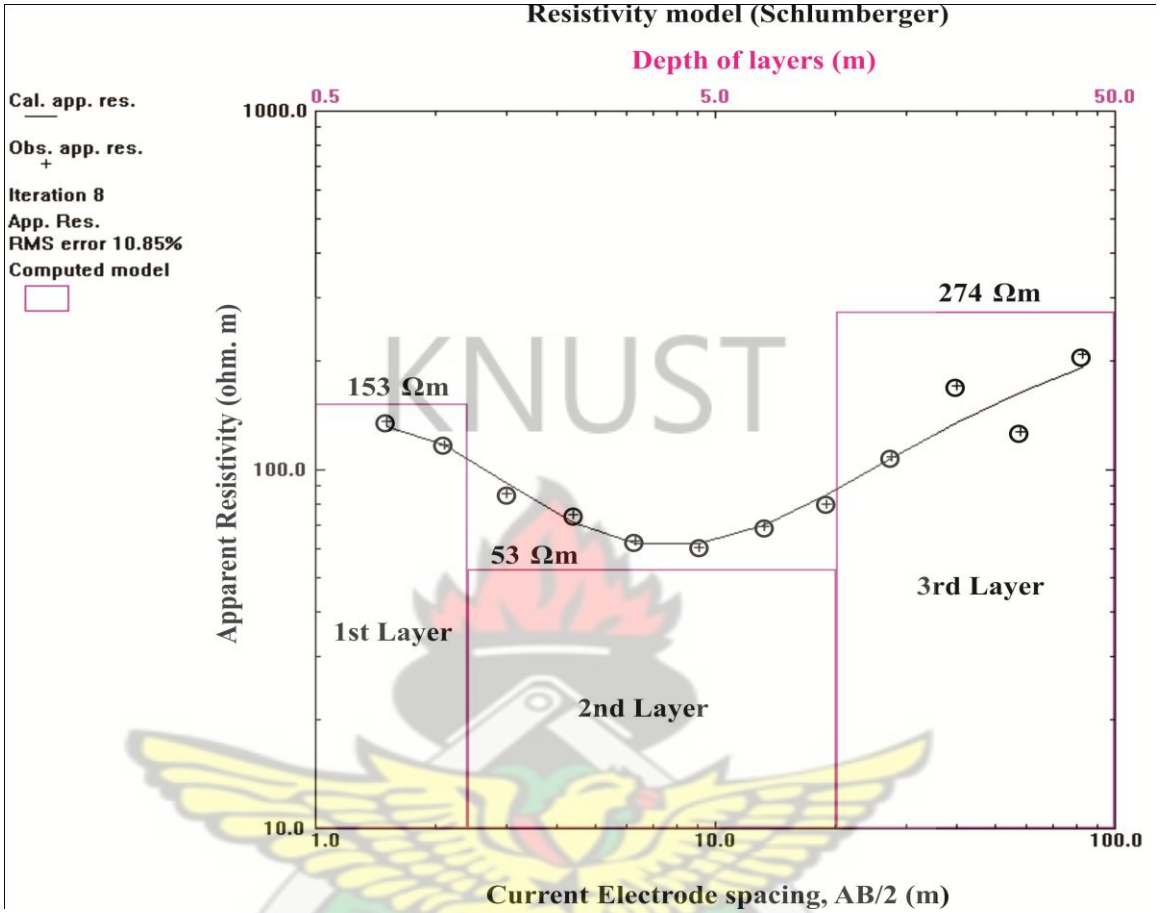

Fig. 4.42 VES curve at station A40 at Kofi Daa-Tano

VES for A80

The sounding results at VES station A80 (as in Figure 4.43) depicts that the first layer is highly weathered and has apparent resistivity and thickness of 27 Ωm and 0.6 m respectively. The second layer directly beneath this is likely to be slightly weathered with 1.1 m thickness and 775 Ωm resistivity. The third layer, similar to the topsoil, is probably highly weathered due to its apparent resistivity of 18 Ωm and thickness of 4.8 m. Underlying this is a very resistive bedrock with an apparent resistivity of 2244 Ωm.

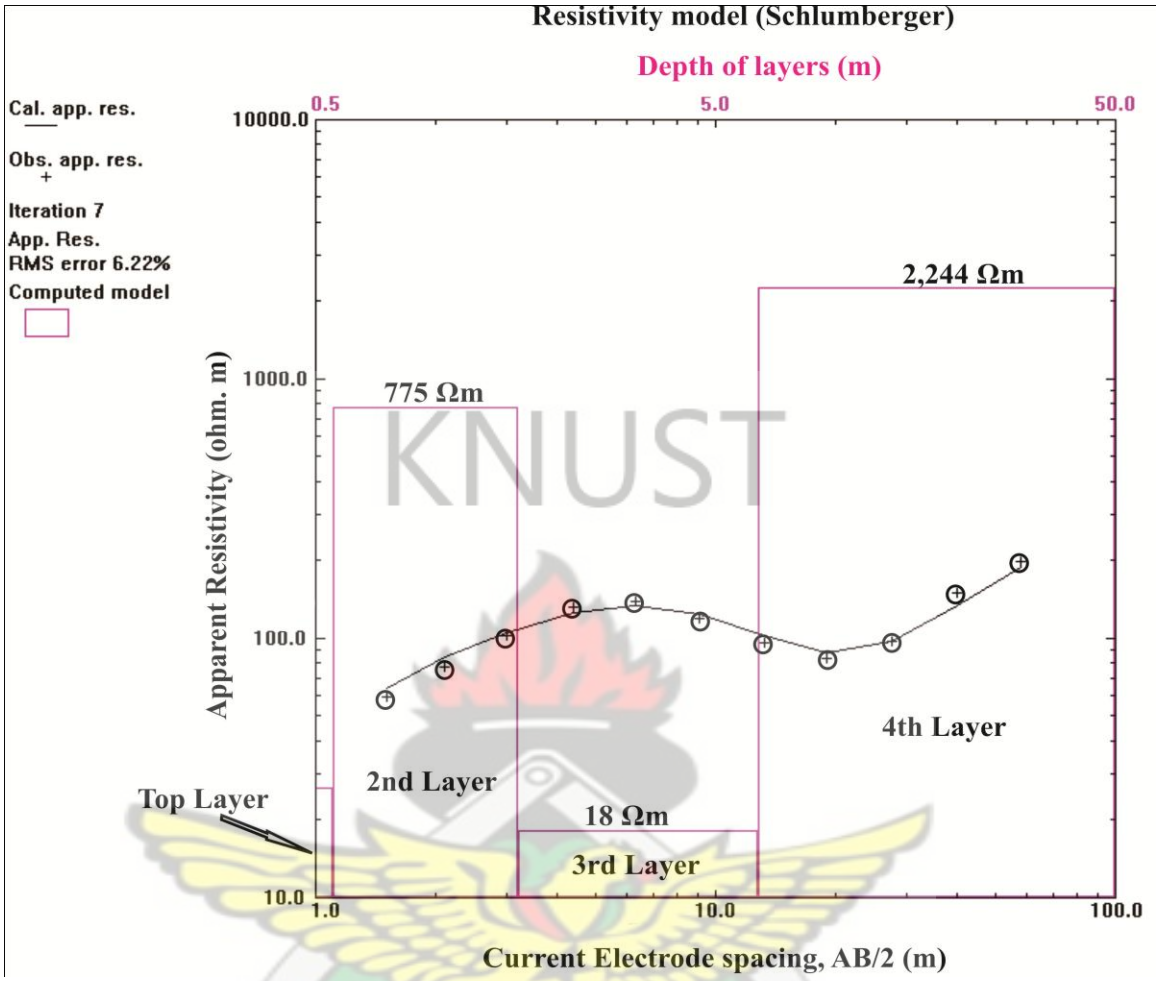

Fig. 4.43 VES curve at station A80 at Kofi Daa-Tano

Three subsurface geological layers underlie the most of this community except at the station A80, which is made up of four lithological layers. The analyses imply that the bedrock is generally moderately weathered hence; groundwater potential is expected to be moderate in this community. The various VES points are ranked in order of their potential water bearing capacity and are presented in Table 4.8. The most suitable point for test drilling is station A40.

Table 4.8 Ranked VES points for test drilling at Kofi Daa-Tano

Community	VES Point	Layer	Apparent Resistivity (Ωm)	Thickness (m)	Depth (m)	Rank
Kofi Daa-Tano	A40	1	153	1.2	1.2	1
		2	53	8.9	10.1	
		3	274	-	-	
	A20	1	49	4.3	4.3	2
		2	18	12.2	16.5	
		3	1594	-	-	
	A80	1	27	0.6	0.6	3
		2	775	1.1	1.7	
		3	18	4.8	6.5	
		4	2244	-	-	

4.1.9 Kwanware

A traverse line of length 380 m was profiled using the electromagnetic method at the 20 m coil spacing in this community. Three potential points A90, A300 and A360 were selected for further depth probing using the VES technique. Figure 4.44 is a layout of the community showing traverse lines and the selected VES points.

The EM traverse was carried out on a profile length of 380 m on and a bearing of 242^0. The apparent conductivity values range from as low as 1 m mhos/m to 26 m mhos/m. As is evident in Figure 4.45, both HD and VD curves behaved erratically. Along a greater part of the profile, the conductivity values of the VD mode were higher than those of the HD mode. Many cross-over points were established along the profile, out of which three (A90, A300 and A360) were selected for VES.

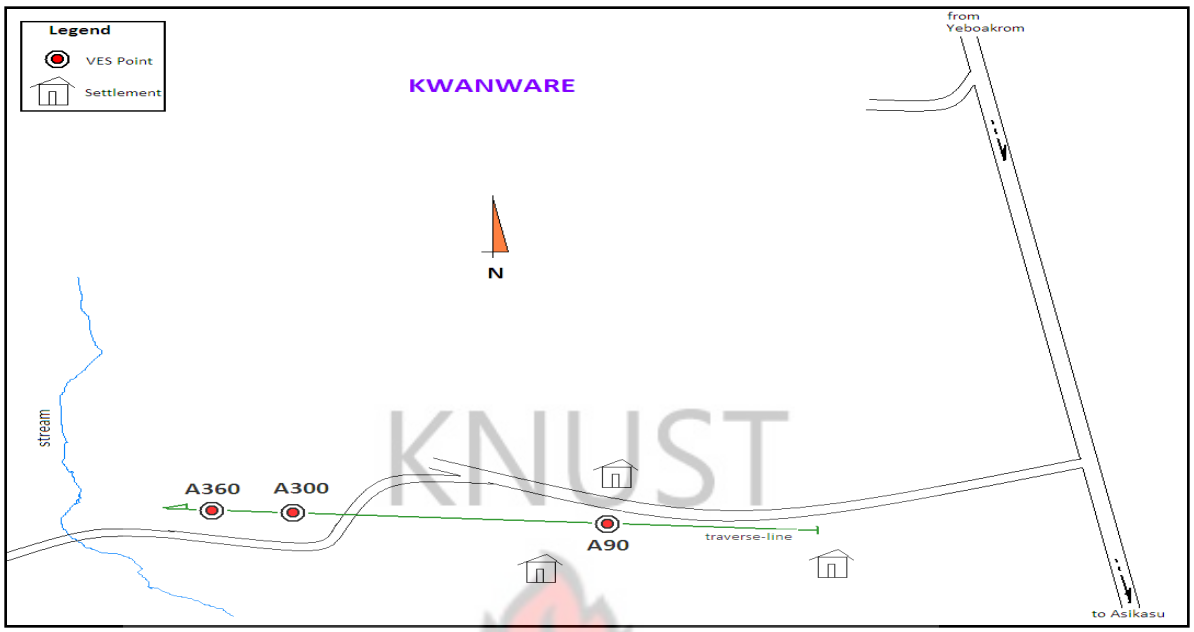

Fig. 4.44 A sketch of the layout of Kwanware community (Not to scale)

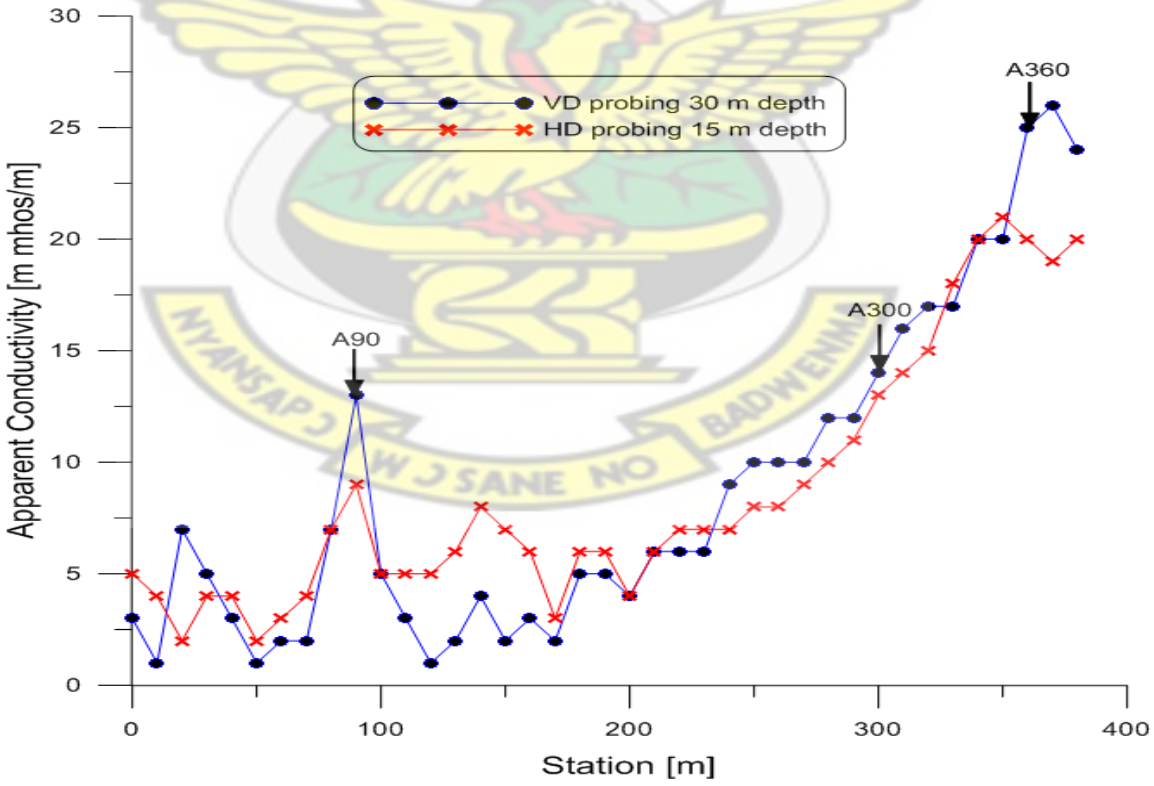

Fig. 4.45 EM terrain conductivity measurements along a profile at Kwanware

VES for A90

The graph of apparent resistivity against depth at station A90 as shown in Figure 4.46 suggests that there exist four layers in the subsurface with resistivity values ranging between 112 Ωm and 2261 Ωm. Resistivity of layer one of thickness 0.7 m is 112 Ωm whilst that of the second layer is 160 Ωm and has a thickness of 4.1 m. The thickness and apparent resistivity of the third layer is 9.1 m and 2261 Ωm respectively. The bottom layer has 167 Ωm resistivity. Analysis of these results suggests that both first and second layers are moderately fractured and are underlain by a highly resistivity third layer. The moderately fractured bedrock is expected to host sufficient quantity of water. This is most likely to be a very good potential borehole drilling point.

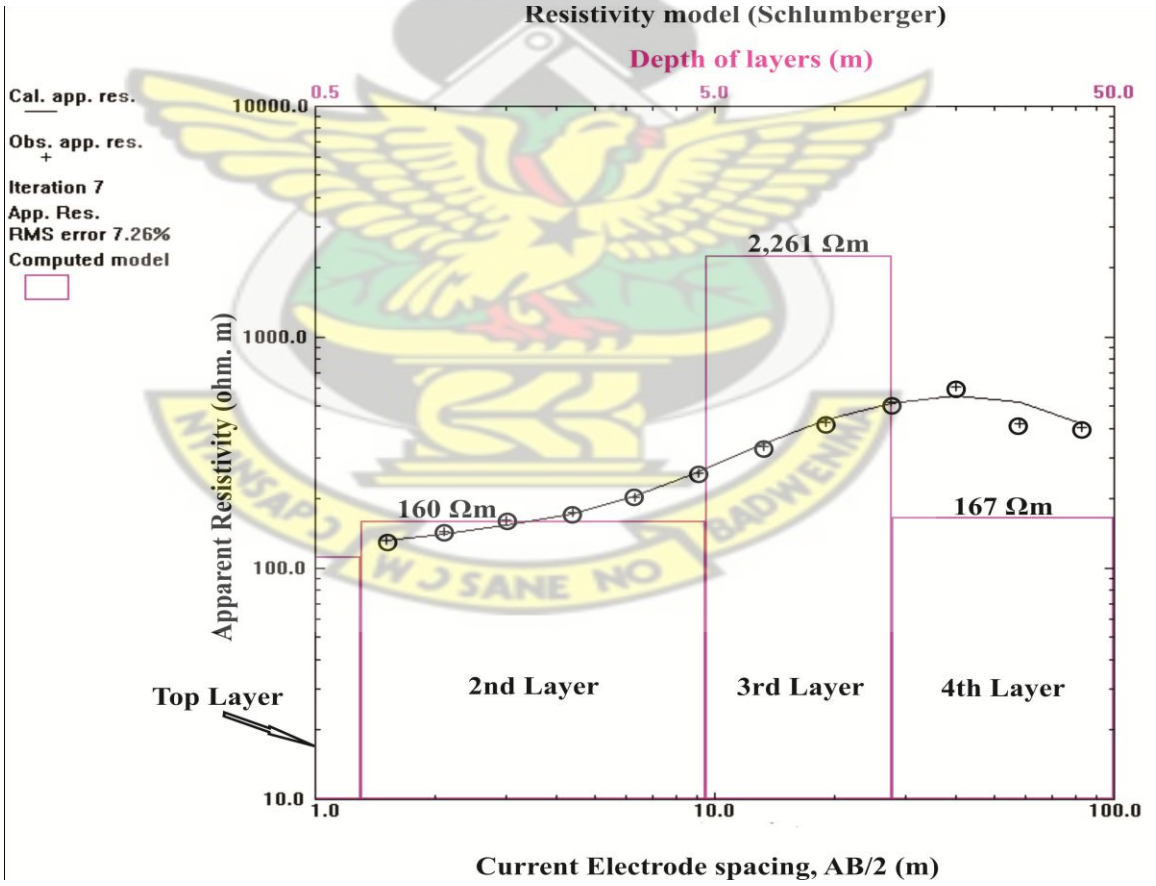

Fig. 4.46 VES curve at station A90 at Kwanware

VES for A300

Resistivity values from the VES at station A300 (as shown in Figure 4.47) range from 36 Ωm to 396 Ωm. The results suggest a highly fractured topsoil, which is 0.6 m thick and has a resistivity of 36 Ωm. Below this is a 396 Ωm resistivity, characteristic of a partially fractured formation with a 1.5 m thickness. Underlying this layer may be a moderately weathered bedrock with an apparent resistivity of 178 Ωm. Water is expected to be accumulated both in the second and third layers.

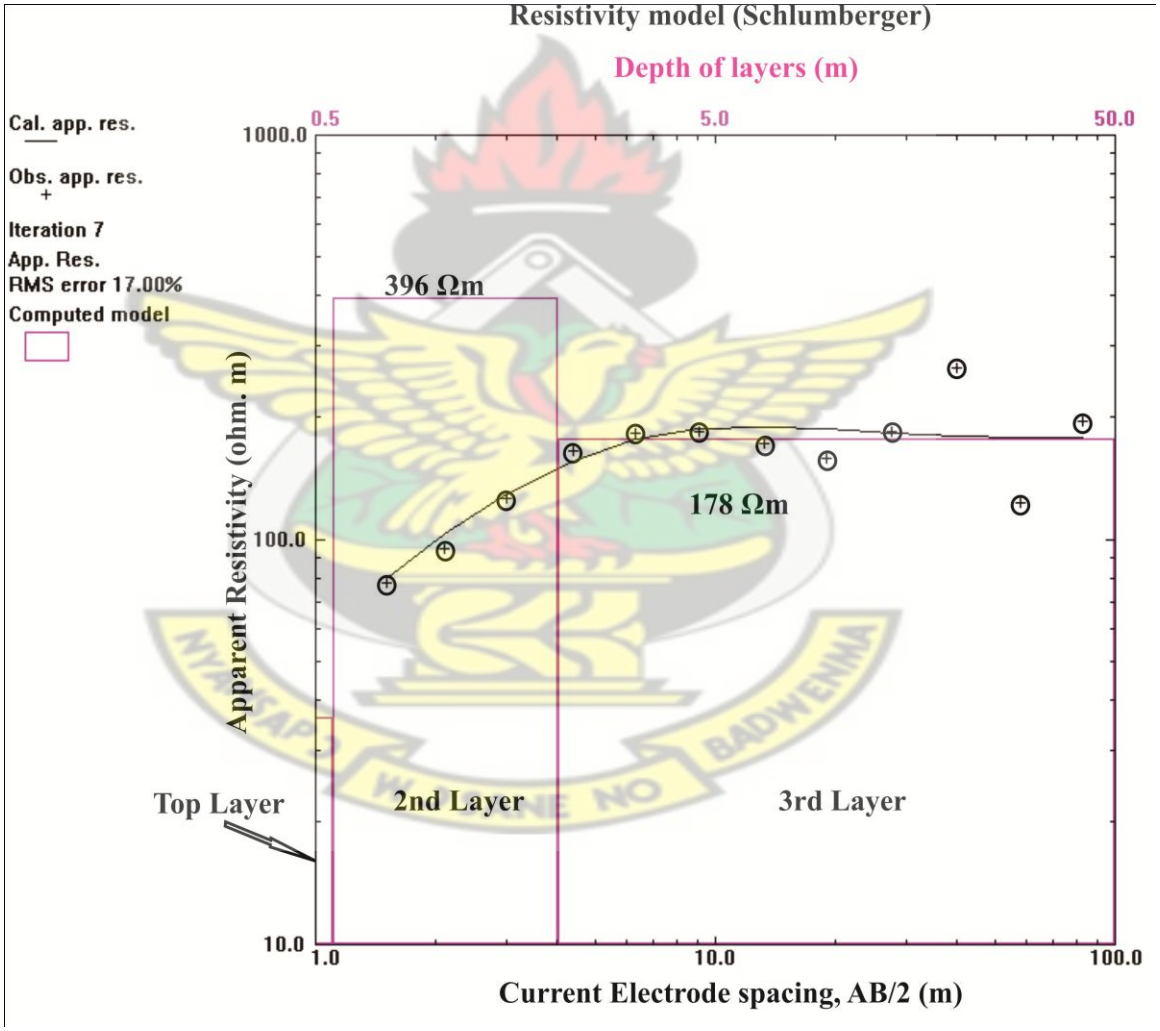

Fig.4.47VES curve at station A300 at Kwanware

VES for A360

The next VES point A360, produced results of apparent resistivity in the range of 118 Ωm and 596 Ωm. The point is made up of three geological layers as shown in Figure 4.48. Layer one is 3.6 m thick and has resistivity of 251 Ωm whereas the second layer has thickness of 5.8 m and an apparent resistivity of 118 Ωm. The bottom layer at this point has a resistivity of 596 Ωm. The results are suggestive of moderately weathered first and second layers with the third layer, only slightly weathered. This site may not be suitable for water accumulation.

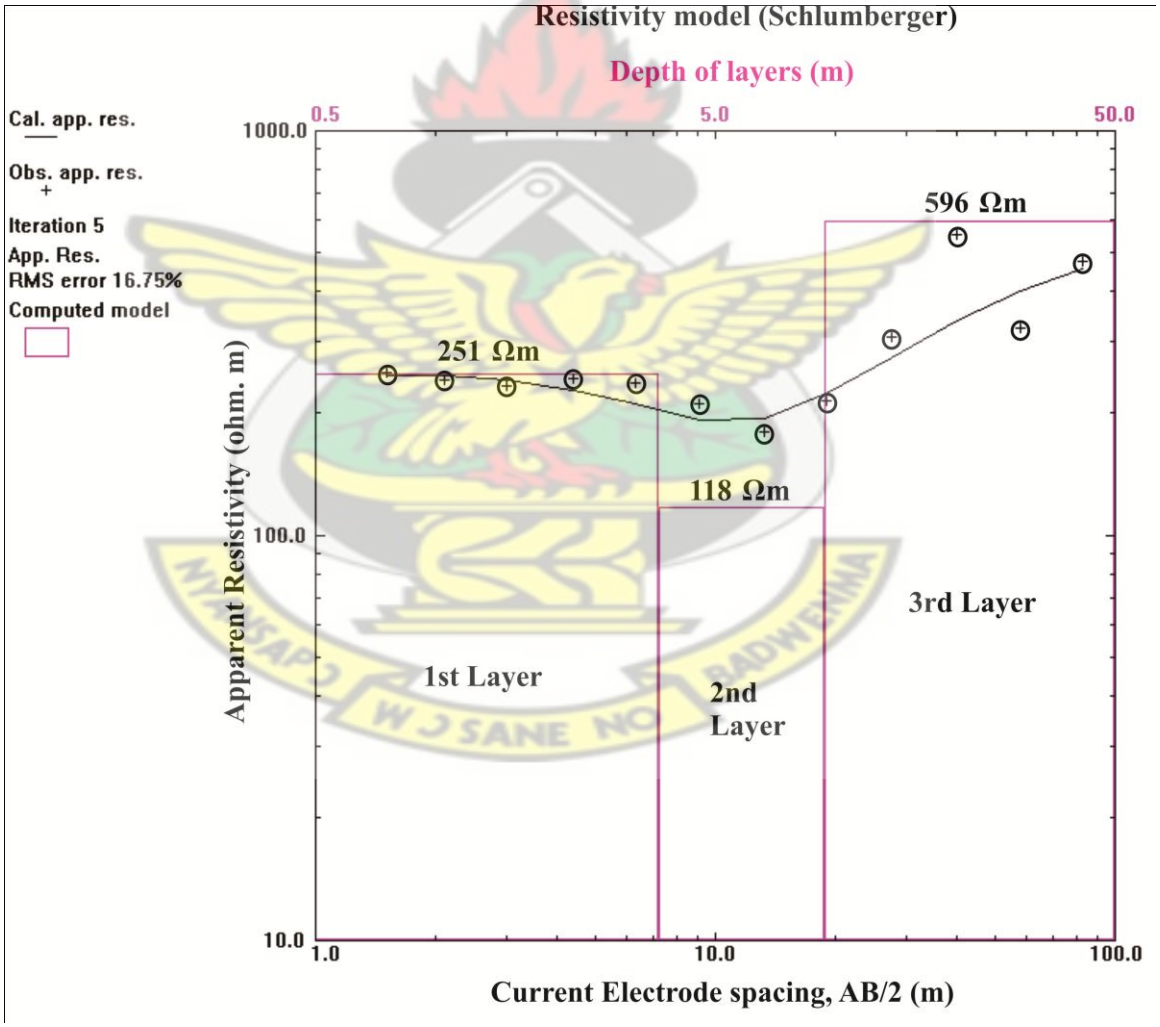

Fig. 4.48 VES curve at station A360 at Kwanware

As the analysis of the three VES stations depict, this community is marked predominantly by three subsurface geological layers even though station A90 suggested otherwise. These three stations have been ranked according to their potential to host groundwater. Station A90 was ranked the first choice for test drilling, whilst station A360 was ranked unsuitable. This is presented in Table 4.9 below.

Table 4.9 Ranked VES points for test drilling at Kwanware

Community	VES Point	Layer	Apparent Resistivity (Ωm)	Thickness (m)	Depth (m)	Rank
Kwanware	A90	1	112	0.7	0.7	1
		2	160	4.1	4.8	
		3	2261	9.1	13.9	
		4	167	-	-	
	A300	1	36	0.6	0.6	2
		2	396	1.5	2.1	
		3	178	-	-	
	A360	1	251	3.6	3.6	3
		2	118	5.8	9.4	
		3	596	-	-	

4.1.10 Maamakrom

EM profiling was conducted along two traverse lines with a total length of 140 m in this community. Out of these two profiles, three potential points were chosen for further investigations using the VES method. The schematic layout showing the profile lines and the VES points are shown in Figure 4.49.

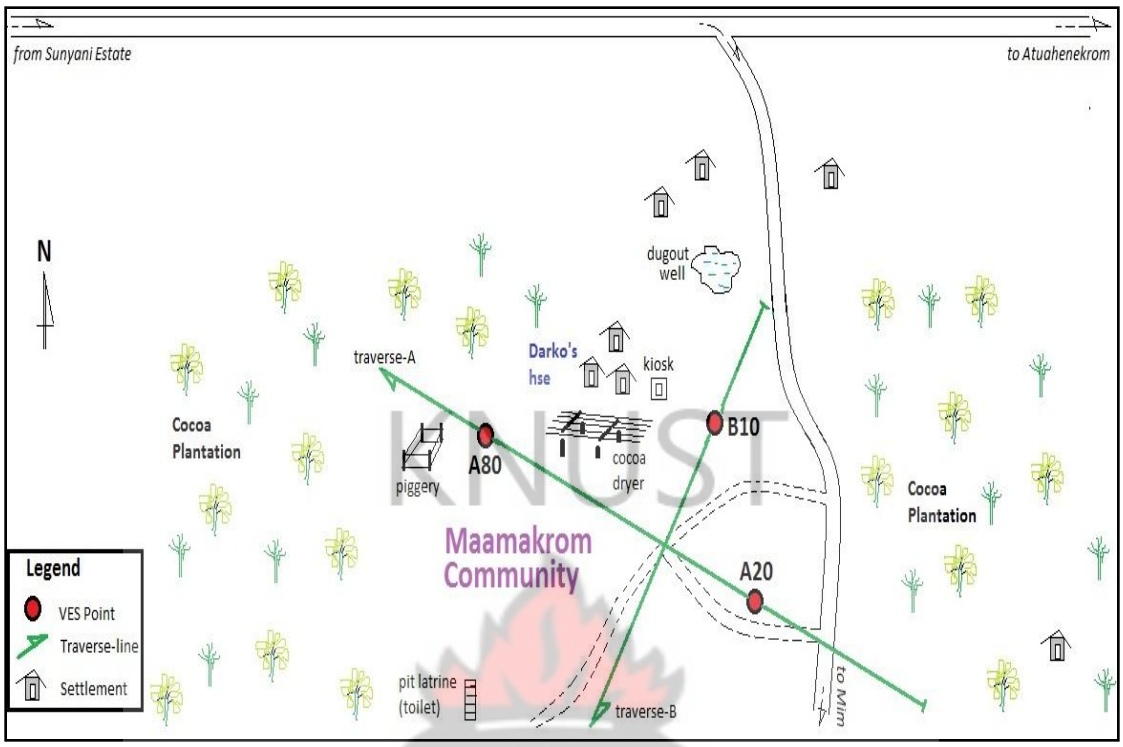

Fig. 4.49 A sketch of the layout of Maamakrom community (Not to scale)

Figure 4.50 is a graph of the variation of EM terrain conductivity with distance along profile A at Maamakrom. From this graph, it was observed that values of the VD mode were comparatively lower than those of the HD mode almost along the whole of the profile suggesting a decrease in conductivity with depth. Conductivity values were generally low along this profile ranging between 1 – 16 m mhos/m. The HD curve begins with an increase in conductivity from 4 m mhos/m to 8 m mhos/m at the 10 m point and then decreased slightly to 3 m mhos/m at the 20 m point where there was a crossover of the VD curve. The apparent conductivity increased to 16 m mhos/m at point 40 m. The curve then declined till it got to the 70 m point at a conductivity of 6 m mhos/m and increased to 12 m mhos/m at the end of the profile. The VD curve on the other hand,

begun with an increase in apparent conductivity from the 1 m mhos/m to the 10 m mhos/m after which there was a steady decline up to point 70 m at 5 m mhos/m. There was an increase in conductivity to 10 m mhos/m at the end of the profile. It is worth noting that the trend of both HD and VD curves was the same from the 70 m point to the end of the profile. Two stations A20 and A80 were chosen for VES along this profile. It is apparent from the EM plot that the conductivity value of the HD curve (12 m mhos/m) at point 80 m was higher than that observed for the VD curve. However, both curves show constant conductivities from this point (80 m) till the end of the profile hence, its selection for further resistivity depth probing.

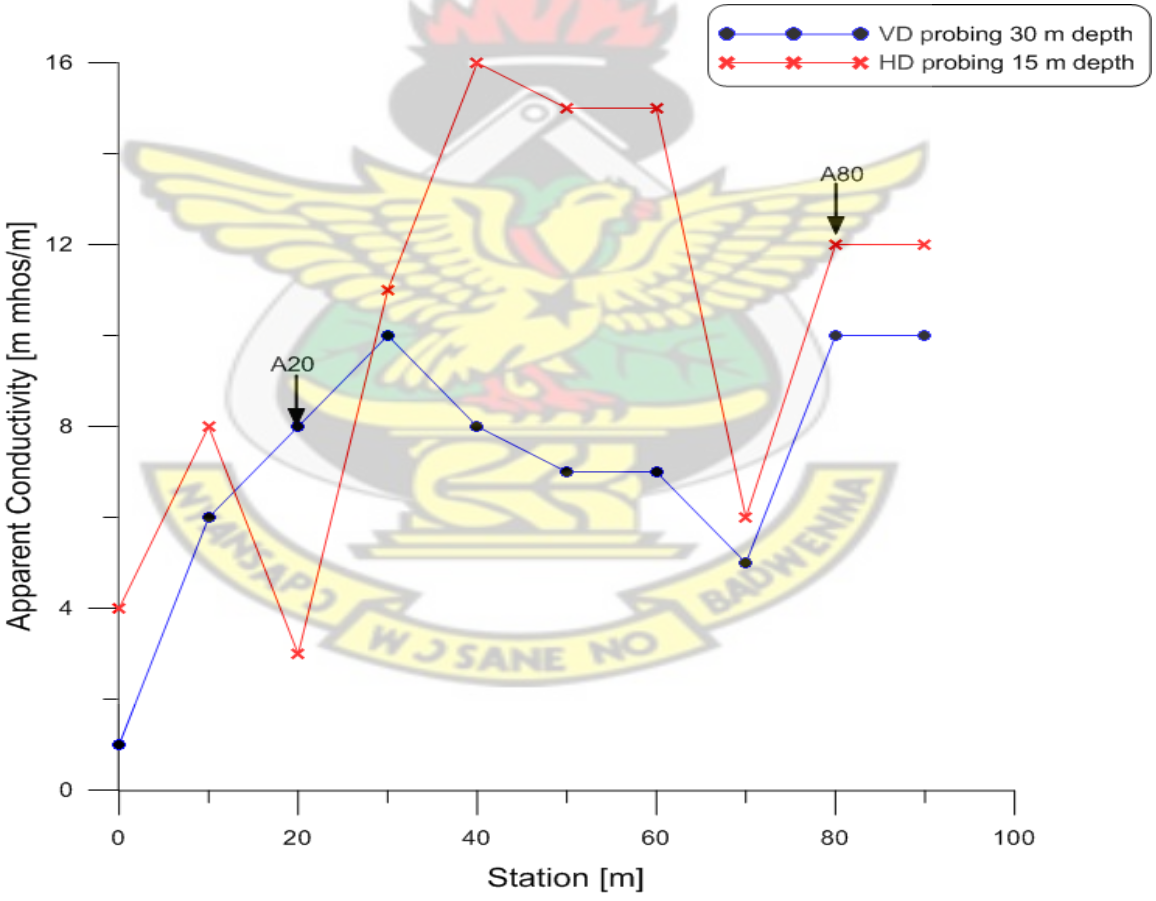

Fig. 4.50 EM terrain conductivity measurements along profile A at Maamakrom

Along profile B however, apparent conductivity values were between 6 and 17 m mhos/m as Figure 4.51 shows. The trend of HD curve showed a gradual increase in apparent conductivity up to 11 m mhos/m at the 30 m point. It then decreased to 9 m mhos/m at point 40 m and increased to 12 m mhos/m at the end of the profile. With the VD curve, values of conductivity were quite higher than the HD values for half of the profile length. The curve started off with a slight increase in conductivity to 17 m mhos/m at the 10 m point and then decreased steeply to the 40 m point at 6 m mhos/m. The curve ended up at 8 m mhos/m conductivity at the end of the profile. One point, B10 was selected for VES along this profile.

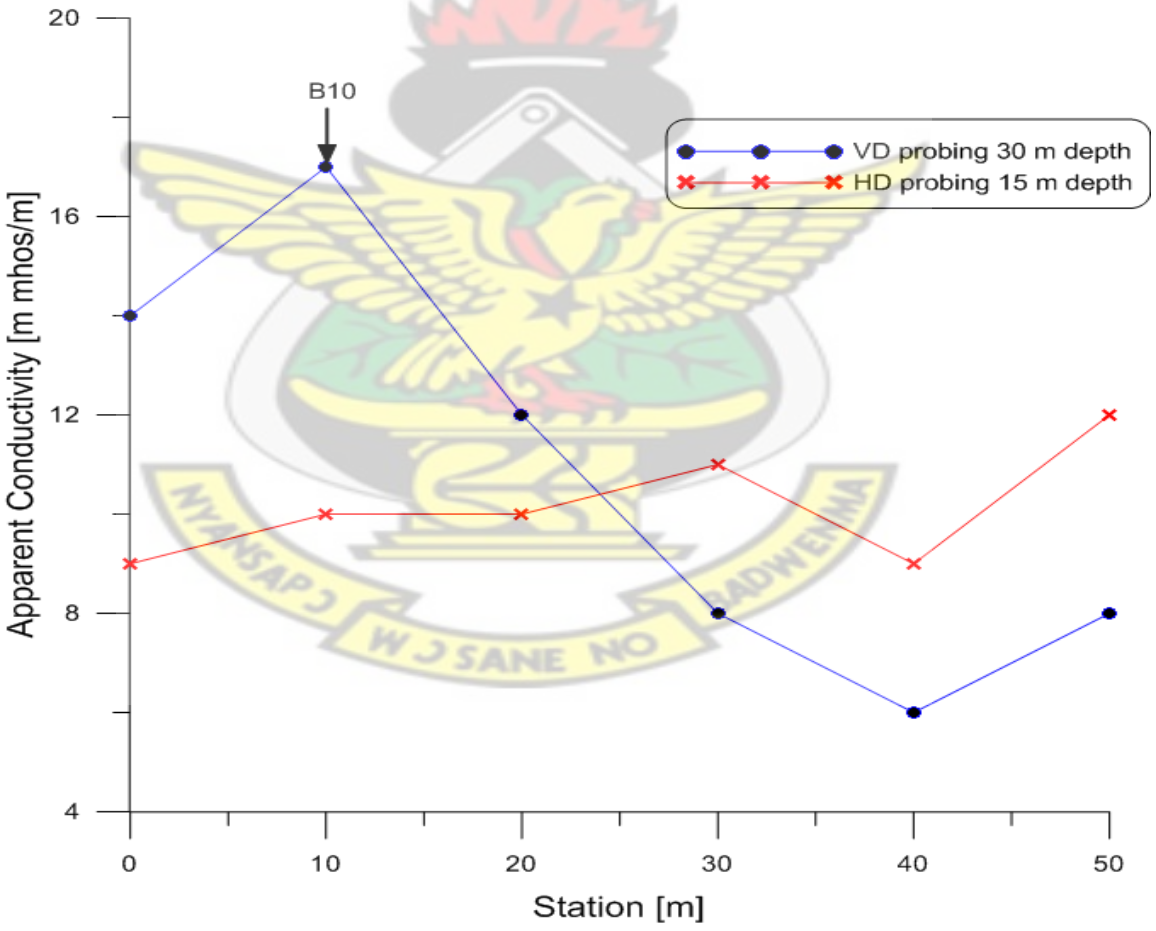

Fig. 4.51EM terrain conductivity measurements along profile B at Maamakrom

The VES curves of variation of apparent resistivity with depth at the three stations are shown in Figures 4.52 – 4.54.Results of the VES conducted in this area indicate a three layered subsurface structure except at station A80, which showed four lithological layers.

VES for A20

Analysis of the VES curve at station A20, Figure 4.52 revealed three geological layers at the subsurface. The topsoil may be fairly weathered and has apparent resistivity of 103 Ωm and a thickness of 3.2 m. The second layer, which is 5.9 m thick, with a 2633 Ωm resistivity is characteristic of a highly resistive formation. Below this is a probably fairly fractured third layer where the aquifer is expected to be intercepted. This layer has an apparent resistivity of 125 Ωm.

VES for A80

Deductions made from the VES curve at station A80 indicates a four layered subsurface structure as shown in Figure 4.53. The top layer is 1.5 m thick and has resistivity of 131 Ωm and is underlain by a second layer of resistivity and thickness of 141 Ωm and 2.2 m respectively. Beneath this is a 35.5 m thick third layer of resistivity, 383 Ωm whilst the fourth layer has 247 Ωm resistivity. All four layers are likely to be equally moderately fractured. This point may not be suitable for borehole drilling.

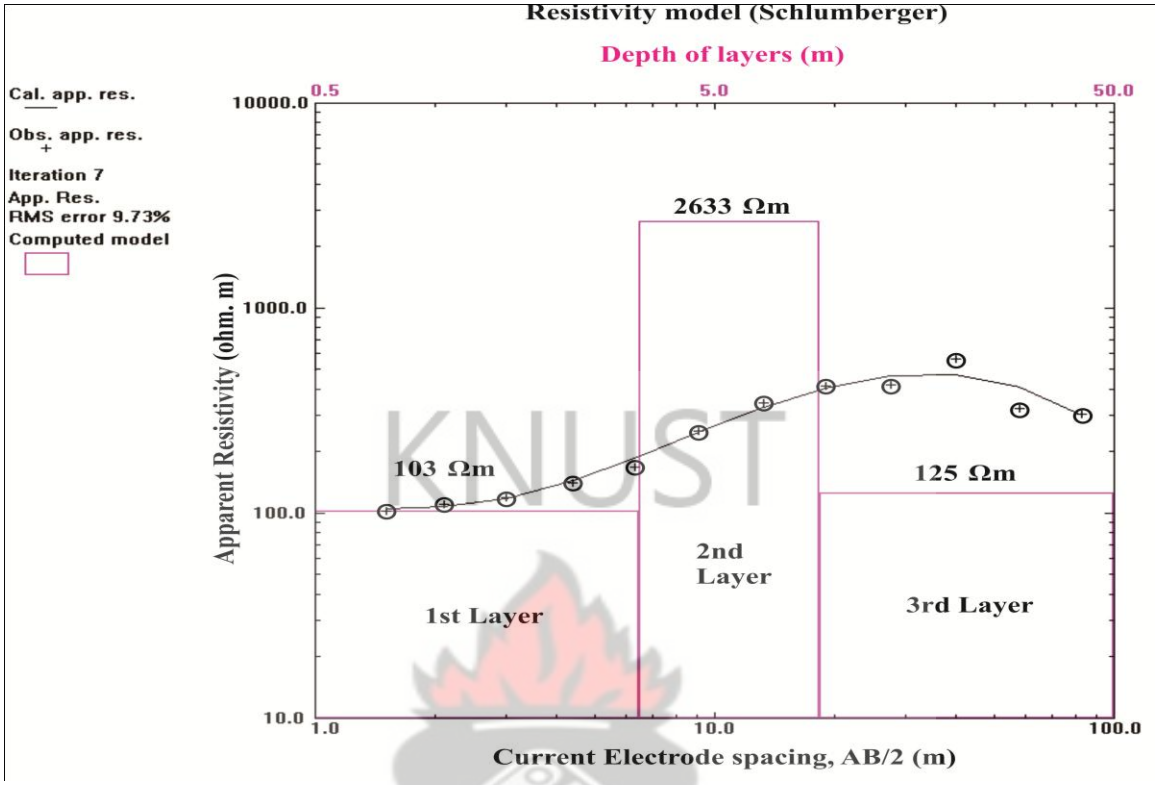

Fig. 4.52 VES curve at station A20 at Maamakrom

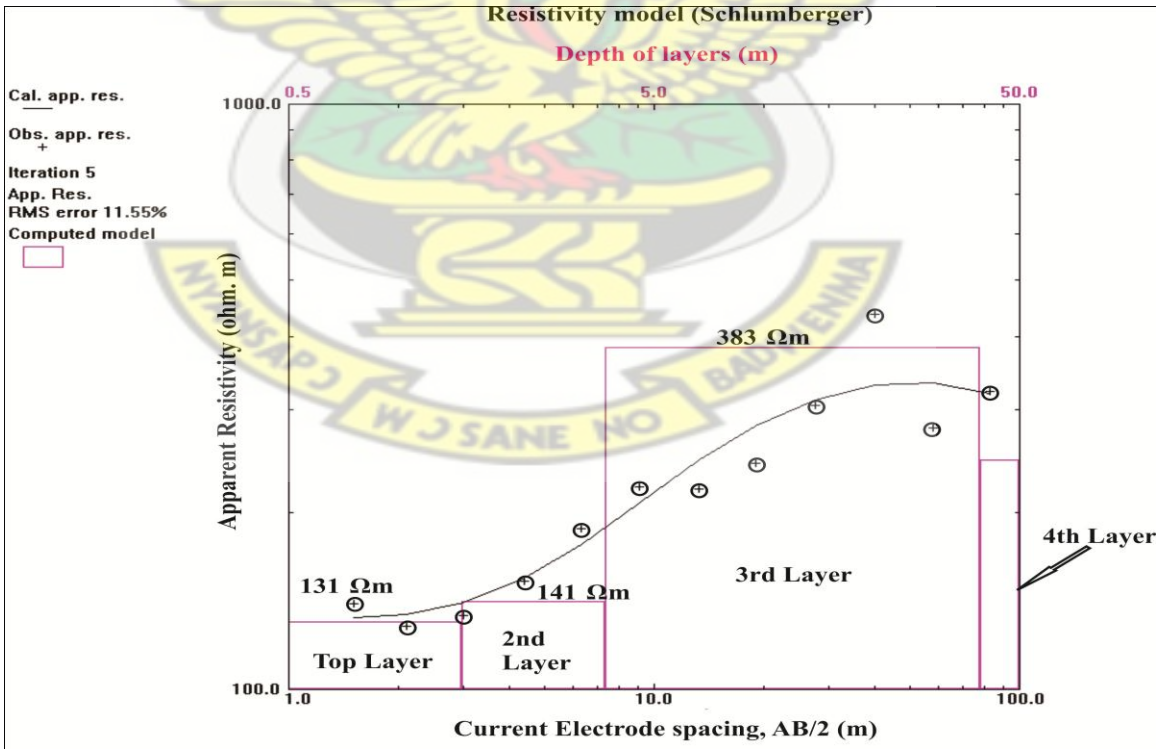

Fig. 4.53 VES curve at station A80 at Maamakrom

VES for B10

Station B10 Figure 4.54 revealed three layers in the subsurface with resistivity values in the range of 114 – 1016 Ωm. The first layer is 1.9 m thick and has a resistivity of 114 Ωm whilst the second layer, with a thickness of 6.7 m has 1016 Ωm resistivity. Below this is a third layer of 120 Ωm apparent resistivity. Deductions from these results suggest a highly resistive second layer sandwiched between two moderately fractured first and third layers. The third layer is expected to host moderate amount of groundwater.

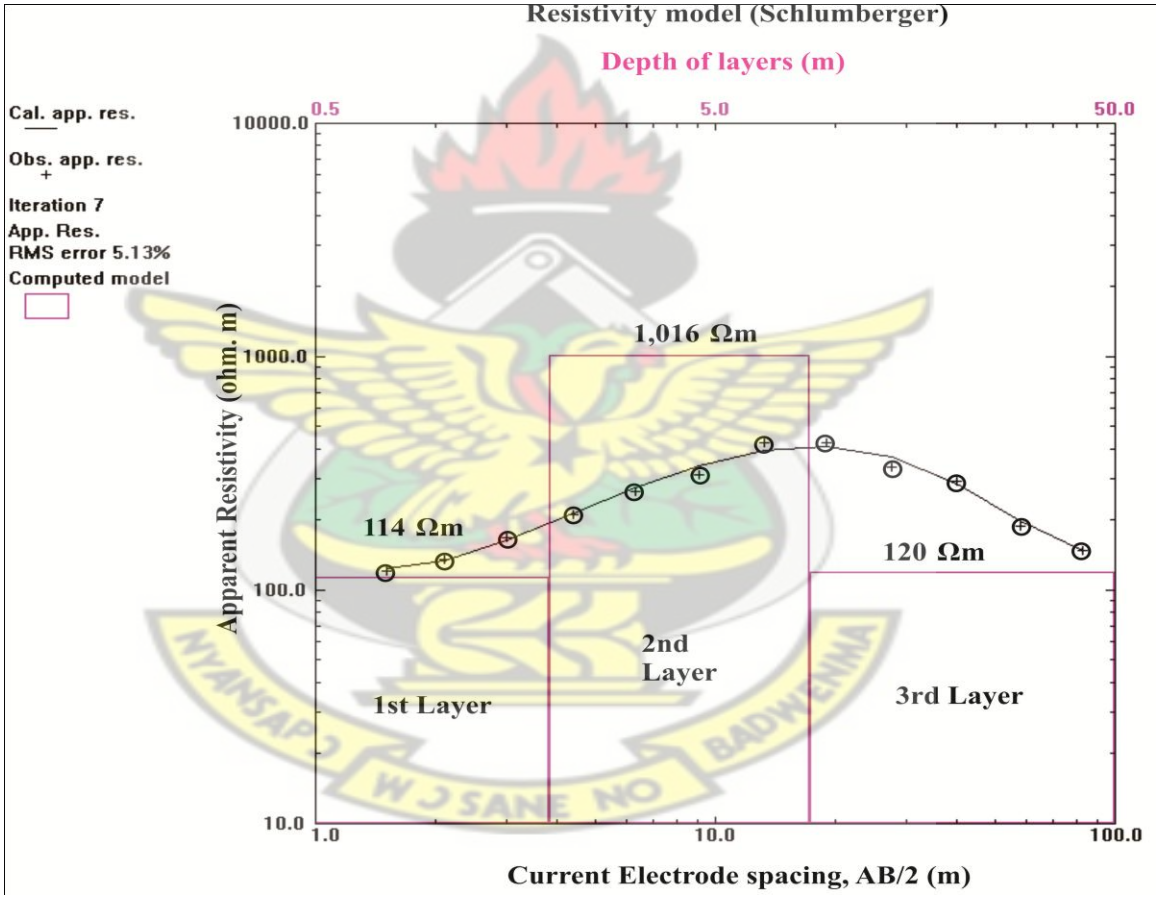

Fig. 4.54 VES curve at station B10 at Maamakrom

Based on the results obtained, the three VES stations were ranked according to their water bearing capacity. Station A20 was the first choice for test drilling and A80, considered unsuitable. This is presented in Table 4.10.

Table 4.10 Ranked VES points for test drilling at Maamakrom

Community	VES Point	Layer	Apparent Resistivity (Ωm)	Thickness (m)	Depth (m)	Rank
Maamakrom	A20	1	103	3.2	3.2	1
		2	2633	5.9	9.1	
		3	125	-	-	
	B10	1	114	1.9	1.9	2
		2	1,016	6.7	8.6	
		3	120	-	-	
	A80	1	131	1.5	1.5	3
		2	141	2.2	3.7	
		3	383	35.5	39.2	
		4	247	-	-	

4.1.11 Nkranketewa

One EM traverse was conducted on a profile length of 170 m and on a bearing of 254^0 from the True North in the community. Three potential points were selected along the profile to access their groundwater potential. These points include A30, A60 and A140.Figure 4.55 shows a layout of the community.

Observations of the graph in Figure 4.56 show that both HD and VD curves were erratic along the profile. However, apparent conductivity values of VD mode were generally higher than the HD mode suggesting higher groundwater prospects in the area. Consequently, three points were selected along the profile for depth probing with the VES method.

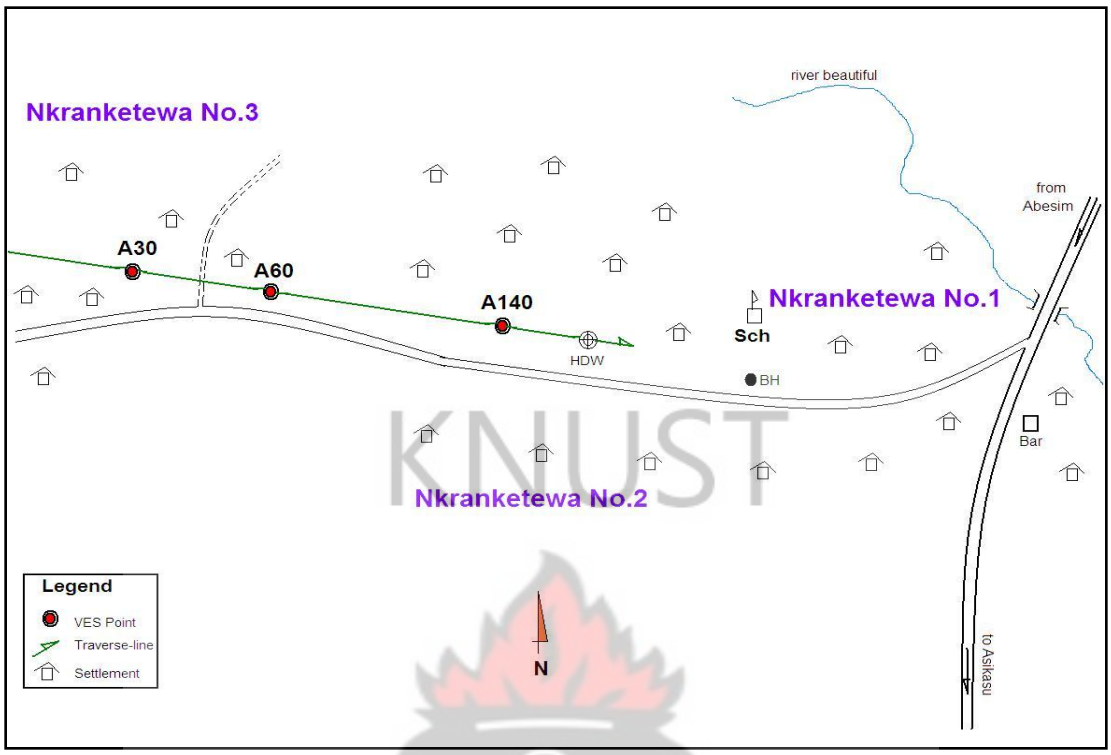

Fig. 4.55 A sketch of the layout of Nkranketewa community (Not to scale)

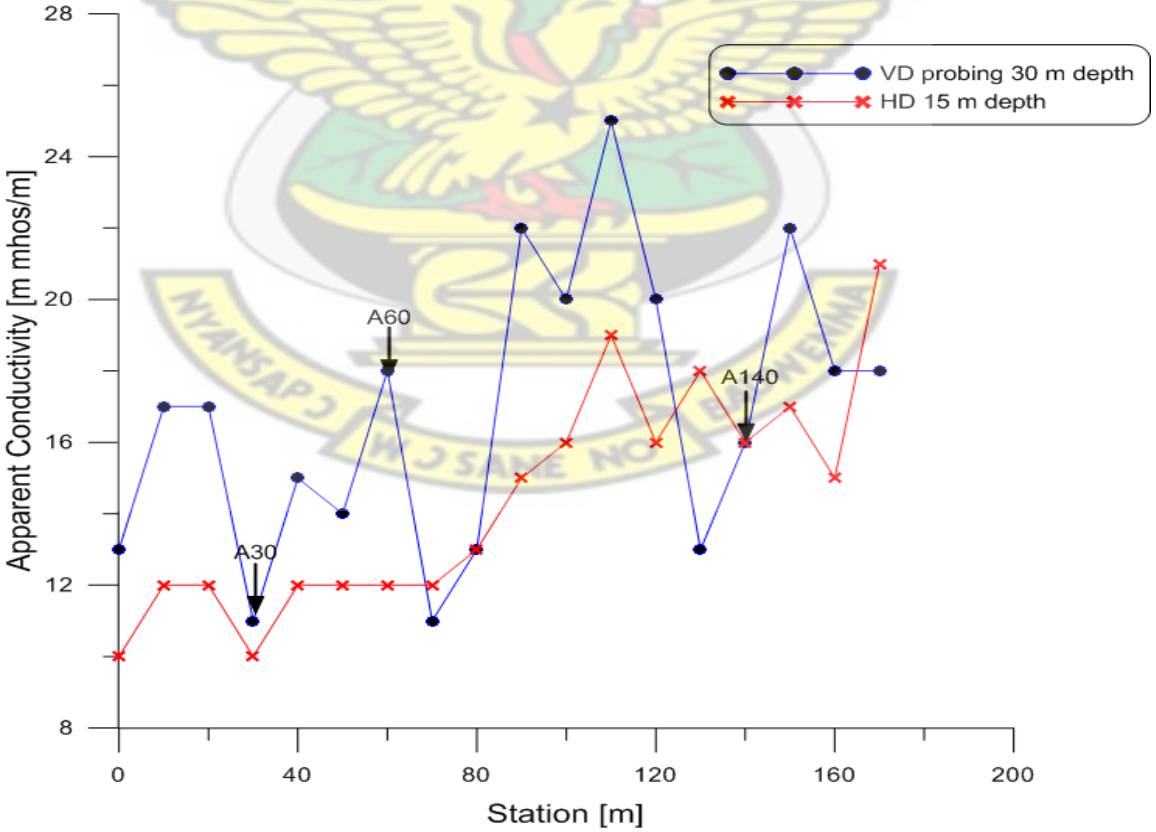

Fig. 4.56 EM terrain conductivity measurements along a profile at Nkranketewa

VES for A30

Station A30 was the first VES point selected along the EM profiling. Results from the depth sounding indicate that this point is underlain by four lithological units with apparent resistivity values between 65 Ωm and 332 Ωm as shown in Figure 4.57. The topsoil is 1.1 m thick and has a resistivity of 86 Ωm; whilst the second layer has resistivity of 65 Ωm and a thickness of 0.9 m. Beneath this is a third layer with apparent resistivity of 332 Ωm and a thickness of 7.5 m whereas the bedrock resistivity is 219 Ωm. Deductions made from these results suggest that all the four layers are fractured. However, the first two layers are diagnostic of highly fractured formations whilst the third and fourth layers could be partially fractured. Groundwater is expected to be accumulated in the third and fourth layers.

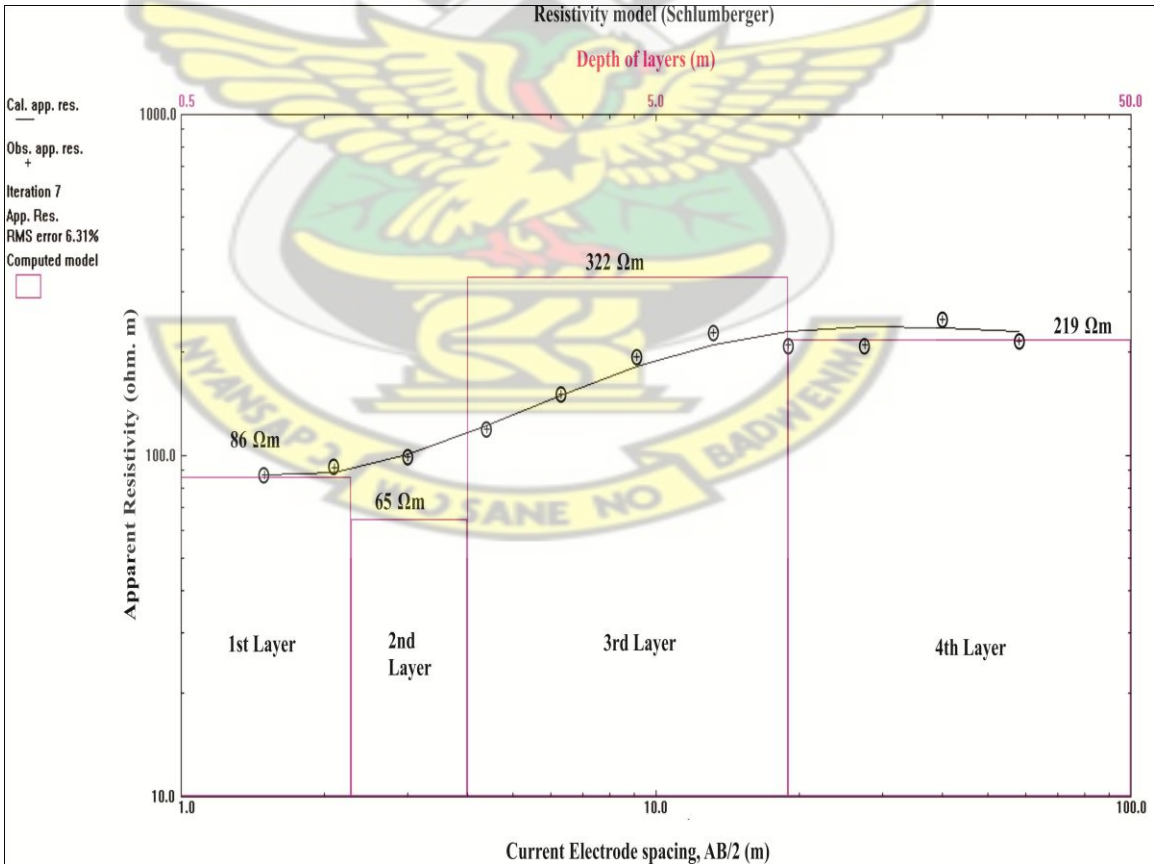

Fig. 4.57 VES curve at station A30 at Nkranketewa

VES for A60

The next VES was established at station A60 Figure 4.58 and the results similarly showed four lithological units in the subsurface. The topsoil, which is diagnostic of a highly fractured formation with a 1.5 m thickness and a 74 Ωm apparent resistivity. The second layer is 3.3 m thick and has 655 Ωm resistivity whilst the third layer has apparent resistivity and thickness values of 120 Ωm and 19.6 m respectively. Underlying this is a fourth layer of 325 Ωm resistivity. Analysis reveal that aside the topsoil being highly fractured, all the other three layers appear to be moderately fractured. Therefore, moderate amount of water is expected to be accumulated in the third and fourth layers.

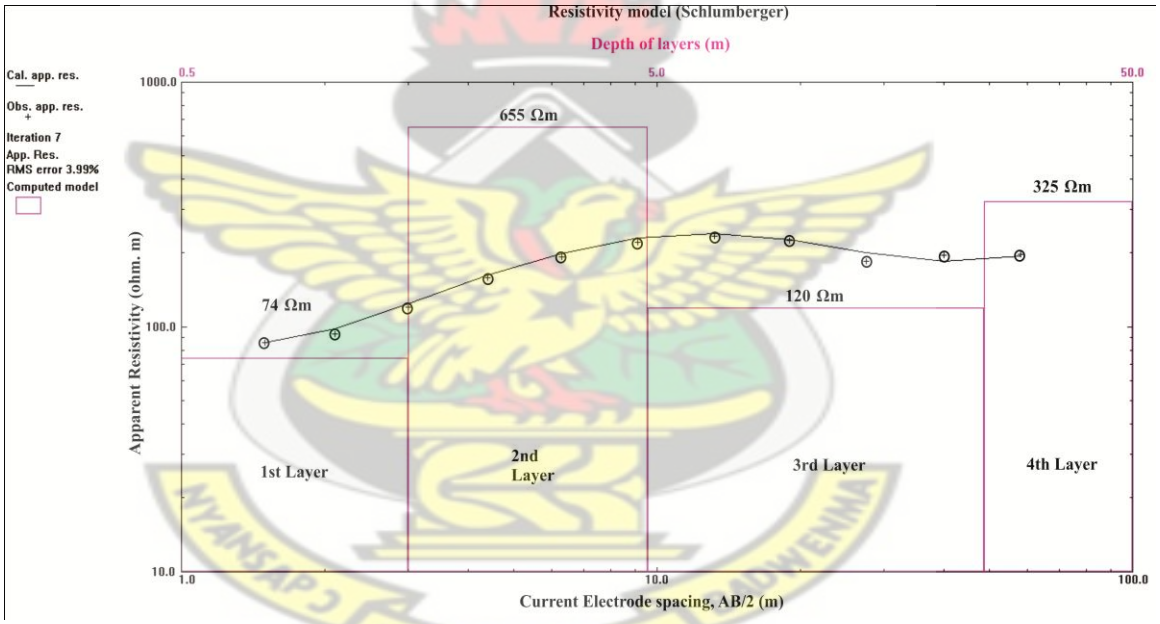

Fig. 4.58 VES curve at station A60 at Nkranketewa

VES for A140

The curve analysis at station A140 depict that the subsurface structure comprises four geological units as is apparent in Figure 4.59. The topsoil has an apparent resistivity of 148 Ωm and a thickness of 1.7 m whereas the thickness of the second layer is 4.1 m and

has 331 Ωm resistivity. Underlying this is a 13.6 m thick third layer, which has a resistivity of 124 Ωm whilst the deepest layer has an apparent resistivity of 247 Ωm. These results suggest that all the four layers are moderately weathered. This site appears to have very good groundwater potentials. Groundwater is expected to be intercepted in the third layer.

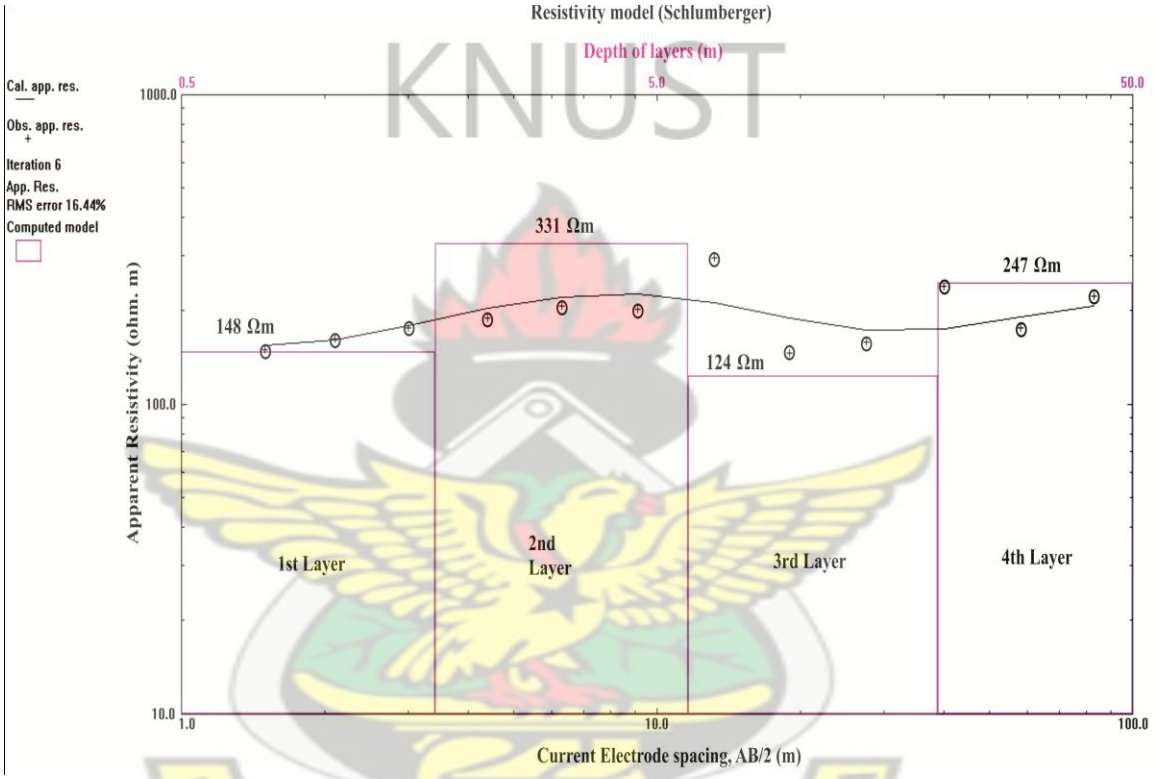

Fig. 4.59 VES curve at station A140 at Nkranketewa

A general observation made was that the area is underlain by four lithological units and that the bedrock is fairly fractured. Groundwater potential is therefore expected to be moderate. For borehole drilling purposes, these stations were ranked due to their groundwater bearing potentials. The first choice for test drilling was station A60 followed by station A140 as the alternate test drilling site. Information on these rankings is presented in Table 4.11.

Table 4.11 Ranked VES points for test drilling at Nkranketewa

Community	VES Point	Layer	Apparent Resistivity (Ωm)	Thickness (m)	Depth (m)	Rank
Nkranketewa	A60	1 2 3 4	74 655 120 325	1.5 3.3 19.6 -	1.5 4.8 24.4 -	1
	A140	1 2 3 4	148 331 124 247	1.7 4.1 13.6 -	1.7 5.8 19.4 -	2
	A30	1 2 3 4	86 65 322 219	1.1 0.9 7.5 -	1.1 2 9.5 -	3

4.1.12 Tano – Ano

The conductivity anomaly of the terrain was delineated by two EM traverses. From the results obtained, three points A10, A90 and B10 were selected for further probing with the VES method. The schematic layout showing the traverse lines and the VES points selected in this community are displayed in Figure 4.60.

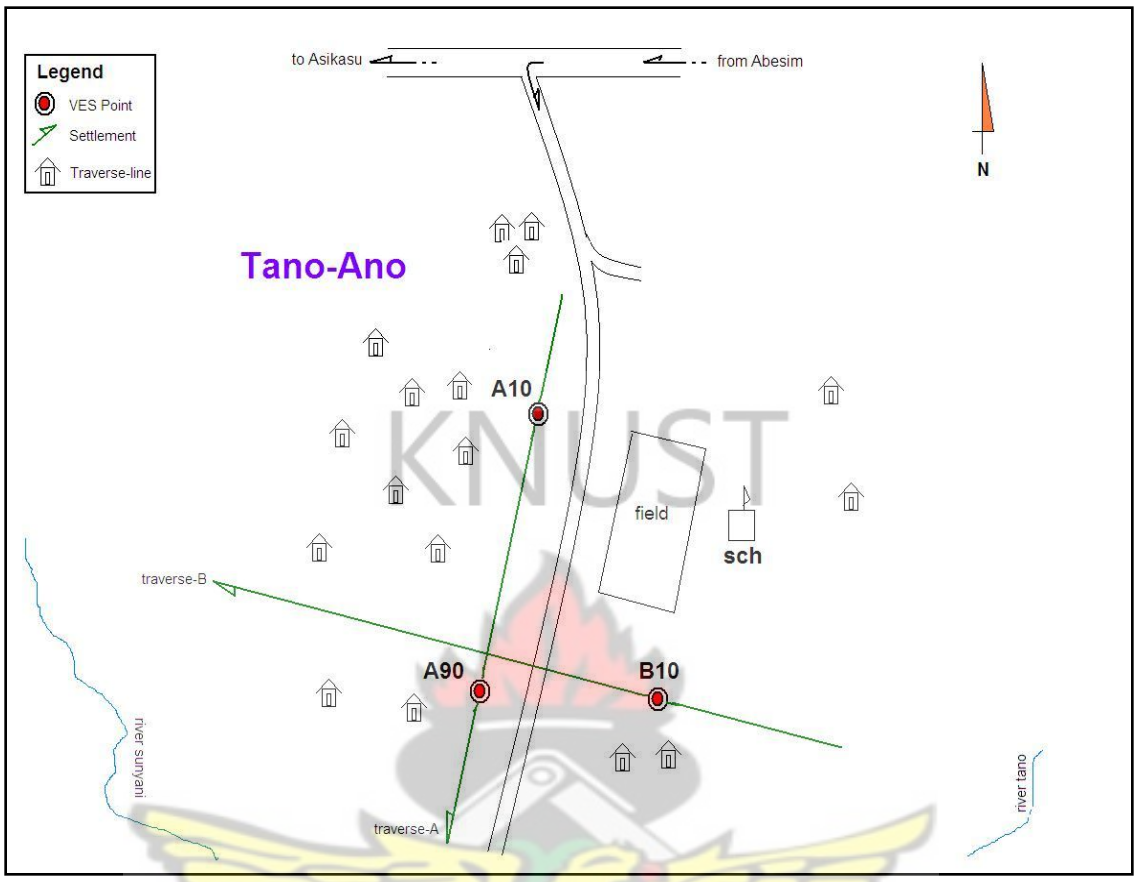

Fig. 4.60 A sketch of the layout of Tano-Ano community (Not to scale)

EM results gathered from the traverse conducted on profile A of length 170 m with the 20 m coil spacing show that the trend of both HD and VD curves were similar. That is, both curves behaved erratically along the entire length of the profile. Apparent conductivities varied from low (3 m mhos/m) to moderate (15 m mhos/m) values with an average of 8.3 m mhos/m. Even though the VD curve showed lower values of conductivity than the HD curve, a few crossover points were obtained along the profile. Two of these crossover points (A10 and A90) were selected for VES as shown in Figure 4.61.

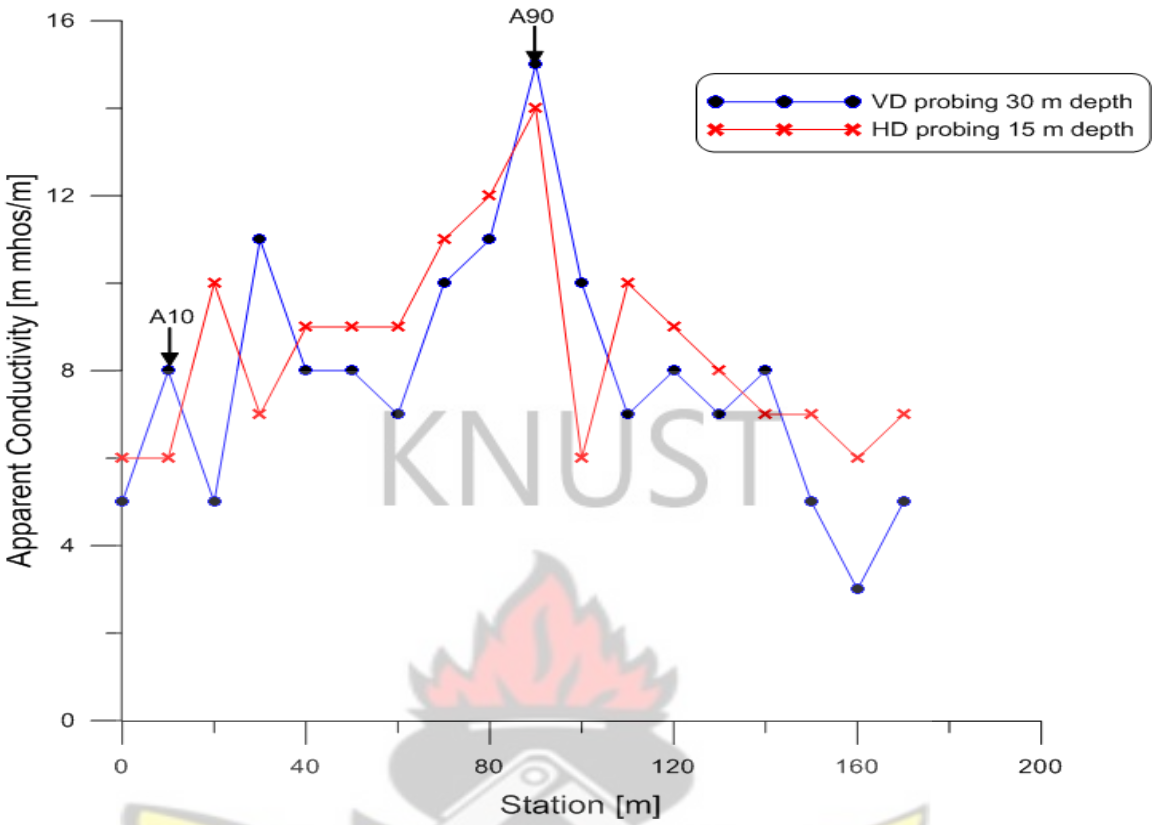

Fig. 4.61 EM terrain conductivity measurements along profile A at Tano-Ano

Profile B was established on a bearing of 320^0 from the True North and a length of 100 m. From the graph of EM response curves with distance (Figure 4.62), there were higher values of the HD mode than of the VD mode except at the beginning of the profile. This suggests a decrease in conductivity with depth. Nevertheless, cross-overs were detected at the 10 m point at 7 m mhos/m and the 60 m point at 10 m mhos/m conductivity. Station B10 was chosen for VES.

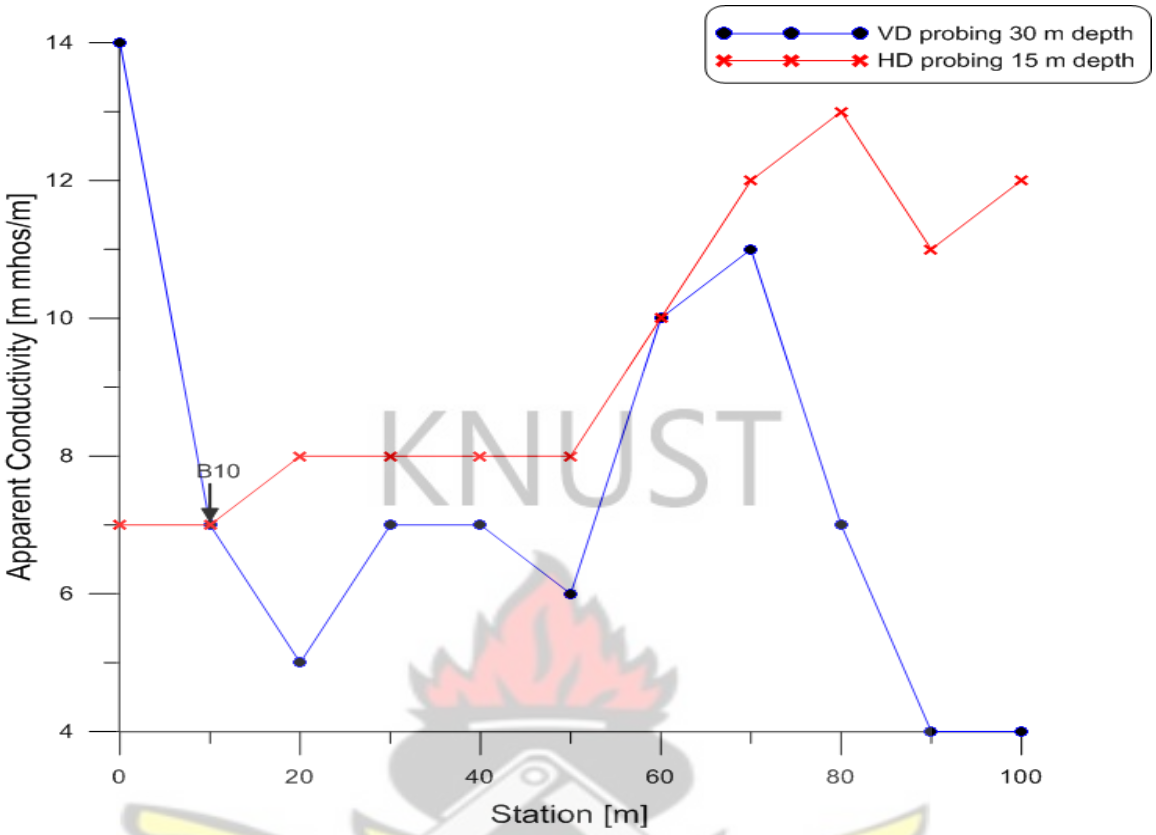

Fig. 4.62 EM terrain conductivity measurements along profile B at Tano-Ano

VES for A10

Station A10 was the first selected VES point. Depth probing at this station revealed three geological layers as in Figure 4.63. The topsoil appeared moderately fractured with a thickness of 2.2 m and a resistivity of 124 Ωm. Beneath this is likely to be a slightly fractured second layer of thickness and apparent resistivity of 23.7 m and 670 Ωm respectively. The third layer which may be highly weathered has an apparent resistivity of 90 Ωm. The layer is expected to host appreciable amount of water.

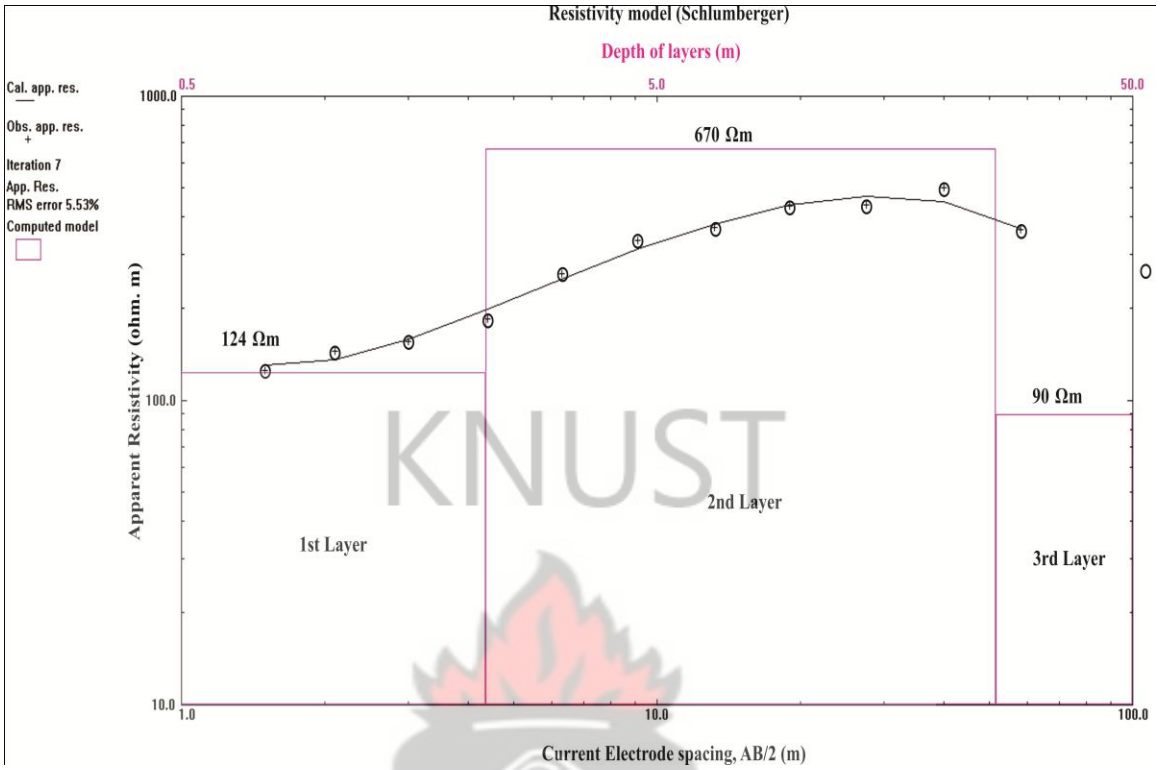

Fig. 4.63 VES curve at station A10 at Tano-Ano

VES for A90

Unlike station A10, results of the VES at station A90 revealed the subsurface structure consist of four geological units. The top layer, 2.5 m thick has a resistivity of 69 Ωm whereas the 1.8 m thick second layer has a resistivity of 33 Ωm. Beneath this is a third layer with thickness and apparent resistivity values of 7.1 m and 1416 Ωm whilst the bottom layer has a 15 Ωm resistivity. Analysis of the curve at this station (Figure 4.64) suggest that, with the exception of the third layer which is probably made of a very high resistive rock, all the other three layers appear to be highly fractured. The fourth layer is a potential zone for groundwater storage.

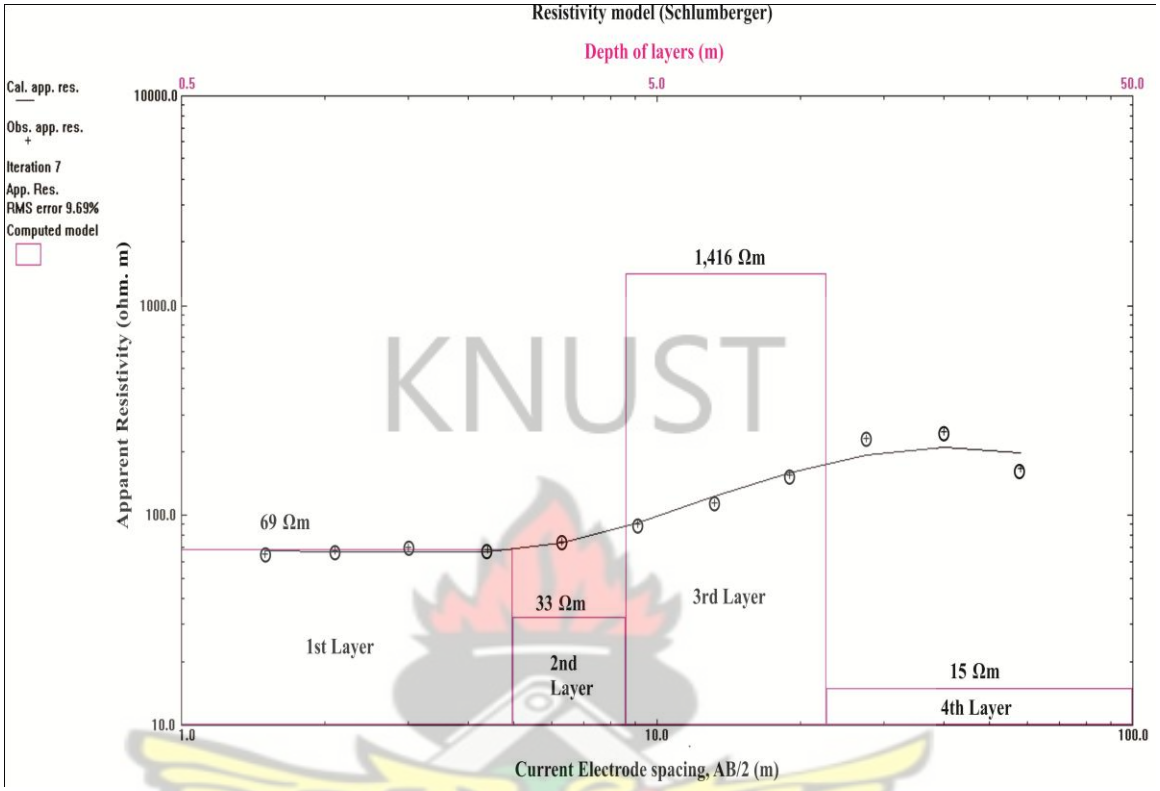

Fig. 4.64 VES curve at station A90 at Tano-Ano

VES for B10

The next sounding station, B10 revealed a three layered subsurface structure as displayed in Figure 4.65. Analysis of the results revealed the possibly highly fractured topsoil of 0.9 m thick with an apparent resistivity of 60 Ωm. The second layer, which may be only slightly weathered is 17.7 m thick and has an apparent resistivity of 736 Ωm. Underlying this is a highly weathered formation of 19 Ωm resistivity. This layer could contain appreciable quantity of groundwater.

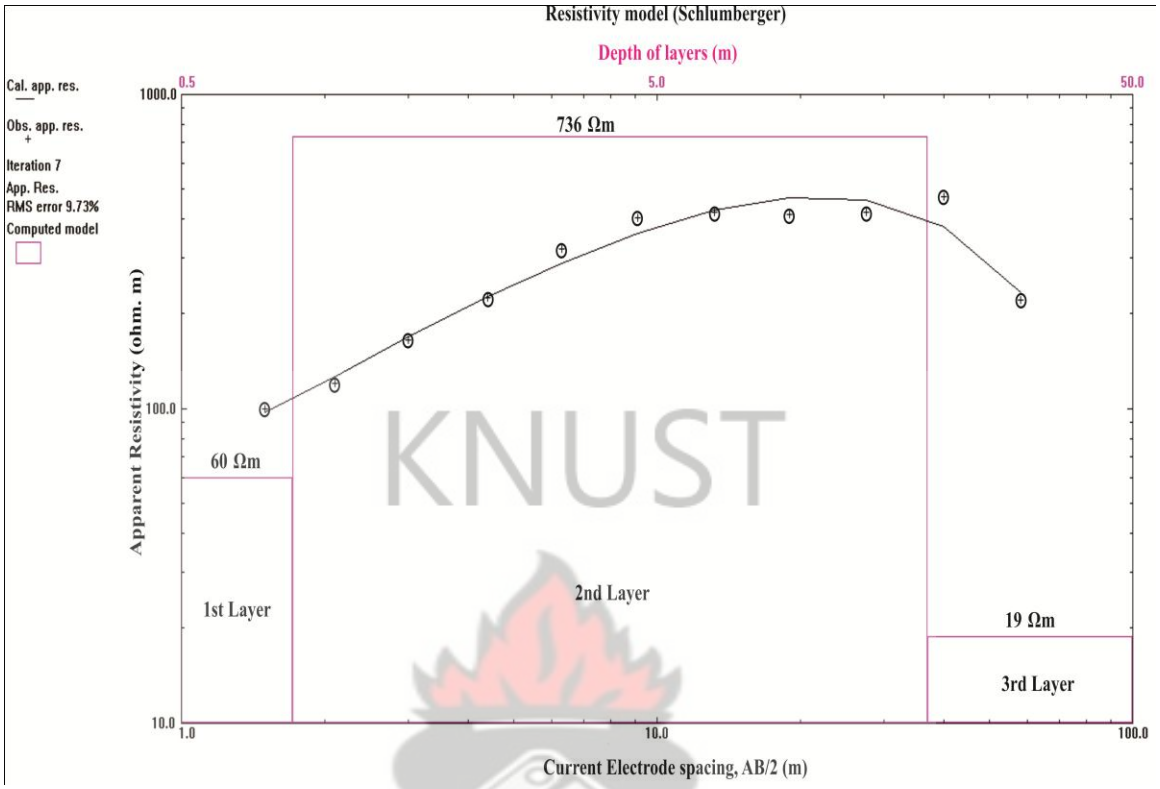

Fig. 4.65 VES curve at station B10 at Tano-Ano

General deductions made from the results indicate that the subsurface structure is underlain by three lithological units except at station A90, which revealed four layers. The bedrock is expected to be moderately fractured. The prospects for borehole drilling in the community appear to be a very high. Nevertheless, some points have relatively higher potentials for groundwater than others. Hence, the depth sounding stations are ranked to help in selecting the test drilling points. Information on this is provided in Table 4.12 below. From the table, station A90 was the best recommended site for test drilling and station B10 was chosen as an alternate site.

Table 4.12 Ranked VES points for test drilling at Tano-Ano

Community	VES Point	Layer	Apparent Resistivity (Ωm)	Thickness (m)	Depth (m)	Rank
Tano - Ano	A90	1	69	2.5	2.5	1
		2	33	1.8	4.3	
		3	1416	7.1	11.4	
		4	15	-	-	
	B10	1	60	0.9	0.9	2
		2	736	17.7	18.6	
		3	19	-	-	
	A10	1	124	2.2	2.2	3
		2	670	23.7	25.9	
		3	90	-	-	

4.1.13 Yeboakrom

EM profiling in Yeboakrom was conducted along two traverse lines of total length 180 m. A total of three vertical electrical soundings were also selected in this community. The three VES points included A60, B30 and SP1. Station A60 was established along profile A, station B30 along profile B and station SP1 was a spot sounding point. A sketch of the layout of this community showing the location of traverse lines and VES points is displayed in Figure 4.66 below.

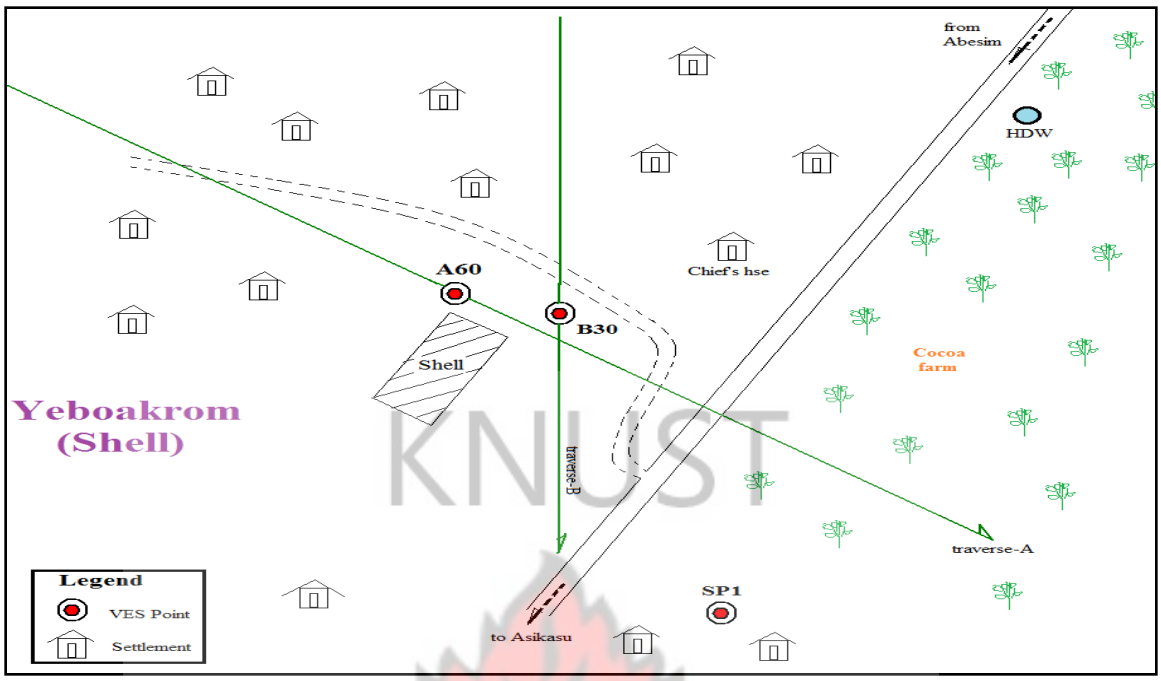

Fig. 4.66 A sketch of the layout of Yeboakrom community (Not to scale)

EM terrain conductivity measurements along profile A was conducted on a bearing of 127^0 from the True North and it had a length of 70 m. Conductivity values ranged between -3 to 12 m mhos/m. As shown in Figure 4.67, the VD values were lower than the HD values up to the 20 m point where it reached a conductivity of 5 m mhos/m. A cross-over point was obtained between 20 m and 30 m points after which the VD values crossed-over and increased till it got to a conductivity of 12 m mhos/m at the 60 m point. The apparent conductivity then decreased to the end of the profile. The trend was somewhat different for the HD curve in that, it began with a decline in apparent conductivity value up to 3 m mhos/m at point 10 m. A steady increase was then observed till it reached the 40 m point at 7 m mhos/m and remained constant at this conductivity value for the rest of the profile. Station A60 was selected for VES.

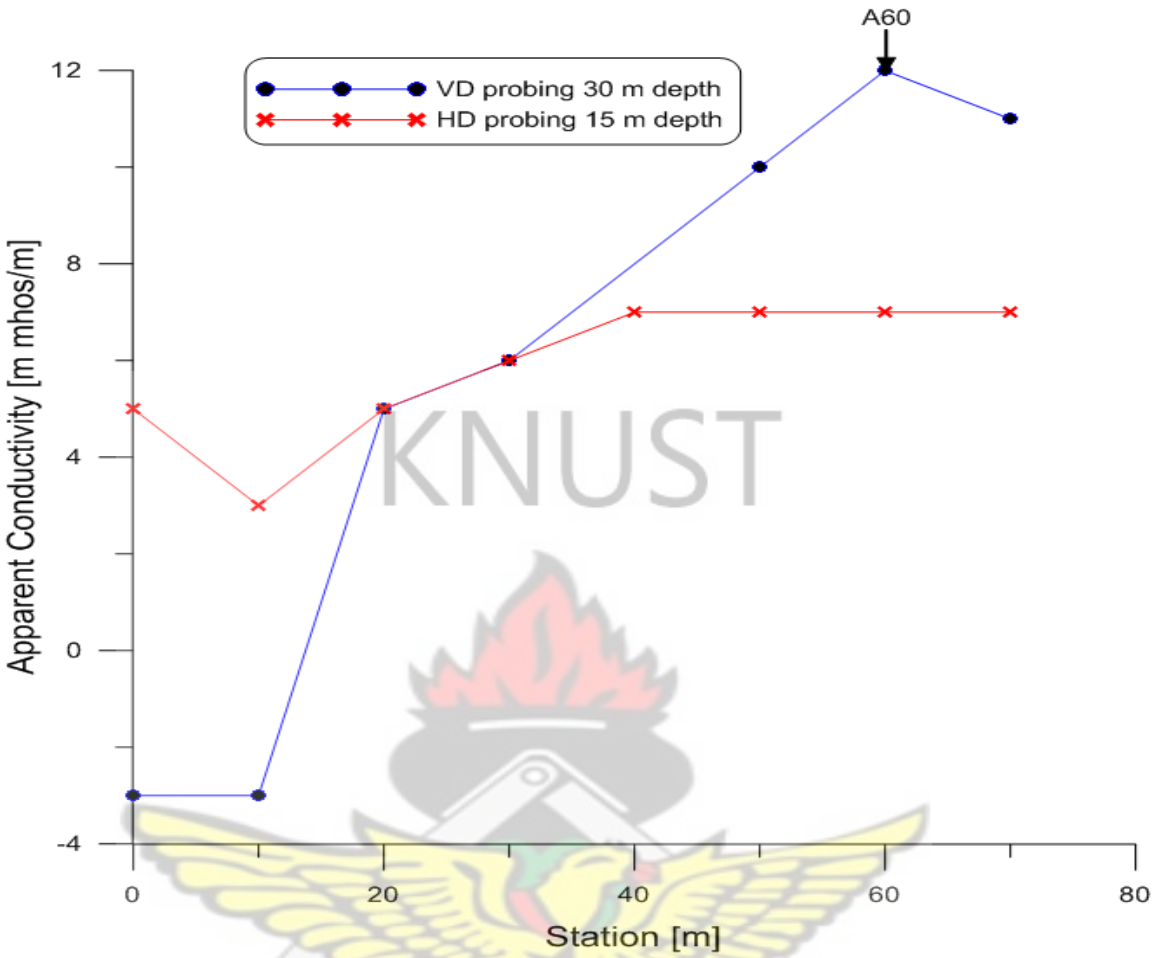

Fig. 4.67 EM terrain conductivity measurements along profile A at Yeboakrom

Along profile B of length 110 m, terrain conductivities measured were in the range of 5 and 11 m mhos/m. Observations made from the curves in Figure 4.68 revealed both HD and VD curves to be erratic. However, HD values remained higher than the VD values suggesting a decrease in conductivity with depth along the profile. Despite this trend, cross-over points were obtained between the 20 m and 30 m points with conductivities of 8 and 9 m mhos/m respectively. Therefore, the 30 m point was selected for further depth probing.

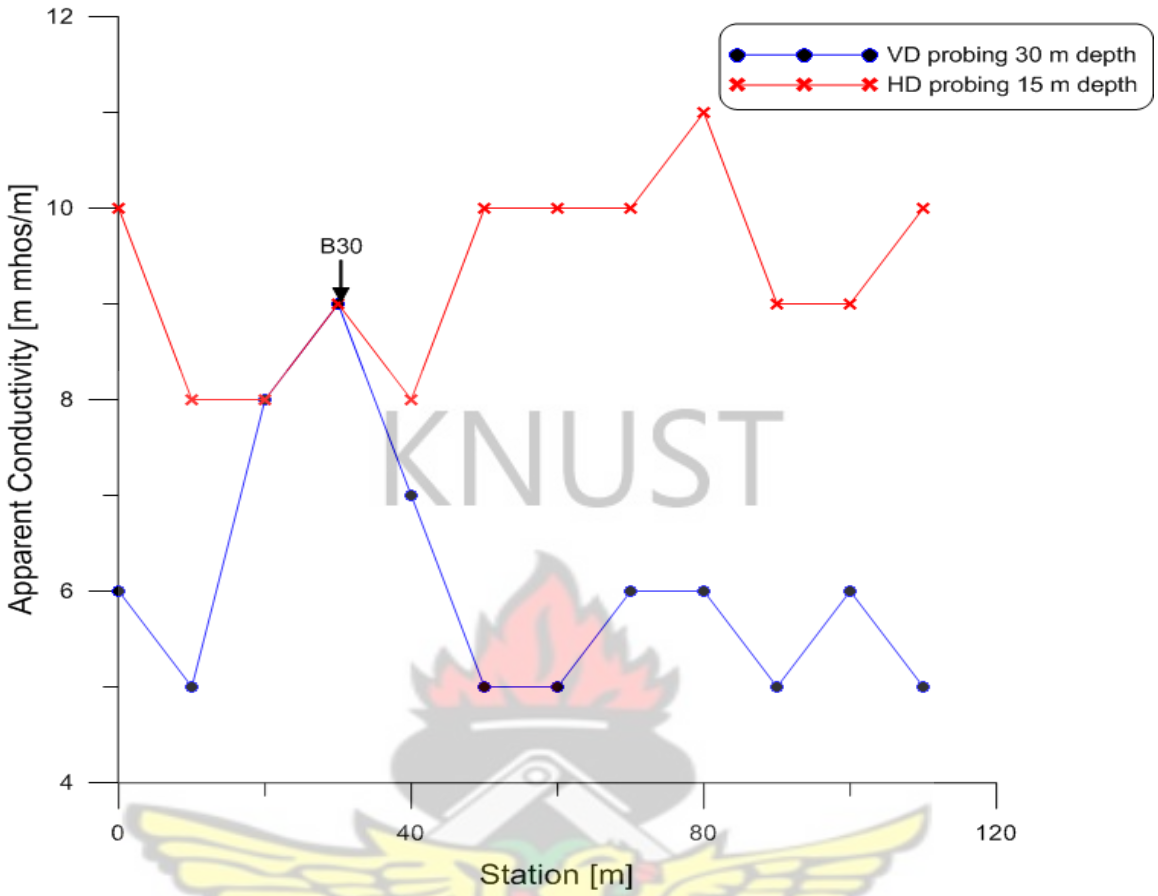

Fig. 4.68 EM terrain conductivity measurements along profile B at Yeboakrom

VES for A60

The first VES point (A60), revealed that the subsurface structure consists of four geological units as shown in Figure 4.69. Analysis of the results obtained suggests that the top layer, which has 0.6 m thickness and 69 Ωm resistivity, is highly fractured. Beneath this is likely to be a fairly fractured formation of apparent resistivity and thickness values of 288 Ωm and 10.7 m respectively. The third layer appears to be only slightly fractured and is 22.8 m thick with a resistivity of 688 Ωm. Underlying this is a moderately weathered bedrock which, is a potential groundwater storage point.

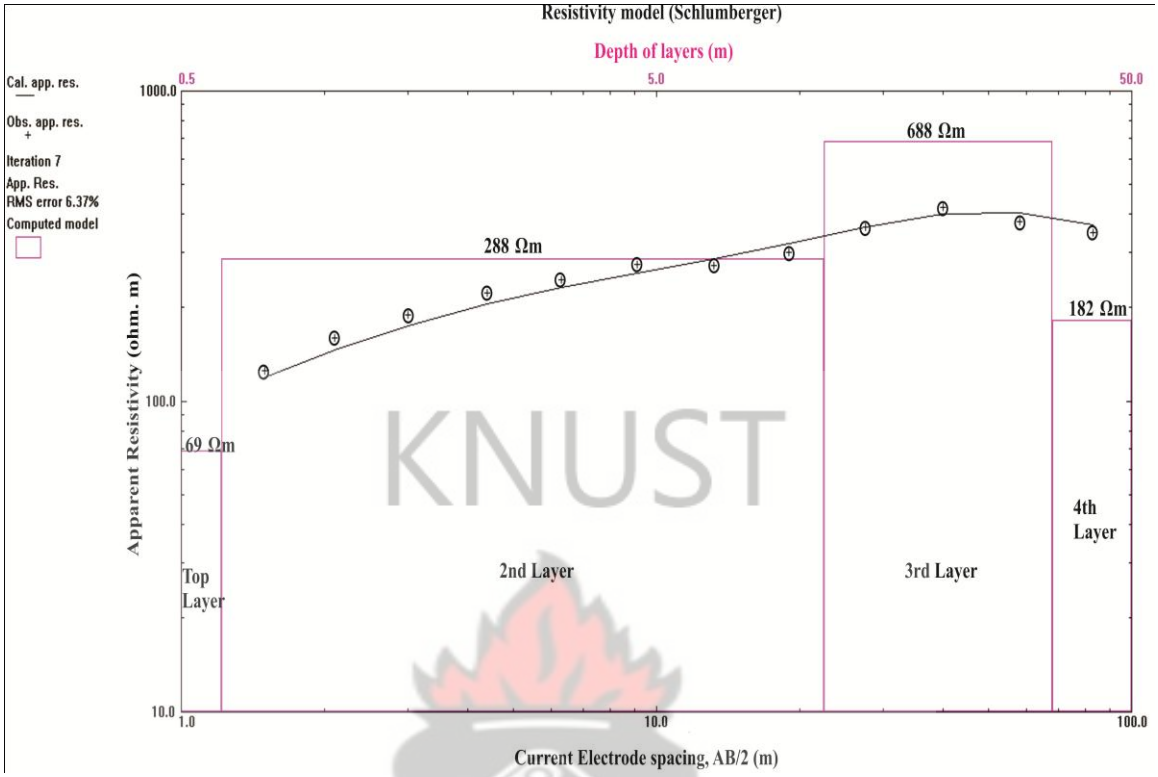

Fig. 4.69 VES curve at station A60 at Yeboakrom

VES for B30

Figure 4.70 shows a graph of apparent resistivity against depth at station B30. The curve reveals three layers in the subsurface. Layer one is 1.2 m thick and has a resistivity of 229 Ωm, whilst layer two has a thickness of 6.2 m and resistivity of 246 Ωm. The deepest layer has an apparent resistivity of 603 Ωm. Deductions made from these indicate that the first two layers may be moderately fractured whilst the third layer appears to be slightly fractured. Not much water is expected at this point.

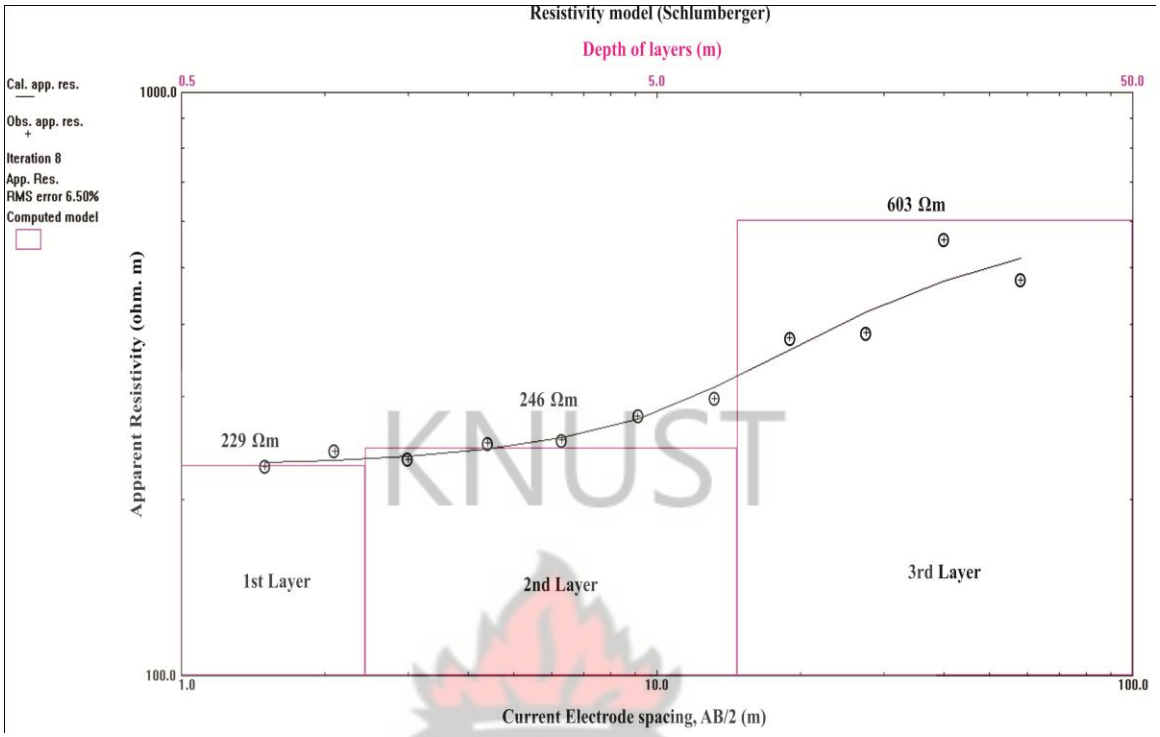

Fig. 4.70 VES curve at station B30 at Yeboakrom

VES for SP1

The curve analysis from the spot sounding at station SP1 indicates the subsurface is made up of three lithological layers. As is apparent in Figure 4.71, apparent resistivity values varied between 122 Ωm and 1749 Ωm. The seemingly moderately fractured topsoil is 3.1 m thick and has a resistivity of 122 Ωm. Below this is characteristic of a highly resistive formation with thickness and apparent resistivity of 10.5 m and 1749 Ωm respectively. The bottom layer, which may be moderately weathered, has an apparent resistivity of 236 Ωm. This layer is expected to host sufficient quantity of groundwater and could be a very good point for borehole drilling.

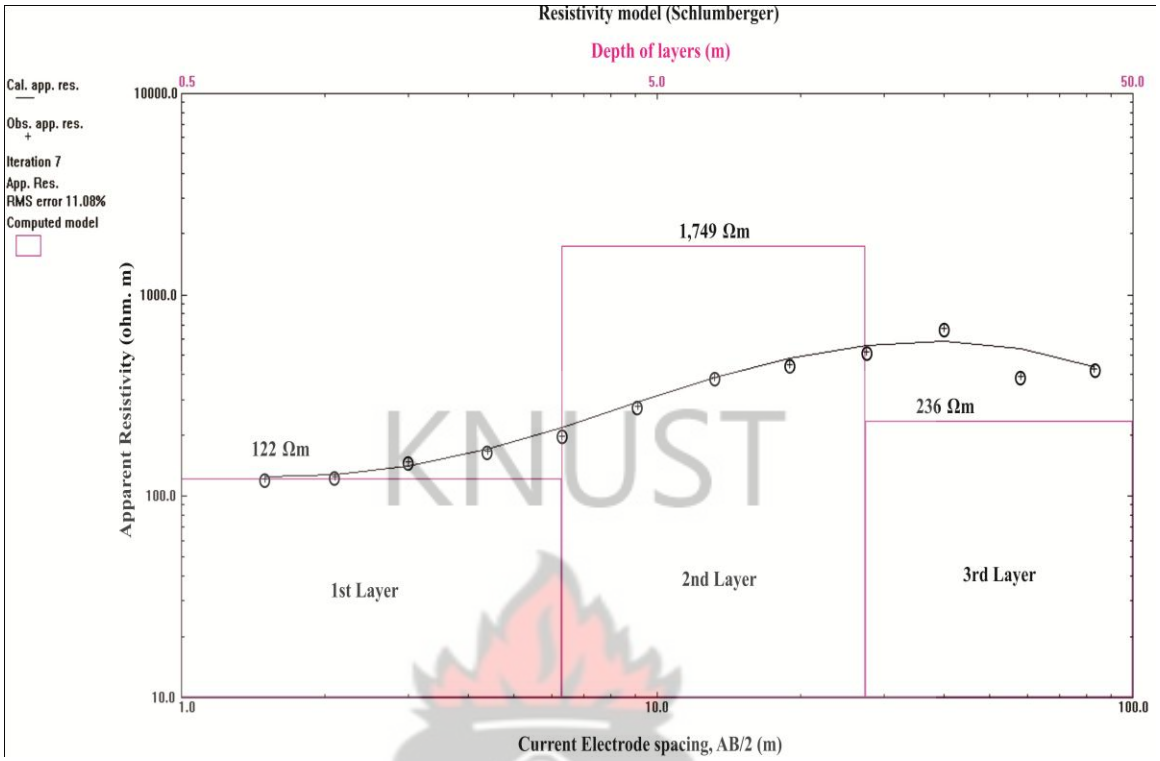

Fig. 4.71 VES curve at station SP1 at Yeboakrom

The general implication of the results is that the community is underlain by three subsurface lithological units except at station A60, which showed four subsurface layers. The aquifer is expected to be located in the bedrock. For purposes of drilling, the various stations are ranked in order of their groundwater potentials as shown in Table 4.13. The VES point SP1 is recommended for drilling with A60 as the alternate drilling point.

Table 4.13 Ranked VES points for test drilling at Yeboakrom

Community	VES Point	Layer	Apparent Resistivity (Ωm)	Thickness (m)	Depth (m)	Rank
Yeboakrom	SP1	1	122	3.1	3.1	1
		2	1749	10.5	13.6	
		3	236	-	-	
	A60	1	69	0.6	0.7	2
		2	288	10.7	11.3	
		3	688	22.8	34.1	
		4	182	-	-	
	B30	1	229	1.2	1.2	3
		2	246	6.2	7.4	
		3	603	-	-	

CHAPTER 5

CONCLUSIONS AND RECOMMENDATIONS

Introduction

The summary of the major findings of this study, the conclusion of the study and the suggestions for further research works are presented in this chapter

5.1 Conclusion

It is worth stating that this project was carried out as part of the efforts being made by Water Research Institute of the CSIR in collaboration with the Physics Department, KNUST to help alleviate water crisis in the rural areas in order to improve their standard of living.

As a conclusion for this research, the geophysics analysis using the electromagnetic and electrical resistivity methods has successfully reached it objectives of investigating the groundwater potential zones in the study area. In the quest for finding suitable locations for siting boreholes in the Sunyani Municipality of the Brong-Ahafo Region of Ghana, the concept of geophysics was applied using the Geonics EM 34-3 and ABEM SAS 1000C terrameter equipments. The subsurface resistivity data collected from the survey were processed with the Grapher 8 and RES1D softwares.

Since the electrical method has proved in the past to be a powerful technique in groundwater studies, it was reasonable to use an integrated approach by combining the electromagnetic and resistivity methods in this research. The electromagnetic method was useful as a reconnaissance tool in predicting potential zones for further probing with the

resistivity survey method (specifically, the vertical electrical sounding method). The vertical electrical sounding also delineated sequence of subsurface lithologies. It was evident that the Birimian rocks underlying the study area are marked with generally low to moderate fractures with the overburden thickness in the range of 20 to 60 m. Hence, groundwater yield is expected to be low to moderate in the district. Altogether, the application of the integrated geophysical data was very useful in delineating prospective aquifer zones to aid in the drilling of boreholes in the beneficiary communities.

Out of the 13 communities surveyed, a total of 18 EM profiles were traversed and 40 vertical electrical soundings conducted. In total, an EMT length of 2.8 km was traversed, and the 40 VES points were selected. The interpretation of the 40 VES points suggested that 13 of them could be considered suitable for borehole drilling. From the analyses of the VES curves, it was revealed that the subsurface structure of 27 out of the 40 VES points were underlain by three layers while the remaining 13 were of four layer types. The predominance of the three layer types as well as the low resistivity values obtained at most of the VES points suggest the extent of fracturing in the project communities. This aided in categorizing the study area into three groundwater potential zones as high, moderate and low.

Conclusions drawn from the interpretation of both the EM and VES data obtained in this study are as follows:

In Adomako community, the third layer of station A20 is a good groundwater potential zone characterized by a resistivity value of 140 Ωm. This zone is likely to be a moderately fractured basement. Likewise, the third layer of station A200 is an

intermediate groundwater potential zone and could be an alternative borehole drilling point in the community. The aquifer layer has a resistivity value of 200 Ωm.

In Ankobea community, the third layer of station A20 may be classified as a good layer with possible significant amount of groundwater. The layer has a very low apparent resistivity of 56 Ωm, and is characteristic of a weathered basement. An intermediate groundwater storage zone in the area is the third layer of station A230 with a resistivity of 116 Ωm.

The third layer of station A60 in Antwikrom community is a potential zone for groundwater storage and has a 378 Ωm resistivity. The second layer of station A20 has an intermediate groundwater storage capacity with a resistivity of 121 Ωm.

The first ranked site for drilling in Abesim Zongo community is station A10. The aquifer layer is characterized by 153 Ωm resistivity. However, station SP1 remains an alternative drilling site with an apparent resistivity of the aquifer layer being 204 Ωm.

In Charleskrom, the fourth layer of station A70 has a very low apparent resistivity of 5 Ωm, diagnostic of weathered bedrock and provides a good potential zone for groundwater storage. An intermediate potential zone to host groundwater in this community is the third layer of station SP1 with a resistivity value of 222 Ωm.

The aquifer is expected to be intercepted in the third layer of station A230 in Domsesre community which is presumed to be a weathered basement of resistivity, 15 Ωm. Appreciable quantity of water is also likely to accumulate in the third layer of station B220 which has an apparent resistivity of 290 Ωm.

Significant amount of water is expected to be hosted in the fourth layer of station A70 in Fokuokrom with a characteristic resistivity of 187 Ωm. Another zone with intermediate

groundwater prospects in the community is the second layer of station SP2. This layer has an apparent resistivity of 49 Ωm.

In Kofi Daa-Tano community, the second layer of station A40 is characterized by a low resistivity of 53 Ωm which is indicative of a fractured layer aquifer. An intermediate groundwater potential zone is similarly observed in the second layer of station A20 which possesses a resistivity of 18 Ωm.

The first ranked point for borehole drilling in Kwanware community is station A90. Groundwater is expected to be stored within the fourth layer. An alternative drilling point in the community is station A300 where the aquifer is characterized by 178 Ωm resistivity.

In Maamakrom village, the third layer of station A20 with resistivity 125 Ωm is marked a good groundwater potential zone whilst the third layer of station B10 is presumed to have an intermediate potential for groundwater storage.

The aquifer at station A60 in Nkranketewa community is expected to be intercepted in the third layer. However, the fourth layer resistivity of 325 Ωm is expected to be moderately weathered basement hence, moderate groundwater potential is expected to be accumulated in this layer as well. Likewise, the third and fourth layers of station A140 are presumed to have intermediate groundwater potential characterized by resistivity values of 124 Ωm and 247 Ωm respectively.

In Tano-Ano community, it is revealed that the fourth layer of station A90 characterized by a very low resistivity of 15 Ωm could represent a highly weathered bedrock and it could be a good groundwater potential zone. For an alternative zone for groundwater

storage, the 19 Ωm resistivity third layer of station B10 which is also indicative of a highly weathered basement is chosen.

In Yeboakrom community, the first choice for test drilling is station SP1. The third layer which is expected to host significant amount of groundwater has an apparent resistivity of 236 Ωm. The alternative drilling site in this community is station A60 where the fourth layer of resistivity, 182 Ωm is expected to contain appreciable quantity of groundwater.

5.2 Recommendations

It is worth considering that all the geophysical methods of exploration have their own limitations and specialities. In view of that, the information and results obtained in this research may not be all that comprehensive and thus, further investigations could still be made. It is therefore suggested that other geophysical methods of investigation be employed to compliment the results obtained.

Due to reasons beyond the control of the investigator, drilling could not be done before the time of the submission of this thesis. It is therefore suggested that, efforts should be put in place to facilitate the drilling of boreholes so as to obtain drill logs which could provide control information regarding the subsurface geology of the area and to ascertain the effectiveness of the methods used.

Finally, it is recommended that the drilling of boreholes should be done in the order suggested in each of the communities.

REFERENCES

Acheampong, S. Y. (1996). *Geochemical Evolution of the Shallow Groundwater System in the Southern Voltaian Sedimentary Basin of Ghana. PhD Dissertation.* University of Nevada, Reno.

Agyekum, A. W. (2002). *Groundwater Resources of Ghana With Focus on International Shared Aquifer Boundaries.* CSIR Water Research Institute Accra, Ghana.

Ahzegbobor, P. A. (2010). 2D and 3D Geoelectrical Resistivity Imaging: Theory and Field Design. *Scientific Research and Essays Vol. 5(23)*, pp. 3592-3605.

Akudago, J. A., Chegbele, L. P., Nishigaki, M., Nanedo, N. A., Ewusi, A., & Kankam-Yeboah, K. (2009). Borehole Drying: A Review of the Situation in the Voltaian Hydrogeological System in Ghana. *J. Water Resource and Protection, 3*, pp. 153-163.

Ameloko, A. A., & Rotimi, O. J. (2010). 2- D Electrical Imaging And Its Application In Groundwater Exploration In Part Of Kubanni River Basin-Zaria, Nigeria. *World Rural Observations;2(2)*, pp. 72.

Anan-Yorke, R. (1971). *Geology of the Voltaian Basin – Special Bulletin of the Geological Survey Department.* Accra: Geological Survey Department.

Apambire, W. B. (1996). *Groundwater Geochemistry and the Genesis and Distribution of Groundwater Fluoride in the Bolgatanga and Bongo Districts, Ghana.* MSc Thesis. Carleton University, Ottawa, Ontario, Canada.

Apambire, W. B., Boyle, D. R., & Michel, F. A. (1997). Geochemistry, Genesis and Health Implications of Fluoriferous Groundwaters in the Upper Regions of Ghana. *Environmental Geology 33 (1)*, pp. 13-24.

Araffa, S. A. S. (2012). *Groundwater Management by Using Hydro-Geophysical Investigation: Case Study: An Area Located at North Abu Zabal City,* National Research Institute of Astronomy and Geophysics, Helwan, Cairo, Egypt.

Arthur, J. L. (2006). *Implications of Family Size on the Quality of Life of People in the Sunyani Municipality. MA Dissertation in Environmental Management And Policy.* University of Cape Coast, CapeCoast.

Asklund, R., & Eldvall, B. (2005). *Contamination of Water Resources in Tarkwa Mining Area of Ghana, MSc Thesis.* Royal Institute of Technology, Lund, Sweden.

Badrinarayanan, T. S. (2002). *Groundwater Exploration.* A Presentation by B Square Geo Tech Services, Kollidam.

Barry, B., Oboubie, E., Andreini, M., Andah, W., & Pluquet, M. (2005). *The Volta River Basin.* International Water Management System.

Barry, B., & Oboubie, E. (2010). Groundwater in sub-Saharan Africa: *Implications for food security and livelihoods.* Ghana Country Status on Groundwater, pp. 18

Bayor, J. S. (2004). *Application of the Electromagnetic and the Electrical Resistivity Methods in Groundwater Exploration in the Tolon-Kumbungu District of the Northern Region of Ghana.*

Beck, A. E. (1981). *Physical Principles of Exploration Methods.* London: Macmillan.

Benson, R. C., Glaccum, R. A., & Noel, M. R. (2000). *Geophysical Techniques for Sensing Buried Wastes and Waste Migration.* EPA/600/7-84/064 (NTIS PB84-198449), 236 pp.

Bosu, J. K. (2004). *Groundwater Exploration in the Granitic Basement in the Assin District of the Central Region Using the Electrical Resistivity Method.*

Carney, J., Colm, J., Chris, T., & McDonnell, P. (2008). *A Revised Lithostratigraphy and Geological Map for the Volta Basin, Derived From Image Interpretation and Field Mapping The Voltaian Basin.* Ghana Workshop and Excursion.

Cudjoe, J. E. (1961). *A Programme for Geophysical Exploration in Ghana. MSc Thesis.* Massachusetts Institute of Technology: pp. 7.

Dahlin, T., & Loke, M. H. (1997). Quasi-3D Resistivity Imaging-Mapping of Three-Dimensional Structures Using Two-Dimensional DC Resistivity Techniques. *Proceedings of the 3rd Meeting of the Environ. Eng. Geophy. Soc.*, (pp. 143-146).

Dapaah-Siakwan, S., & Gyau-Boakye, P. (2000). Hydrological Framework and Borehole Yields in Ghana. *Hydrogeology Journal 8*, pp. 405-416.

Darko, P. K. (2001). *Quantitative Aspects of Hard Rock Aquifers: Regional Evaluation of Groundwater Resources in Ghana. Ph.D Thesis.* Charles University, Prague, Czech Republic.

Driscoll, F. D. (1986). *Groundwater and Wells.* St. Paul, MN: Johnson Screens.

Eke, K. T. & Igboekwe, M. U. (2011). Geoelectrical Investigation of Groundwater in Some Villages in Ohafia Locality, Abia State, Nigeria. *British Journal of Applied Science & Technology* 1(4): 190-203.

Freeze, R. A., & Cherry, J. A. (1979). *Groundwater.* Eaglewood Cliffs, NJ: Prentice Hall.

Gill, H. E. (1969). A Ground-water Reconnaissance of the Republic of Ghana, With a Description of Geohydrologic Provinces. *US Geological Survey Water Supply Paper 1757-K*.

Gilson, E. W., Nimeck, G., Bauman, P. D., & Kellett, R. (2000). Groundwater Exploration in Prairie Environments. *Journal of Environmental and Engineering Geophysics*, pp. 1-5.

Gyau-Boakye, P., & Dapaah-Siakwan, S. (2000). Groundwater as a Source of Rural Water Supply in Ghana,. *Journal of Applied Science and Technology (JAST), Vol 5, Nos. 1 & 2*, pp. 77-86.

Hirdes, W., & Nunoo, B. (1994). The Proterozoic Paleoplacers at Tarkwa Gold Mine, SW Ghana: Sedimentology, Mineralogy, and Precise Age Dating of the Main Reef and West Reef, and Bearing of the Investigations on Source Area Aspects. *Geologisches Jahrbuch D 100*, pp. 247–311.

Hiscock, K. M. (2005). *Hydrogeology: Principles and Practice.* Wiley-Blackwell.

Jones, W. B. (1978). *The Stratigraphy and Age of the Voltain System, Ghana.* (Unpublished Report of the Ghana Geological Survey).

Junner, N. R. (1935). *Gold in the Gold Coast.* Ghana Geol. Surv. Mem., No. 4 64 p.

Junner, N. R. (1940). *The Geology of the Gold Coast and Western Togoland.* Bull. Geol. Surv. Gold Coast, vol. 10. 40p.

Junner, N. R., & Bates, D. A. (1945). *Reports on the Geology and Hydrology of the Coastal Areas East of the Akwapim Ranges.* Ghana Geological Survey Memoir No. 7.

Kearey, P., & Brooks, M. (2002). *An Introduction to Geophysical Exploration.* Third Edition, Blackwell, London.

Kesse, G. O. (1985). The Mineral and Rock Resources of Ghana. *Rotterdam, A.A. Balkema*, pp. 95-156.

Key, R. M. (1992). *An Introduction to the Crystalline Basement of Africa. In : The Hydrogeology of Crystalline Basement Aquifers in Africa.* Geological Society Special Publication 66: pp. 29-57.

Kresic, N. (2007). *Hydrogeology and Groundwater Modeling (3rd ed.).* New York, London: CRC Press/Taylor& Francis.

Lashkarripour, G. R. (2003). An Investigation of Groundwater Condition by Geoelectrical Resistivity Method: A Case Study in Korin Aquifer, Southeast Iran. *Journal of Spacial Hydrology. 3(1)*, pp. 1-5.

Leube, A., Hirdes, W., Mauer, R., & Kesse, G. O. (1990). The Early Proterozoic Birimian Supergroup of Ghana and Some Aspects of its Associated Gold Mineralization. *Precambrian Research, 46*, pp. 139-165.

Liopis, J. L., & Simms, J. E. (1994). *Seismic Refraction and Electromagnetic Surveys at Fort Detrick, Maryland.*

Loke, M. H. (1999). *Electrical Imaging Surveys for Environmental and Engineering Studies.*

MacDonald, A. M., Davies, J., & Dochartaigh , B. É. (2002). *Simple Methods for Assessing Groundwater Resources in Low Permeability Areas of Africa.* Commissioned Report CR/01/168N.

MacDonald, A., Davies, J., Calow, R., & Chilton, J. (2005). *Developing Groundwater; A Guide for Rural Water Supply.* Practical Action Publishing Ltd. Bourton on Dusmore, Rugby, Warwickshire, UK. pp. 1, 7 – 12, 64 – 106.

Martin, N., & Van de Giesen, N. (2005). Spatial Distribution of Groundwater Use and Groundwater Potential in the Volta River Basin of Ghana and Burkina Faso. *IWRA Water International, 30 (2)*, pp. 239–249.

McDowell, P. W., Barker, R. D., Butcher, A. P., Culshaw, M. G., Jackson, P. D., McCann, D. M., et al. (2002). *Geophysics in Engineering Investigations.*

McNeill, J. D., & Snelgrove, F. B. (1995). *Electromagnetic Geophysical Methods Applied to Groundwater Exploration and Evaluation.* Geonics Limited.

Milesi, J. P., Feybesse, J. L., Dommanget, A., Ouedraogo, M. F., Marcoux, E., Prost, A., et al. (1990). West African Gold Deposits in their Lower Proterozoic Lithostructural Seeting. *Chron. Rech. Min., v. 497*, pp. 3-98.

Ndlovu, S., Mpofu, V., Manatsa, D., & Muchuweni, E. (2010). Mapping Groundwater Aquifers Using Dowsing, Slingram Electromagnetic Survey Method and Vertical Electrical Sounding Jointly in the Granite Rock Formation: A Case of Matshetshe Rural Area in Zimbabwe. *Journal of Sustainable Development in Africa (Volume 12, No.5).*

Nejad, H. T., Mumipour, M., Kaboli, R., & Najib, O. A. (2011). Vertical Electrical Sounding (VES) Resistivity Survey Technique to Explore Groundwater in an Arid Region. *Journal of Applied Sciences 11 (23): 3765-3774.*

Nyarko, E. S., Aseidu, D. K., Osea, S., Dampare, S., Zakaria, N., Hanson, J., et al. (2012). Geochemical Characteristics of the Basin-type Granitoids in the Winneba Area of Ghana. *Proceedings of the International Academy of Ecology and Environmental Sciences 2(3)*, pp. 177-192.

Ó Dochartaigh, B. É., Davies, J., Beamish, D., & MacDonald, A. M. (2011). BGS Consultancy: UNICEF IWASH Project, Northern Region, Ghana. Final Report. *British Geological Survey Open Report, OR/11/017. 69pp*.

Obuobie, E., & Boubacar, B. (2010). Groundwater in sub-Saharan Africa: Implications for Food Security and Livelihoods, Ghana Country Status on Groundwater. pp. 18.

Odoh, B. I., Utom, A. U., & Nwaze, S. O. (2012). *Groundwater Prospecting in Fractured Shale Aquifer Using an Integrated Suite of Geophysical Methods: a Case History from Presbyterian Church, Kpiri-Kpiri, Ebonyi State.* SE Nigeria, p-ISSN: 2163-1697.

O'Donovan, G., & Lacey, A. (2011). Technical Report on The Asuogya Licence, Ghana NI. pp. 43-101.

Oghenekohwo, O. F. (2008). *A Comparison of Resistivity and Electromagnetics as Geophysical Techniques.* Msc Thesis, African Institute for Mathematical Sciences, Capetown, South Africa.

Paine, J. G. (2000). *Identifying and Assessing Groundwater in the Lower Rio Grande Valley, Texas,Using Airborne Electromagnetic Induction.* MSc Thesis. The University of Texas at Austin.

Pigois, J. P., Groves, D. I., Fletcher, I. R., McNaughton, N. J., & Snee, L. W. (2003). Age Constraints on Tarkwaian Palaeoplacer and Lode-gold Formation in the Tarkwa-Damang District, SW Ghana. *Mineralium Deposita 38*, pp. 695–714.

Reynolds, J. M. (1997). *An Introduction to Applied and Environmental Geophysics.* John Wiley and Sons Ltd.

Rosen, S., & Vincent, J. R. (1999). *Household Water Resources and Rural Productivity in Sub- Saharan Africa: A Review of the Evidence.* Development Discussion Paper No. 673, Harvard Institute for International Development, Harvard University.

Schwarz, S. D. (1988). Application of Geophysical Methods to Groundwater Exploration in the Tolt River Basin, Washington State. *Geotechnical and Environmental*

Studies Geophysics, Vol II. Soc. Exploration Geophysicist: Tulsa, OK, pp. 213-217.

Sen, Z. (1995). *Applied Hydrogeology for Scientist and Engineers.* ISBN 1-56670-091-4.

Shehu, A. D. (1998). *Application of Electromagnetic and Direct-Current Resistivity Methods to Groundwater Exploration in Selected Villages in Ningi L.G.A. Bauchi State.* MSc Thesis.

Sheriff, R. E. (1991). *Encyclopedic Dictionary of Exploration Geophysics 3rd edn.* Tulsa: Society of Exploration Geophysicists.

S. M. A. (2010). *Municipal Medium Term Development Plan Document.*

S. W. D. A. (2010). *Municipal Medium Term Development Plan Document.*

Smedley, P. L. (1996). Arsenic in Rural Groundwater in Ghana. *Journal of African Earth Sciences 22 (4)*, pp. 459-470.

Straton, J. A. (1941). *Electromagnetic Theory.* McGraw-Hill Book Co.

Taylor, P. N., Moorbath, S., Leube, A., & Hirdes, W. (1988). Geochronology and Crustal Evolution of Early Proterozoic Granite-Greenstone Terrains in Ghana/West Africa. *Abst., International Conference on the Geology of Ghana with Special Emphasis on Gold Comm.* 75th Anniversary of Ghana Geol. Surv. Dept., Accra. pp. 43-45.

Telford, W. M., Gerdart, L. P., & Sheriff, R. E. (1990). *Applied Geophysics.* 2nd Ed. Cambridge University Press.

Unihydro, L. (2002). *Baseline Study and Inventory of Water Resources in the Northern Region of Ghana. AFD Rural Water Supply and Sanitation Project in the Northern Region.*

Vogelsang, D. (1994). *Environmental Geophysics: A Practical Guide.* Springer Verlag ISBN 10: 0387579931.

W.V.I. (1997). *Unihydro, Adaklu Anfoc Hydrofac Supervision Report Prepared for Regional Coordinator/Programme Manager, VRCWSP, Ho.*

Ward, S. H., & Hohmann, G. W. (1987). *Electromagnetic Theory for Geophysical Applications.* Dept of Geology and Geophysics, University of Utah.

Walton, J. (2010). *Surface Investigations of Groundwater.*

WARM. (1998). *Water Resources Management Study, Information 'Building Block' Study. Part II, Volta Basin System, Groundwater Resources.* Accra: Ministry of Works and Housing.

WHO/UNICEF. (2000). *Global Water Supply and Sanitation Assessment 2000 Report, New York, Geneva: Joint Monitoring Programme for Water Supply and Sanitation (JMP).*

Wightman, W. E., Jalinoos, F., Sirles, P., and Hanna, K. (2003). *"Application of Geophysical Methods to Highway Related Problems."* Federal Highway Administration, Central Federal Lands Highway Division, Lakewood, CO, Publication No. FHWA-IF-04-021

WRI. (2001). *Groundwater Resources Assessment of Ghana.* Technical Report, Water Research Institute (CSIR), Accra.

APPENDIX 1

Sample Results of the Electromagnetic Measurements

Community:	Adomako	**District:**	Sunyani Municipal
Bearing:	151°	**Profile Length:**	210 m
Profile No.	A	**Date:**	11/03/2013

STATION	**20-m Separation**		Remarks
	HD	**VD**	
0	10	7	
10	10	4	
20	11	12	peg
30	10	12	
40	14	12	mark
50	11	12	
60	12	12	
70	11	11	
80	12	14	peg
90	13	15	roof
100	13	13	peg
110	13	11	
120	13	12	
130	13	11	
140	11	13	septic
150	8	14	
160	12	14	
170	12	14	
180	11	13	
190	11	12	
200	11	13	peg
210	11	12	

APPENDIX 2

Sample Results of the VES Measurements

Location	**ADOMAKO SUNYANI**	Date:	**11-Mar-13**
District	**MUNICIPAL**	Coordinate:	**7.30694^{o}N, 2.33038^{o}W**
Station	**A20**	Altitude:	**288 m** *amsl*

L/2 (m)	a/2 (m)	Resistance (Ohms)	Multiplying Factor	Apparent Resistivity (Ohm-m)
1.5	0.5	13.250	6.3	83.5
2.1	0.5	8.140	13.1	106.6
3.0	0.5	5.290	27.5	145.5
4.4	0.5	3.110	60.0	186.6
6.3	0.5	1.967	124.0	243.9
9.1	0.5	1.135	259.0	294.0
13.2	0.5	0.560	547.0	306.3
13.2	5.0	6.516	47.0	306.3
19.0	0.5	0.267	1133.0	302.5
19.0	5.0	2.853	106.0	302.4
27.5	0.5	0.134	2375.0	318.3
27.5	5.0	1.382	230.0	318.0
40.0	0.5	0.055	5026.0	276.4
40.0	5.0	0.557	495.0	275.8
58.0	5.0	0.168	1049.0	176.2
58.0	25.0	1.023	172.0	176.0
83.0	5.0	0.080	2156.0	172.5
83.0	25.0	0.437	394.0	172.0